

**DEVELOPMENT OF STATISTICAL FORECAST
MODELS OF SUMMER CLIMATE AND
HYDROLOGICAL RESOURCES
OVER SOUTHERN AFRICA**

Mark R Jury

WRC Report No. 903/1/02



Water Research Commission



DEVELOPMENT OF STATISTICAL FORECAST MODELS OF SUMMER CLIMATE AND HYDROLOGICAL RESOURCES OVER SOUTHERN AFRICA

**A report to the WRC
by Mark R Jury
Environmental Studies Dept
University of Zululand**

Based on research in the period 1997-2001

Assisted by:

MSc researchers: N Mwafurirwa, M Gwazantini, M Matitu, E Matari, E Nkosi

PhD researchers: E Mpeta, A Yeshanew, A Kozakiewicz

Post-Doc researchers: J L Melice, S Engert

WRC Report No 903/1/02

ISBN No 1-86845-936-5

December 2002

Disclaimer

This report emanates from a project financed by the Water Research Commission (WRC) and is approved for publication. Approval does not signify that the contents necessarily reflect the views and policies of the WRC or the members of the project steering committee, nor does mention of trade names or commercial products constitute endorsement or recommendation for use.

Executive Summary

Introduction

This research project seeks to develop prediction models for water, climate and related resources from the following realisations: - the climate of southern Africa often exhibits large departures from average; - these unexpected events impact water resources and economic activity; - climate fluctuations are related to nearby tropical ocean – monsoon conditions; - the fluctuations can be replicated using various climate and oceanic indices; and - regression equations can be formulated at useful lead-times to predict the climate.

The methodology presented here is simple and easily implemented with a small PC and internet connection. This is not to say that statistical modelling is of limited value. Such models can be trained directly on a desired resource at long lead-times (here defined as 3 to 6 months in advance). Statistical models compete favourably with numerical models at lead times greater than three months. However the assumption of history 'repeating itself' is not to be taken lightly. In this regard, we are fortunate to be able to employ new analysis techniques: to test the stability of relationships, to achieve optimum solutions and to recognise limitations. In this research we have explored predictors other than sea surface temperature, considering that tropical wind circulations and air pressure play important roles in forcing the tropical ocean into an anomalous state, and in transmitting these effects to wider areas via slowly evolving 'waves'. Through our efforts we have uncovered key indices that distinguish the linearly predictable component of climate around southern Africa.

Background

The availability of water in southern Africa is constrained by fluctuations in summer rainfall. Economic activity subsides during drought years, whilst rivers and their dams overflow in flood years causing destruction. Accurate long-range forecasts of streamflows and area- rainfall could play a useful role in mitigating the effects of climate variability. The research is aimed at developing climatic inputs to hydrological models at regional level.

This research has carried forward the successful initiative of an earlier WRC project on long-range rainfall forecasting (WRC 672). This saw the development of multi-variate models for seasonal-lead time forecasting of summer rainfall. Model validations gave skill test correlations averaging about 70%, considered to be some of the highest in the world for seasonal lead times (Jury, 1996). Their success can be traced to the wide range of climatic predictors uncovered by earlier WRC projects (WRC 278 of 1994, and WRC 436 of 1996).

The statistical models employed up to 1998 were based on a training period from 1971-1993. Updating of the models to the present (1998) was considered necessary to capture recent patterns of global ocean-atmosphere coupling and influences of tropical Atlantic ENSO events. This new research benefited from the NCEP re-analysis data set. Overlap between the predictors ensured that an understanding of climate dynamics could develop in parallel with statistical model formulation and testing. Models with forecast lead times of two seasons were then formulated.

Original aims

The original aims of this WRC project, as outlined in the accepted proposal included:

(a) Historical analysis of streamflow and rainfall over southern Africa, with emphasis on inter-annual variability of water resources.

(b) Meteorological analysis of monthly National Center for Environmental Prediction (NCEP) geophysical data, leading to the formulation and extraction of suitable climatic predictors in the period 1958-1998.

(c) Development of statistical long-lead forecast models for hydrological targets which can address the varying influences of the El Nino Southern Oscillation (ENSO).

(d) Assessment of how long-lead forecasts can be taken up in the hydrological decision-making process.

(e) Development of skilled manpower through environmental science research.

In retrospect, the project has achieved these objectives, with most emphasis on aims a, b, and c.

Consolidated summary

The section provides a consolidation of results for each facet of the project. In the early stages of the project, efforts were placed on extending the earlier results of the WRC 672 project, using the same predictors and new hydrological target data. Predictive models were formulated for a number of southern African water resources:

Target	Algorithm	r^2 fit
Midmar	$+.44(aVang)+.37(oNiV)-.73(oAtlw)$	= 64
Pongo	$-.76(aWip)+.25(aMaurV)$	= 61
Vaal	$-.71(oSlp)-.29(aElu)+.26(aWCI-AbP)$	= 52
Gariiep	$+.39(aVang)-.78(oSlp)-.45(oSocnS)$	= 71
Hartebees	$-.41(aElv)-.43(aCIst)+.44(aWCI-AbP)$	= 46
Zambezi	$-.44(aArBst)-.49(oAtlW)+.73(oATpc2)$	= 73

In one of the studies performed in 1998, hydrological anomalies over Africa were assessed using annual flow data for the Nile, Niger, Congo, Senegal, Zambezi, and Orange Rivers; and Lakes Victoria and Malawi. Significant correlations were uncovered between the various rivers hence it was concluded that hydrological anomalies are widespread across Africa. A composite analysis of years with high and low flow, determined a sensitivity to coupling between the zonal circulation over the tropical Atlantic and ENSO phase.

In studies developed through an exchange visit of Belgian scientist Jean-Luc Melice, scale-interactions in intra-seasonal to decadal climate variability were investigated using the continuous wavelet transform (CWT) technique applied to two long-term data sets: the Nile River flow and Durban rainfall. For Durban rainfall the

annual cycle accounts for 33% of variance, whilst inter-annual fluctuations explain 10%, mainly focused on 2.3 and 4 year bands. Associations between these data sets and the Pacific pressure index of El Nino (SOI) and the Atlantic SST (N-S) dipole were uncovered and again demonstrate the widespread nature of inter-annual forcing over Africa.

In a study performed by senior student S.E. Nkosi, it was demonstrated that summer rainfall over SE Africa increases when easterly flow is present off northern Madagascar in the tropical Indian Ocean. The composite analysis of wet and dry years reveals deep easterly flow differences in the band 5° - 20°S. Convection is reduced over the South Indian Ocean (0 - 30°S, 60° - 110°E) whilst increased over SE Africa. SSTs increase southeast of Madagascar in the latitude band 25° - 35°S and couple with an anticyclonic circulation, which transfers moisture westward to SE Africa. SST in the tropics are below normal, hence the poleward thermal gradient is reduced and the associated subtropical jet stream shifts polewards to 40°S during wet years.

The study of drought over southern Africa by N. Mwafurirwa revealed a meandering of the sub-tropical jet stream around a standing rossby wave with a ridge on 20°E and trough on 55°E. The structure is such that equatorward flow and subsidence is produced over southern Africa. Considering the equation: $f \int d\omega = \int \mathbf{V} \cdot \nabla (\zeta + f) dp$; and substituting appropriate theoretical and observed values; the vertical motion anomaly (w) is found to be $-2 \cdot 10^{-3} \text{ m s}^{-1}$. This is sufficient to overcome local weather events, surface heating and moist inflows, and produce widespread drought conditions over southern Africa.

In the study by M. Gwazantini, variations in key water resources in tropical southern Africa were analysed. Wet years were examined and found to be characterised by an influx of moist monsoonal air from the NE, a zonal overturning cell connected to the tropical south Atlantic, and a subtropical trough over Mozambique. Predictor indices were extracted from environmental fields exhibiting precursor signals at one season lead-time (JAS for DJF). An outcome was the development of predictive models to forecast changes in the inflow to Lake Malawi and other water resources of southern Africa. A more general outcome of this work was the generation of meaningful information on the relative influence of various global and regional climatic fluctuations.

A study initiated by the project leader in 2000 led to an in-depth analysis of monsoons around Africa as predictors of rainfall. For southern African rainfall, SST differences between the southwest and central-west Indian Ocean and the rotational component of monsoon flow in the central Indian Ocean (which controls ocean dynamics) play significant roles. For east African rainfall, the surface zonal wind in the east equatorial Indian Ocean is a key determinant. Westerly (easterly) winds in the east Indian Ocean favor rainfall in southern (east) Africa, and serve to indicate the strength of the zonal direct circulation and the east-west SST gradient. The implication is that East Africa shares a maritime rainfall regime with the west Indian Ocean, whilst convection over southern Africa is inversely related. The study went further to analyse mechanisms underlying warm and cool events in the tropical Indian

Ocean. Composite warming is maintained through reduced evaporation and reduced ocean entrainment, while increased radiative fluxes also contribute. The OND season is when the fluxes most actively modify SST, and also when the ocean and atmosphere are most strongly coupled (eg. cloud depth adjusts to SST). The findings provide support for the use of monsoon indices in predictive models for African rainfall at two-season lead-time (eg. 6 months). Recognizing that our knowledge of ocean-atmosphere coupling around Africa is limited, it is suggested that greater *in-situ* measurements be gathered as part of GOOS and CLIVAR activities.

In the comprehensive PhD study of senior student E. Mpeta, a principal component analysis of low-resolution African rainfall and temperature, and Atlantic and Indian Ocean SST, SLP, U and V wind was done. Five regional targets and 20 predictors were formulated and models were developed over a 30 year training period, yielding the following results:

Target	Most Significant Predictors	Fit ($r^2\%$)
Rain pc1 Africa south of Zambezi	U pc2r + SLP pc3 eq. E. Indian zonal wind + N-S dipole of press. in Atlantic	20

The models are based on continuous time series, filtered with CWT to isolate variability in the 1.5 – 9 year band. The southern African temperature has a high explained variance (partially due to upward trend), contributed by SST varying in-phase in the west Atlantic and central Indian Oceans. The work demonstrates that dipole (or two-area) predictors have considerable value. Of the key area predictors for southern African rainfall: at zero lag the dipole in SST between the SW Indian Ocean and the western tropical Indian Ocean provides a high degree of predictability. At six month lead time the east Indian Ocean zonal wind is a useful lead-time indicator of southern African rainfall.

Using a high resolution rainfall data set, the project leader interacted with German scientists to produce an optimum regionalisation of African rainfall. Rotated principal component solutions were calculated for a varying number of PC modes from 10 to 24. Cross-correlations were computed between the consequent area-indices. The correlation function displayed an inflection point at a 15-mode solution, providing a guide to the size of areas used for the training of predictive models. The consequent models are listed below, with claims of 'fit' deflated using techniques as outlined later. With a range of models to choose from, an ensemble mean can be calculated to provide a more reliable answer.

Nov-Mar Rain training (yrs)	Multivariate algorithm	lead	adj r^2	fit
E South Africa	-.63(wiU)+.34(naSST)-.30(eiP)	JAS	33	19
E South Africa	-.44(wiU)+.38(naSST)-.28(atlw2)	SON	28	19
E South Africa old	+.45(angSST)-.53(ciSST)+.49(niV)	SON	32	22

W South Africa	+ .29(ciEvap) - .55(eiP) + .38(swiSST)	JAS	32	39
W South Africa	+ .30(seaSST) + .49(eiU) + .32(QBO30)	SON	35	39
W South Africa	- .69(atlw2) - .46(eiV)	JAS	33	22

old

In summary, this WRC project has successfully studied, formulated and implemented models to predict the variability of southern African climate and water resources, 3 – 6 months in advance. The project has built on past efforts and drawn ideas from graduate students and collaborating scientists, to provide southern African water and resource managers with optimum statistical forecasts via the internet website:

< http://www.1stweather.com/forecasts/cip_seasonal_outlook.shtml >

The benefits of uptake of this predictive information can be expected to reduce economic risks by over R10 billion per annum in South Africa. During the lifespan of this WRC project, forecasts were issued each spring and the models consistently foretold of the wet conditions that ensued. Further work should seek to separate the spectral components of the climate system into biennial, interannual and decadal bands, which could see the lead-time of accurate forecasts increased from 3-6 months to one year.

Capacity Building and Collaboration

Capacity building during the WRC project took the form of numerous MSc and PhD students, providing support data analyses and interpretation as part of their own thesis development. Many of the graduate researchers had considerable operational experience and were drawn from meteorological services in the SADC. The following students made important contributions and resulted in the project's objectives being met. MSc researchers: N Mwafurirwa (Malawi), M Gwazantini (Malawi), M Matitu (Tanzania), E Matari (Tanzania), E Nkosi (South Africa), PhD researchers: E Mpeta (Tanzania), A Yeshanew (Ethiopia), A Kozakiewicz (Poland/South Africa), Post-Doc researchers: J L Melice (Belgium), S Engert (Germany), all supervised by Prof M. R. Jury. In addition, a number of collaborating international scientists provided useful inputs, including: A Phillip (Univ Wuezburg), S. Mason (IRI, Scripps Inst.), B. Huang (Univ Maryland), D. Enfield (AOML, NOAA), and W. White (Scripps Inst.).

Preface

Chapter one outlines the objectives of the project, and chapter two - the initial work that resulted in models for water resources. Chapters 2 – 6 derive from journal articles in press that were produced as part of the project research, and consider the regional climatic processes underpinning predictability. Chapters 7 – 8 discuss model development and project wrap-up, including recommendations for further work.

Contents

	Page
Executive Summary	
Chapter 1 – Introduction, background and initial success	1
Chapter 2 – River flows across Africa and the tropical Atlantic circulation	6
Introduction	
Data and methods	
Results	
Discussion	
References	
Chapter 3 – Analysis of long-term data sets: predictability in historical context	23
Introduction	
Data and methods	
Results	
Discussion	
References	
Chapter 4 – Indian Ocean circulation and rainfall over southeast Africa	33
Introduction	
Data and methods	
Results	
Discussion	
References	
Chapter 5 – Composite wet and dry spells and implications for predictability	42
Introduction to rainfall and drought analysis	
Data and methods	
Results	
Discussion	
References	
Introduction to Lake level - wet spell study	60
Data and methods	
Results	
Discussion	
References	

Chapter 6 – Analysis monsoon indices and ENSO stability using NCEP data	73
Introduction	
Data and methods	
Results	
Discussion	
References	
Chapter 7 – Determination of predictors and targets, regionalisation and development of statistical models	100
Chapter 8 – Summary and recommendations – advances in predictability of southern African climate	112

Acknowledgements

This research report to the Water Research Commission of South Africa is made possible by their financial support. In the capacity building section above, the various graduate students contributing to the project were identified. Most valuable contributions came from E Mpeta and A Phillip, whose work toward PhD is represented in chapters 8 and 9, respectively. The advice from the WRC steering committee ensured the success of the project. Finally the host institution via the NRF provided many of the computer resources that enabled data analysis.

Chapter 1 – Introduction, Background and Initial Success

This WRC project is aimed at formulating regional climate predictors, applying these to indices of local water resources, and developing skilful statistical forecast models at lead-times suitable for strategic planning (eg. 3-6 months). In doing so, an improved understanding of inter-annual climate variability is gained and expertise is enhanced.

The water resources of southern Africa are dependent on how summer rainfall responds to regional and global circulation patterns. Past research has established that it is possible to predict about 50% of the variance for hydrological targets. Statistical models have been formulated based on regional predictors using stepwise multivariate linear regression. The long range forecasts have predicted the correct tercile category in 8 of the last 10 years, and correctly anticipated the near-normal conditions that occurred in 1998 and 1999 and the floods of 2000. These models have demonstrated an ability to capture the mix of regional and remote climate signals in a skilful manner. In addition to extending the existing knowledge base to new target data, it was recognised that too many predictors had been generated in the earlier WRC research project. Hence a consolidation phase was necessary. To this end, principal component analyses of SST, air pressure and wind components was conducted over the Atlantic and Indian Ocean domain. The results were assessed as potential predictor inputs, following sensitivity tests on the annual cycle and the application of rotation. Correlation analysis was performed using the principal component time scores with respect to rainfall and temperature over Africa south of 10N.

Other avenues of research employed composite analyses based on changes in catchment inflow. A mathematical explanation was formulated to relate how warming of the tropical Indian Ocean causes an eastward circulation toward lower latitudes and sinking motions over southern Africa. Another analysis investigated the spatial scale of hydrological anomalies and found that drought and flood conditions are widespread and related to the tropical Atlantic circulation. A conceptual model was developed.

To further consolidate the predictors indices were extracted from NCEP reanalysis products for comparison with continuous and seasonal rainfall indices over Africa. The aim was to determine how well a few key tropical monsoon indices 'track' fluctuations of African climate at simultaneous and 6-month lead time. Much of this analysis was performed on low resolution rainfall data sets. To further analyse the spatial structure of rainfall anomalies, a regionalisation of high resolution rainfall was carried out for Africa south of 15 N. Various PCA solutions were analysed and cross-correlated. A change in the correlation function was determined for a 15 PC solution, and this was deemed the appropriate spatial scale for climate prediction. Further statistical techniques were investigated to determine whether the lead time could be increased from one season to one year, using a spectral decomposition into biennial, interannual and decadal climate components. One of the motivations for this work is the increasing impact that rainfall and water resources have on the South African economy as illustrated in fig 1-1.

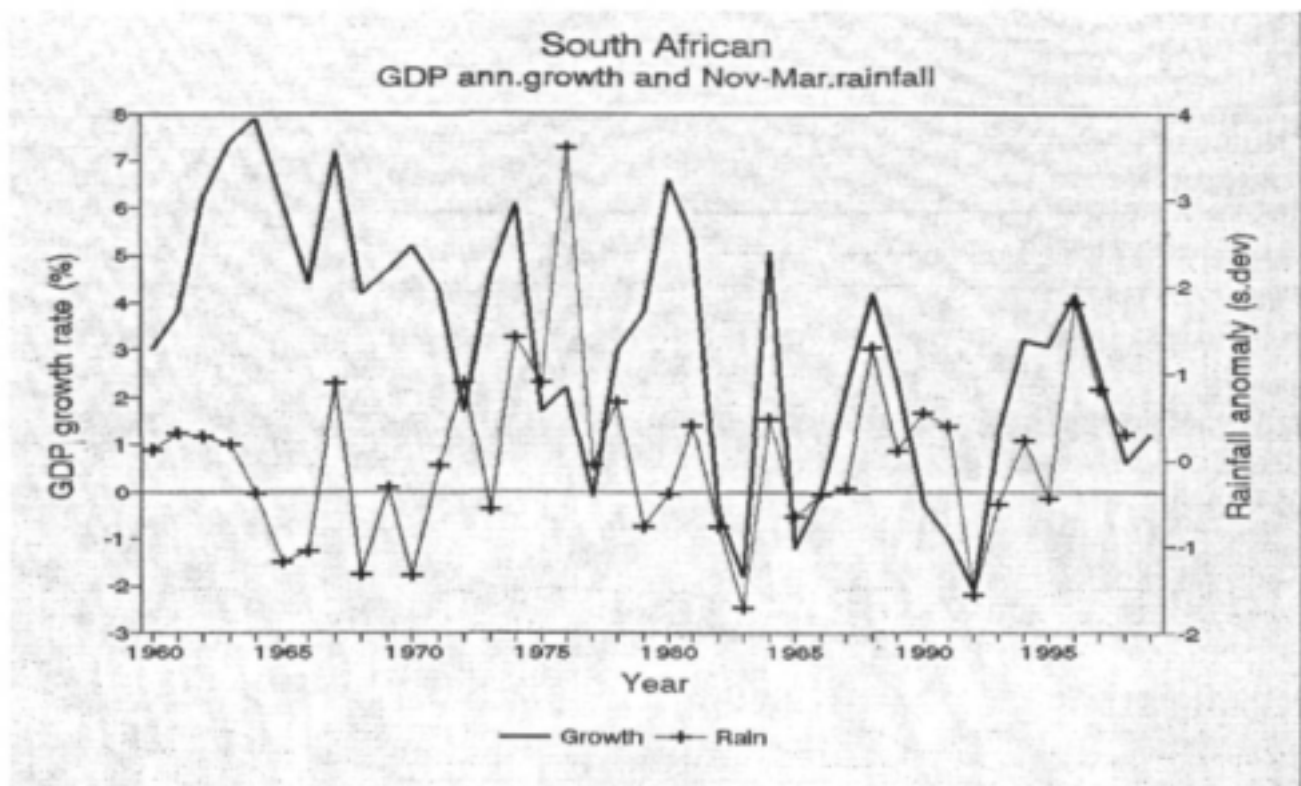


Fig 1-1 Comparison of annual growth rate and South African summer rainfall over the period 1960-1998. Economic swings are $\pm 2\%$, or about R 25 billion. Since 1980s half of GDP variance is associated with rainfall ($r^2 = 48\%$).

Some of the best research is often an extension of previously generated ideas and information. In the predecessor WRC project 672 (Jury et al 1997), a prediction system was developed with demonstrated success in operational application to summer rainfall, temperature and maize yield in the period 1991-1996. It was recognised that the existing prediction system could be applied to new data on water resources. Following a workshop in Pretoria in 1997, Prof W. Alexander provided a hydrological database for the major water supplies of South Africa in spreadsheet format. It contained monthly catchment inflow data either measured from streamflow records or estimated from rain gauge data in the appropriate area. The targets considered for application of climate prediction methodology included the Gariep dam inflow, the Pongolapoort inflow, the Vaal dam inflow and the Hartebeespoort inflow. Many had time series of streamflow or estimated inflow dating to the 1920s. All hydrological information was quality-checked and naturalised using standard techniques common in the field of hydrology, to remove artificial effects: dam construction or abstraction. Additional hydrological data were obtained from sources north of South Africa, including the Zambezi streamflow above Victoria Falls. The new target data were applied to previously identified climate predictors using step-wise multi-variate regression. These predictors met the required criteria in that they were spatially averaged over areas $> 10^6 \text{ km}^2$, temporally averaged over three month time periods,

originated from surface data collected across the tropical oceans, and exhibited a degree of persistence or stability. The sub-set of hydrologically-sensitive predictors are listed in table 1-1 below:

Table 1-1 Most valuable predictors from earlier WRC project

Predictor	Parameter	Area / borders	Lat, long.
aVang	meridional wind	west of Angola	5 S, 5 E
aWCI-ABp	air pressure	south-north dipole	2 N, 55 E
oSiP	air pressure	south Indian Ocean	12 S, 55-77 E
oAtlw	upper zonal wind	central Atlantic	2 S, 20 W
aPac2	sea surface temp.	east Pacific Ocean	2 S, 100 W
oNiV	meridional wind	northern Indian Ocean	12 N, 65 E
oSocnS	sea surface temp.	Southern Ocean	45 S, 10-40 E
aCist	sea surface temp.	central Indian Ocean	2 S, 62 E
aEiU	zonal wind	eastern Indian Ocean	2 S, 77 E
aEiV	meridional wind	eastern Indian Ocean	2 S, 77 E
aWiP	air pressure	western Indian Ocean	2 S, 47 E
aMaurV	meridional wind	Mauritius area	17 S, 55 E

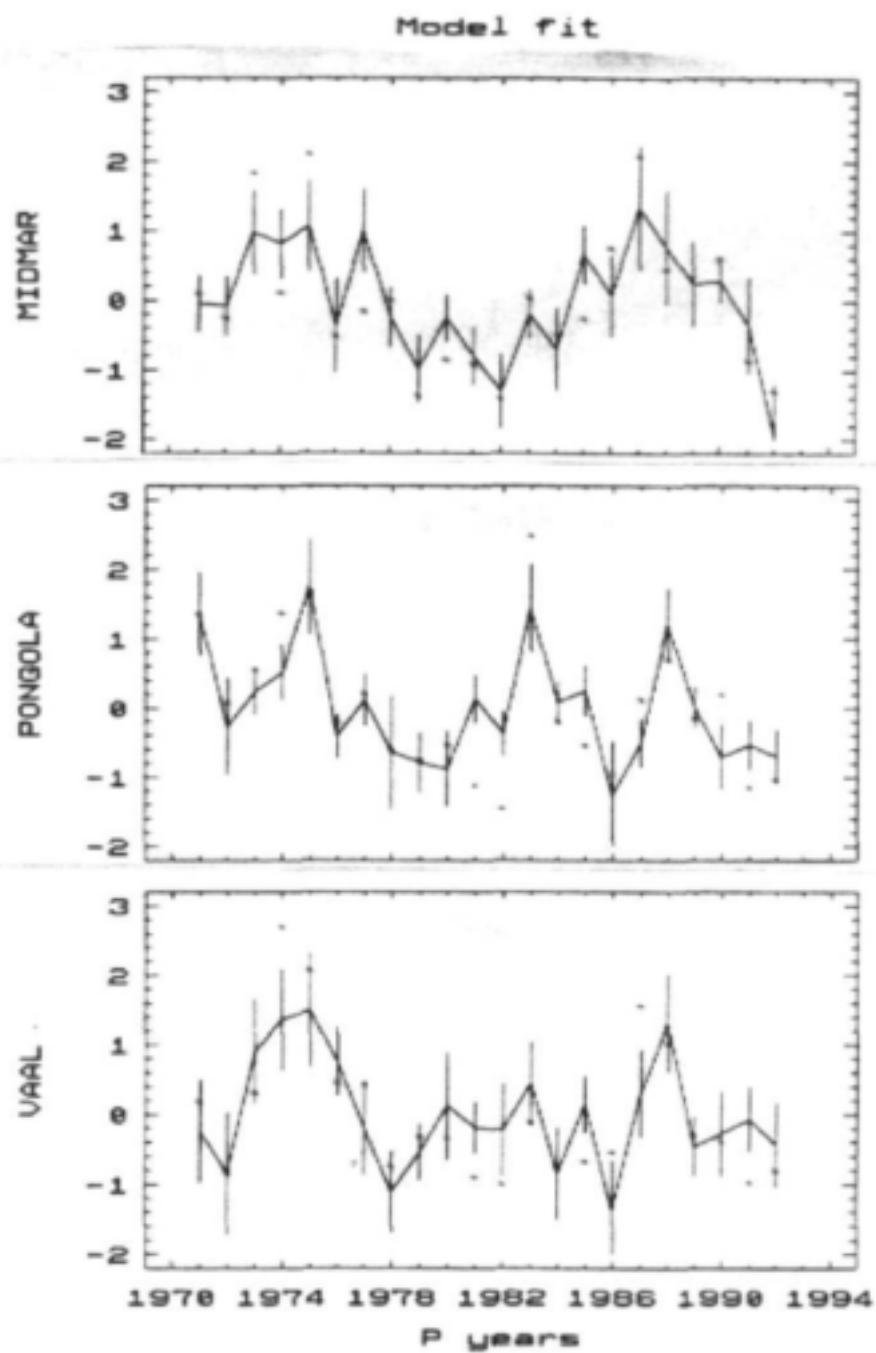
a = JAS o = SON months

The predictors include 4 meridional wind indices, 3 air pressure indices, 3 SST indices, and 2 zonal wind indices. Only 1 index is from the Pacific, 2 from the Atlantic, and the remainder are from the tropical Indian Ocean (8). This pool of predictors was submitted for multi-variate model development using the step-wise regression technique. Predictors within the individual models were screened for co-linearity above a threshold r^2 of 20%. A useful level of hindcast fit was achieved (table 1-2). Although 'hindcast fit' is for the entire training period, the tercile hit-rate from objective validation is consistent with it.

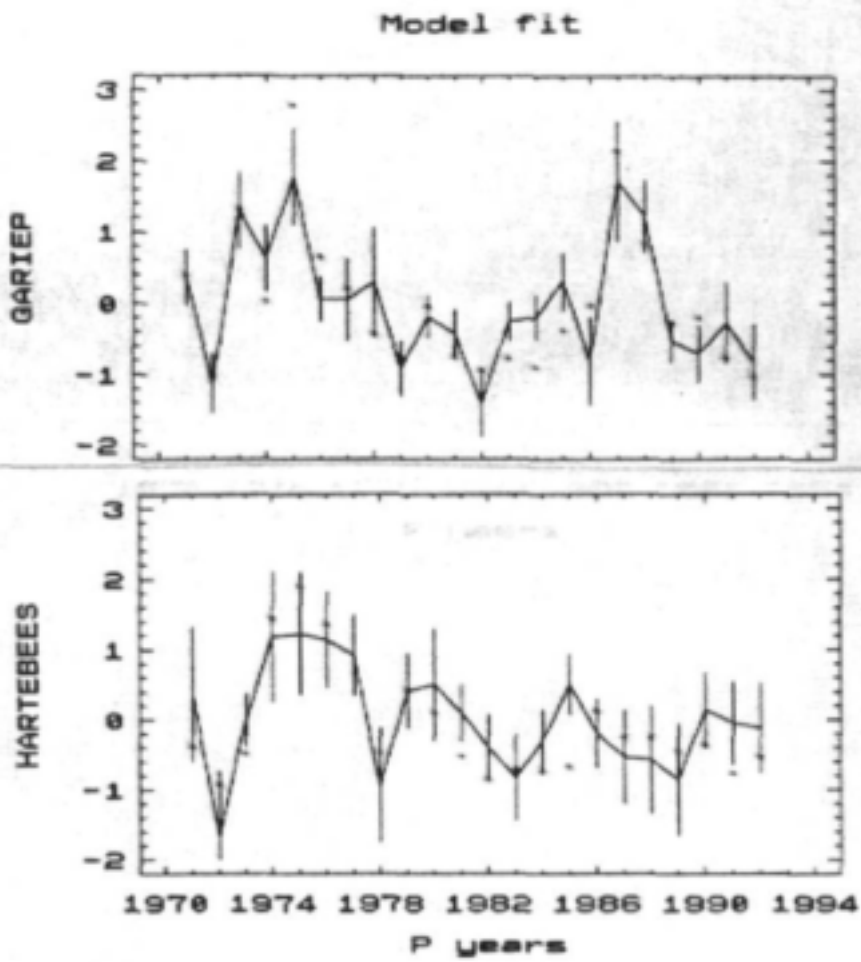
Hence an early success of this WRC project was to extend the research to include new hydrological target data, formulate predictive algorithms, evaluate model performance (figs. 1-2 and 1-3) and implement the results.

Table 1-2 Models for hydrological targets

Target	Algorithm	r^2 fit
Midmar	$+0.44(aVang) + 0.37(oNiV) - 0.73(oAtlw)$	= 64
Pongo	$-0.76(aWiP) + 0.25(aMaurV)$	= 61
Vaal	$-0.71(oSiP) - 0.29(aEiU) + 0.26(aWCI-AbP)$	= 52
Gariiep	$+0.39(aVang) - 0.78(oSiP) - 0.45(oSocnS)$	= 71
Hartebees	$-0.41(aEiV) - 0.43(aCist) + 0.44(aWCI-AbP)$	= 46
Zambezi	$-0.44(aArBst) - 0.49(oAtlW) + 0.73(oATpc2)$	= 73



Figures 1-2 Illustration of 6-month-lead models fitted to hydrological observations over the period 1971-1993.



Figures 1-3 Illustration of 6-month-lead models fitted to hydrological observations over the period 1971-1993.

Chapter 2 – River flows across Africa and the tropical Atlantic circulation

Introduction

Ancient civilizations in Africa were dependent on a regular flow of water in the Nile, and in other major rivers: Niger, Congo, Senegal, Zambezi, Orange; and the rift valley lakes: Victoria, Malawi. These water resources nurtured the evolution of man and enabled societal and economic advances. Their statistics are impressive: the Nile extends 6650 km in length, the Congo yields an annual runoff of 1250 km³, whilst the volume of Lake Malawi is 7200 km³. However, Africa's rivers flow irregularly and fluctuations over millennia have occurred as a result of changes in the overlying monsoons.

Intra-decadal climate variability is typically more pronounced where tropical convection spills north and south over more arid landscapes. Ancient civilizations engaged in agricultural activities in these marginal lands, despite the risk of multi-year drought and flood (Nicholson 1981). Whilst the seasonal shifts of rainfall could be anticipated, runoff is such a small fraction of rainfall that vulnerability is high in the African savanna. Farquharson and Sutcliffe (1998) show that annual runoff is low (< 200 mm) and more variable (coefficient of variation ~ 0.5) for annual rainfall totals < 1200 mm. In contemporary times, an explanation for the inter-annual fluctuation of African river flows has remained an elusive problem (Servat et al. 1998). The flow of the Nile and Congo Rivers is influenced by Pacific El Niño Southern Oscillation (ENSO) phase (Amerasekera et al. 1997); so it is thought that further research on year-to-year changes in tropical climate may lead to a better understanding of hydrological extremes in Africa. Interaction between the regional circulation around the tropical Atlantic and convective patterns over the adjacent continents is the subject of this paper.

The tropical Atlantic Ocean and its overlying atmosphere contain many similarities with the equatorial Pacific in terms of air-sea coupling processes. Although warm events similar to El Niño occur in the Atlantic, it is a narrower ocean basin and the continental influences of South America and Africa are more apparent. The asymmetry of the African landmass with respect to the adjacent ocean basin induces a north-south temperature gradient and a monsoon regime over the Gulf of Guinea. To the west, deep convection is confined to a narrow strip that spans the Atlantic Ocean with a northward tilt toward Africa (Servain et al. 1998). The inter-tropical convergence zone (ITCZ) over the east Atlantic experiences a seasonal migration, from 14°N in August to the equator in March. This region of moisture flux convergence and latent heating overlies higher sea surface temperature (SST). South of the equator southeasterly trades are strong and steady. An equatorial cold tongue coupled with coastal upwelled water induces stratiform convection there. In the Gulf of Guinea winds are more meridional and rotate clockwise becoming more westerly over Africa, in the process modulating inflow to continental rainfall regimes. Most of the tropical Atlantic gains heat radiatively and evaporation losses are found to be low (Hastenrath and Lamb 1978). Cyclonic wind stress west of Angola produces an uplifted thermocline, which is sensitive to ocean-atmosphere coupling processes (Jury et al. 2000).

Studies of inter-annual climate variability have revealed two Atlantic modes: an equatorial ENSO-type every 2 to 5 years; and opposing sea surface temperature (SST) anomalies in northern and southern subtropics with a more decadal rhythm. Basin-scale winds and associated equatorial waves play a significant role in the generation of SST anomalies and coherent atmospheric responses and impacts (Nicholson and Entekhabi 1987; Servain 1991; Zebiak 1993; D'Abreton and Lindesay 1993; Curtis and Hastenrath 1995; Mehta and Delworth 1995; Huang et al. 1995; Tourre et al. 1998). Interannual variability is found to be weak and unstable compared with the tropical Pacific. ENSO in the Atlantic signals may be identified through shifts of the ITCZ and associated wind shear. Tourre and White (1995) and Delecluse *et al.* (1994) indicate that ENSO coupling in the tropical Atlantic is part of a global perturbation, which can explain a significant portion of African rainfall variability (Hastenrath, 1990; Ropelewski and Halpert, 1987). It is the intention of this paper to add to this research on linkages between African climate and the tropical Atlantic.

In the North Atlantic, the atmospheric circulation is dominated by low frequency adjustments of pressure known as the North Atlantic Oscillation (Lamb and Pepler 1987; Deser and Blackmon 1993; Kushnir 1994; Hurrell 1995). Alternating bands of high and low pressure and related wind stress anomalies extend from the mid-latitudes through the Azores High to the tropical Atlantic; and modulate the latitudinal disposition of rainfall over Africa (Houghton and Tourre 1992; Enfield and Mayer 1997; Servain et al. 1998; Lamb 1978; Hirst and Hastenrath 1983; Folland et al., 1986; Lough, 1986; Lamb and Pepler, 1987; Wagner and daSilva, 1994; Janicot et al., 1996; Jury 1997, Ward, 1998). A question to be considered in this study is - How do circulation patterns over the tropical Atlantic produce widespread convective anomalies over Africa?

Observational studies using composites of extreme rainfall seasons in West Africa have revealed a consistent N-S dipole structure in SST (Hastenrath and Heller, 1977; Moura and Shukla, 1981; Wolter 1989). Servain's (1991) dipole index showed significant correlation with regional precipitation in South America and Africa. In addition to the meridional displacement of the ITCZ, the stability of low level air affects precipitation well north of the Guinea coast (Fontaine *et al.*, 1995, Eltahir and Gong 1996) where west African rivers (the Senegal and Niger) are fed.

The Nile River flow has been extensively studied and linked with the global ENSO (Quinn 1992, Eltahir 1996), as defined by Pacific SST and the southern oscillation index (SOI) of zonal pressure. The correlation between the Nile flow and the Pacific Nino3 SST index in the period 1871-1997 is -0.54 at zero lag (Eltahir and Wang, 1999). Warming in the equatorial eastern Pacific causes an indirect circulation and sinking motion over the source of the Nile. Less rain falls over Ethiopia in the June-October season leading into an El Nino event. This Nile - ENSO association, first outlined by Bliss (1925) in the context of the southern oscillation, is unstable at times yet offers predictive potential. If many of the other rivers in Africa are correlated with the Nile and with each other, then understanding ENSO responses across the oceans near Africa would enable the application of widespread mitigation strategies. The known

response of the tropical Atlantic to ENSO (Saravanan and Chang 2000) is likely to create opposing climatic conditions over parts of South America, so this hypothesis is tested with the results presented here.

Data and methods

To understand the inter-annual variability of river flows across Africa; annual streamflow data were obtained for a number of rivers, including:

Blue Nile, tributary at Roseris, Sudan, draining the Ethiopian highlands,

White Nile, outflows at Jinja, Uganda from Lake Victoria,

Niger at Koulikoro, Mali, draining Guinea,

Senegal at Bakel, draining eastern Senegal / western Mali

Congo at Brazzaville, draining the northern and central basin,

Zambezi at Victoria Falls, draining western Zambia,

Orange above Gariep dam, draining the Lesotho highlands

Malawi lake inflows.

The data are based on quality-checked hydrographic records, naturalized for known anthropogenic effects (eg. dams built), and published in scientific reports. The time series were available from 1950-1995 as cumulative streamflow in cubic kilometers per year. In the case of Lake Malawi, changes in its level from the lowest to the highest point of the rainy season were obtained. Eltahir (1996) and Farquharson and Sutcliffe (1998) have analysed the seasonal cycle using monthly records. Southern Africa streamflow increases from January to April. Northern rivers exhibit highest flows from July to October. Annual streamflow data are assumed to represent the cumulative seasonal behaviour, and generally exhibit close agreement with catchment rainfall, with a 1-2 month lag in most cases. The hydrographic data, except for the flows from Lakes Victoria and Malawi, contained near-linear trends averaging -1% per annum in the 1950-1995 period. These could be attributed to multi-decadal oscillations in rainfall and to agricultural use and human consumption. To investigate year-to-year variability a more stationary record is necessary, so the average downtrend was removed. The annual records were analysed for auto-correlation and Pearson's product cross-correlations were calculated over the 45 year period. Finally, an index of African water resource variability was constructed from the five time series exhibiting significant cross-correlations. To support the hypothesis of opposing hydrological behaviour in South America, streamflow data for the Amazon and Parana Rivers are compared using similar statistical methods.

To establish climatic factors governing fluctuations in continental-averaged streamflow, National Centre for Environmental Prediction (NCEP) reanalysis data were consulted. This data set provides monthly averages of numerous atmospheric fields from 1958 to present. The observations are model-reconstructed as described by Kalnay et al. (1996). Here use is made of winds at three levels: surface, 3 km and 12 km, estimates of convective activity from outgoing longwave radiation, and two indicators of circulation – the streamfunction (rotational flow) and velocity potential (divergent flow). Observational densities vary through the record and may influence the result. Surface data inputs increased over most of Africa after 1958, however over

West Africa data densities increased significantly after 1967. Hence some of the earlier wet years may be less reliable. Oceanic influences are characterised by SST. Ship data densities were highest over the tropical Atlantic in the period 1968 to 1988. Although radiosonde profile inputs have been consistent through the period, aircraft and satellite wind data increased after 1978 and 1988 respectively.

To describe climate teleconnections affecting African river flows, a hemispheric scale domain of analysis is utilized and gridded data are averaged over annual or half-yearly periods, following tests to determine stability of the pattern. Environmental conditions for the five years with highest river flows: 1961, 1962, 1968, 1977, 1978 are contrasted with five years with lowest flows: 1971, 1972, 1982, 1983, 1991 by subtraction of the low-flow composite field from the high-flow field. The aim is to place hydrological events over Africa into a regional context, and to consider what climatic signals are present. The intra-composite consistency is evaluated for key areas and biases are identified. The low flow years occur about a decade later than high flow years, during which time the low-frequency Atlantic SST dipole inhibited West African rainfall. Hence the interaction of mixed low frequency climate modes may be assessed in the composite. It is pointed out that the western Pacific is omitted in the illustrations, as environmental differences there are small and apparently inconsequential.

Results

Temporal analysis of river flows

Table 2-1 provides details of trend, persistence and association. Many rivers still have considerable downward trends after removal of the mean. The Niger is amongst the most desiccated since 1950, followed by the Senegal. Sahel rainfall corroborates the drying trend across West Africa over the four decades considered here. The Zambezi exhibits a drying trend, however catchment rainfall is quite stationary. The auto-correlation at one year lag, as a measure of persistence, suggests that equatorial water resources are least variable. The White Nile (78%) is followed by the Congo (61%) and experience bimodal rainy seasons. The Niger, Senegal and Zambezi rivers are swept by unimodal rainy seasons controlled by the latitude of inter-tropical convergence. Auto-correlation is in the range 42% to 53%, the catchments lie west of 20°E, and rainfall is more influenced by the tropical Atlantic. Further east, the Orange and Blue Nile rivers and Lake Malawi exhibit higher frequency variability, presumably of ENSO and biennial type contributed from the Indian Ocean. The residual persistence (AC+1) in the hydrological time series requires that the degrees of freedom be deflated by a factor of two.

Spectral characteristics of annual river flows over the period 1950-1995 are as follows: Blue Nile, 2.7 year cycle dominant, secondary cycles at 6.6 and 15.3 years, Congo, 6.6 and 15.3 year cycles present, quasi-biennial cycle absent, Orange (in the south), 15.3 cycle present, quasi-biennial cycle at 2.3 years, Zambezi, most spectral energy around 5.6 years, White Nile (Lake Victoria outflow), 'step' increase in 1962 disturbs cyclic analysis, Niger and Senegal, multi-decadal trends dominant; Malawi inflow, spectral energy at 7.7 and 5.6 years, quasi-biennial at 2.4 years. When all the cross-correlated rivers are combined, spectral energy is strongest at 6.6 years, whilst a secondary cycle is present at 2.4 years. Multi-decadal trends give rise to an

artificial cycle near the record length (46 years). The 6.6 year cycle is consistent with low-frequency ENSO variability, whilst the 2.4 year cycle may be modulated by the quasi-biennial oscillation of stratospheric momentum.

Cross-correlations are high for a number of rivers, but lower for the Orange, Senegal and White Nile. The first two are at the poleward edges of the Africa's rainy belt. Much of East Africa, which experiences a dry boreal summer, is known to receive surplus rainfall during ENSO warm phase (Ogallo et al. 1988; Kabanda 1995), hence the generally weaker relationships for the White Nile (Lake Victoria). Cross-correlations between the Zambezi, Congo, Blue Nile, Niger and Malawi flows are sufficient ($p < .05$) to justify combining their individual standardized departures into a single African river index (fig 3-1), which is geographically balanced: with two south, one central and two northern rivers. The highest year on record is 1961 (Lake Victoria rose ~ 2 m, yet ENSO amplitude was minimal). Other high flow years are of comparable magnitude. Low flow years include the 1983 El Nino event, and the years leading into the El Ninos of 1973 and 1992. The cross-correlations listed in table 2-1 are calculated within the calendar year, eg. southern flows from January to April are compared with northern flows from July to October. Calculated the other way, with the northern rivers leading by 6 months, cross-correlations are of similar magnitude. Hence the climatic forcing contains such memory that both austral and boreal summers are similarly affected, and meridional or seasonal propagation is not a strong concern.

Composite climatic structure

The NCEP reanalysis data for composite high and low flow years identify the large-scale ocean and atmospheric conditions necessary for the development of extreme hydrological events across Africa. As mentioned earlier, sensitivity tests with different combinations of rivers listed in table 2-1 and years (6 month lead/lag), gave essentially similar results. SST difference fields for the 1st and 2nd half of the composite year are shown in figure 2-2. In the January to June period when southern rivers are flowing most strongly, SST differences (in high flow years) indicate below normal temperatures off the coasts of Peru and Ecuador. This oceanic pattern is consistent with La Nina conditions in the eastern equatorial Pacific. SST differences are also negative in the sub-tropical South Atlantic and in the tropical western Indian Ocean. The sub-tropical north Atlantic is warmer than usual and creates a dipole pattern known to anticipate good rains across the Sahel.

In the July to December period La Nina conditions persist and strengthen in the eastern Pacific and west Indian Ocean. At this time of the year, the northern water resources are replenished. Although many of the oceanic features are persistent, considerable warming occurs in the tropical South Atlantic. An equatorial plume of positive SST differences spreads west from Gabon and Angola with respect to high flow years. Warming is also found around the perimeter of the South Atlantic high pressure cell along 35°S. These changes in the marine environment are coupled to an atmospheric circulation response.

Surface wind differences are illustrated in fig 2-3 for the composite calendar year. Across most of the North Atlantic, westerly winds are evident and exhibit axes of significant differences

near 35°N and over the equatorial Atlantic. The flow rotates cyclonically over West Africa during high flow years, bringing Guinea monsoon air northward into the Sahelian zone. There is a circulation response in the Indian Ocean, fueling convective activity over the southern African catchments. Easterly wind differences from the equatorial South Indian Ocean are drawn toward Africa along 10°S and interact with poleward flowing monsoon air across the eastern highlands and Zambezi Valley. The Indian easterlies (Atlantic westerlies) overlie lower (higher) SST, suggesting that evaporative fluxes and upwelling dynamics sustain the oceanic features.

Wind differences at the 700 hPa level exhibit a more coherent pattern coupled with ENSO phase. Over the eastern Pacific, enhanced easterlies are present in the composite circulation pattern. These provide atmospheric momentum to sustain the equatorial upwelling found in the SST difference map. In the tropical Atlantic a singular axis of westerly wind differences is found along the Guinea coast. The anomalous flow interacts with the African easterly jet associated with convective wave trains across the Sahel (Thorncroft 1995), providing additional cyclonic vorticity in rainy years. The two axes of flow differences align on 5°S in the Pacific and on 5°N in the Atlantic, as the continental asymmetry dictates. Low level divergence is inferred across South America. Over the sub-tropical South Atlantic, cyclonic circulations represent a weakening of the high pressure cell associated with the SST warming trend. Descending (ascending) motions occur at the western (eastern) end of the tropical Atlantic wind axis, in this composite scenario.

Upper level wind differences (fig 2-4) are dominated by enhanced easterly flow over the tropical Atlantic (10°S-20°N, 0-60°W) which bifurcate over Africa into two sub-tropical axes. The northern axis lies along 20°N and supports the tropical easterly jet emanating from India in the boreal summer, whilst the southern axis lies along 15°S. In the mid-latitudes of the north Atlantic and over South Africa, upper wind differences are westerly. The circulation creates a 'C'-shaped streamfunction (rotational circulation) pattern extending from the western tropical Atlantic symmetrically across northern and southern Africa.

The upper level velocity potential pattern (fig 2-5) identifying the divergent circulation illustrates two centres of action over Africa (10°N, 30°E) and South American (10°S, 60°W). During high flow years the upper divergent cell is located over Africa, below which corresponding ascending motion and convection occur. In contrast, upper convergence, descending motion and drought are indicated for South America from Peru to Paraguay. The result suggests that extreme hydrological years are characterised by opposing climate anomalies over the two continents. This is supported by outgoing longwave radiation (OLR) differences illustrating increased convection over much of Africa concentrated in two axes along 10°N and 30°E. A NW-SE band of reduced convection is found over southwestern Brazil. OLR differences along the north coast of South America are of the same sign as over Africa.

Elsewhere across the globe (eg. the western Pacific warm pool), oceanic heat and atmospheric circulation differences in extreme hydrological years are insignificant. Hence it is suggested that an east Pacific La Nina coupled with a warm tropical Atlantic gives rise to a near-

zonal overturning circulation which alternatively benefits sub-Saharan Africa at the expense of sub-Amazonian South America.

Intra-composite anomalies for key areas

The consistency of environmental anomalies is assessed for 10 x 10 degree key areas: SST in the E. Pacific (equator, 95°W) and N. Atlantic (25°N,25°W), zonal wind at 700 and 250 hPa over the tropical Atlantic (2°N,20°W), and the upper velocity potential over Africa (10°N,30°E) and S. America (10°S,60°W). It is found that east Pacific SST in the three warm years of 1972, 1982, 1983 most influence the overall pattern, whilst the north Atlantic differences are weak. For Atlantic winds, the first two years 1961 and 1962, and the 1983 El Nino make a large contribution. The upper velocity potential dipole is largely contributed by values in the 1960s when observations were sparse. Opposing anomalies for SST in the East Pacific and North Atlantic key areas are consistent and correspond with a tilted zonal wind pattern linking the Pacific ENSO and the Atlantic dipole. Other influential or inconsistent cases include: upper zonal winds in 1977 and 1978, and velocity potential over South America in 1971 and 1972. Although some biases exist, the intra-composite differences are adequate to justify interpretation of climatic structure for extreme hydrological years over continents bordering the tropical Atlantic.

Discussion

Regional ocean-atmosphere coupling has been related to African river flows. Interannual variability of the Nile, Congo, Niger, Zambezi, and Lake Malawi were found to be significantly cross-correlated ($p < .05$) over the period 1950-1995, following removal of the mean trend for all rivers. A combined African river flow index was formulated to analyse climatic factors governing extreme years and composites of NCEP reanalysis fields for high (1961, 1962, 1968, 1977, 1978) and low (1971, 1972, 1982, 1983, 1991) flow years were compared. SST differences with respect to high flow years indicated: sustained La Nina conditions in the east Pacific, an inter-hemispheric dipole in the Atlantic (warm – north), below normal SST in the west Indian Ocean, warming of the equatorial east Atlantic, (consistent with its opposing response to Indo-Pacific ENSO), and an inactive west Pacific warm pool.

Regarding the atmospheric circulation, upper wind differences were easterly and symmetrical about the equator. Such a pattern may explain why inter-annual variability of water resources south of the equator are correlated with those of the north at leads and lags of six months. Westerly wind differences were found over the tropical Atlantic from the surface to 600 hPa, particularly along the Guinea coast during high flow years. A zonal overturning circulation is revealed in the NCEP reanalysis data.

Composite difference fields for OLR and upper velocity potential demonstrated two distinct centers of action on either side of the tropical Atlantic. Convection over Africa (along two axes: 10°N, 30°E) was found to be offset by sinking motions over South America (NW-slanted axis: 10°S, 60°W). It is not clear how much of the signal may be attributable to observational trends, or to a real decadal rhythm in the divergent atmospheric flow.

To test the assumption of convective polarity between the two continents, annual river flow data for South America were obtained (Amerasekera et al. 1997). Tropical Amazon River flows are uncorrelated with the African river index ($r = +0.01$). The sub-tropical Parana River exhibits a gradual rising trend and is significantly negatively correlated ($r = -0.31$), more so with the Niger River ($r = -0.42$). It is concluded that convective polarity in this climate mode applies to South America west and south of the Amazon catchment, in agreement with Amerasekera et al. (1997). Further research employing longer records could evaluate ENSO influence by stratifying cases accordingly.

In this study widespread hydrological anomalies over the adjacent continents of Africa and South America were found to be sensitive to coupling between the zonal circulation over the tropical Atlantic, the global ENSO phase and the Atlantic dipole. These geophysical features interact to delay the change of ENSO phase, creating a 'two-years-at-a-time' hydrological impact. Under these conditions the wave one pattern in the global divergent circulation shifts, and centres of opposing action 'close up' over South America and Africa as shown schematically in 3-6. The argument is simple: climatic anomalies over the two continents are governed by ENSO-regulated coupling of the Pacific Ocean and the Atlantic Walker cell. This interaction affects the sustainability of food and water resources and the economic well-being of over one billion people. Prediction and mitigation of these hydrological events is more likely given the widened scope of scientific activities in the World Climate Research Program in the coming decade.

References

- Amerasekera, K N, Lee, R F, Williams, E R, Eltahir, E A B, 1997, ENSO and the natural variability in the flow of tropical rivers, *J Hydrology*, 200, 24-39
- Bliss, E W, 1925, The Nile flood and world weather, *Mem. Roy. Meteor. Soc.*, 4, 36, 53-84.
- Curtis, S and Hastenrath, S, 1995, Forcing of anomalous sea surface temperature evolution in the tropical Atlantic during Pacific warm events, *J Geophys Res.* 100, 15835-15847.
- Delécluse, P., J. Servain, C. Levy, K. Arpe, and L. Bengtsson, 1994: On the connection between the 1984 Atlantic warm event and the 1982-83 ENSO. *Tellus*, 46A, 448-464.
- D'Abreton, P.C. and Lindesay, J.A. 1993: Water vapour transport over southern Africa during wet and dry early and late summer months. *International Journal of Climatology* 13, 151-170.
- Deser, C and Blackmon, M L, 1993, Surface climate variations over the North Atlantic during winter, 1900-1989. *J Climate* 6, 1743-1753.
- Eltahir, E A B, 1996, El Nino and the natural variability in the flow of the Nile River, *Water Resources Research*, 32, 131-137.
- Eltahir, E A B, and Gong, C, 1996, Dynamics of wet and dry years in West Africa, *J Climate*, 9, 1030-1042.
- Eltahir, E A B, and Wang, G, 1999, Nilometers, El Nino and climate variability, *Geophys Res Letters*, 26, 4, 489-492.

- Enfield, D B and Mayer, D A, 1997, Tropical Atlantic SST variability and ENSO, *J Geophys Res* 102, 929-945.
- Farquharson, F, and Sutcliffe, J V, 1998, Regional variations of African river flows, in *Water resources variability in Africa in the 20th century*, eds (E Servat, D Hughes, J-M Fritsch, M Hulme), Proc. Conf IAHS 252, 161-169.
- Folland, C.K., Palmer, T.N., and Parker, D.E., 1986: Sahel rainfall and worldwide sea temperatures, 1901-85. *Nature*, 320, 602-607.
- Fontaine, B., S. Janicot, and V. Moron, 1995: Rainfall anomaly patterns and wind field signals over West Africa in August (1958-1989). *J. Climate*, 8, 1503-1510.
- Hastenrath, S, and Lamb, P.J., 1978, Heat budget atlas of the tropical Atlantic and eastern Pacific Oceans, Univ Wisconsin Press 103 pp.
- Hastenrath, S., and L. Heller, 1977: Dynamics of climatic hazards in Northeast Brazil. *Quart. J. Roy. Meteor. Soc.*, 103, 77-92.
- Hastenrath, S., 1990: Decadal-scale changes of the circulation in the tropical Atlantic sector associated with Sahel drought. *Int. J. Climatology*, 10, 459-472.
- Hirst, A.C. and Hastenrath, S. 1983: Atmosphere-ocean mechanisms of climate anomalies in the Angola - tropical Atlantic sector. *J. Phys. Oceanogr.*, 13, 1146-1157.
- Houghton, R W and Tourre, Y, 1992, Characteristics of low frequency sea surface temperature fluctuations in the tropical Atlantic, *J Climate*, 5, 765-771.
- Huang, B., J.A. Carlton and J. Shukla, 1995: A numerical simulation of the variability in the Tropical Atlantic Ocean, 1980-88. *J. Phys. Oceanogr.*, 25, 835-854.
- Hurrell, J W, 1995, Decadal trends in the North Atlantic Oscillation: regional temperatures and precipitation, *Science*, 269, 676-679.
- Janicot, S., Moron, V. and Fontaine, B. 1996: Sahel droughts and ENSO dynamics. *Geophysical Research Letters* 23, 515-518.
- Jury, M R, 1997, Southeast Atlantic warm events: composite evolution and consequences for southern African climate, *S African J Marine Science*, 17, 21-28.
- Jury, M R, Mulenga, H, and Rautenbach, H, 2000, Tropical Atlantic variability and Indo-Pacific ENSO: statistical analysis and numerical simulation, *Global Atmos. Ocean System*, 7, 107-124.
- Kabanda, T A. 1995, Seasonal and intra-seasonal dynamics and precursors of rainfall over northern Tanzania, MSc thesis, Univ. Cape Town, 219 pp.
- Kalnay, E, et al., 1996, The NCEP/NCAR reanalysis 40-year project, *Bull. Amer. Meteor. Soc.*, 77, 437-471.
- Kushnir, Y, 1994, Interdecadal variations in the North Atlantic sea surface temperature and associated atmospheric conditions, *J Climate*, 7, 141-157.
- Lamb, P.J., 1978, Large-scale tropical Atlantic surface circulation patterns associated with Subsaharan weather anomalies. *Tellus*, A30, 240-251.
- Lamb, P.J. and Pepler, R.A., 1987: North Atlantic Oscillation: Concept and Application. *Bulletin of the American Meteorological Society*, 68, 1218-1225.

- Lough, J.M., 1986: Tropical Atlantic sea surface temperatures and rainfall variations in Subsaharan Africa. *Mon. Wea. Rev.*, 114, 561-570.
- Mehta, V M and Delworth, T, 1995, Decadal variability of the tropical Atlantic Ocean surface temperature in shipboard measurements and in global ocean-atmosphere model, *J Climate*, 8, 172-190.
- Moura, A. and J. Shukla, 1981: On the dynamics of droughts in northeast Brazil: observations, theory, and numerical experiments with a general circulation model. *J. Atmos. Sci.*, 38, 2653-2675.
- Nicholson, S.E., 1981: Rainfall and atmospheric circulation during drought periods and wetter years in West Africa. *Mon. Wea. Rev.*, 109, 2191-2208.
- Nicholson, S.E. and Entekhabi, D. 1987: Rainfall variability in equatorial and southern Africa: relationships with sea surface temperatures along the southwestern coast of Africa. *J Clim Appl Meteor*, 26, 561-578.
- Ogallo, L J, Janiowiak, J E, and Halpert, M S, 1988, Teleconnections between seasonal rainfall over east Africa and global sea surface temperature anomalies, *J Meteor Soc Japan*, 66, 6, 807-821.
- Quinn, W H, 1992, A study of southern oscillation –related climatic activity 622-1990 incorporating Nile river flood data, in *El Nino: Historical and Paleoclimate Aspects of the Southern Oscillation*, ed Diaz, H F, and Markgraf, V, 119-142.
- Ropelewski, C.F. and Halpert, M.S. 1987a: Precipitation patterns associated with El Niño/Southern Oscillation. *Monthly Weather Review*, 115, 1606-1626.
- Saravanan, R, and Chang, P, 2000, Interaction between tropical Atlantic variability and El Nino-Southern Oscillation, *J Climate*, 13, 2177-2194.
- Servain, J., 1991: Simple climatic indices for the tropical Atlantic Ocean and some applications. *J. Geophys. Res.*, 96, 15,137-15,146.
- Servain J., Wainer I., McCreary J. P., and Dessier A., 1998 : Relationship between the equatorial and meridional modes of climatic variability in the tropical Atlantic. *Geophysical Research Letters*.
- Servat, E., D. Hughes. J-M Fritsch, M. Hulme, eds., 1998, Regional variations of African river flows, in *Water resources variability in Africa in the 20th century*, I A H S, publication 252, 462 pp.
- Thorncroft, C.D., 1995: An idealized study of African easterly waves. 3, More realistic basic states. *Quart. J. Roy. Meteorol. Soc.*, 120, 983-1015.
- Tourre, Y. M., and W. B. White 1995: ENSO signals in global upper-ocean temperature. *J. Phys. Oceanogr.*, 25, 1317-1332.
- Tourre Y. M, B, Rajagopalan and Y Kushnir, 1998: Dominant patterns of climate variability in the Atlantic Ocean during the last century. In press *J. Climate*.
- Wagner, R.G., and A. da Silva, 1994: Surface conditions associated with anomalous rainfall in the Guinea coastal region. *Int. J. Climatol.*, 14, 179-199.

Ward, M.N., 1998: Diagnosis and short-lead time prediction of summer rainfall in tropical North Africa and interannual and multidecadal timescales. *J. Climate*, 11, 3167-3191.

Wolter, K. 1989: Modes of tropical circulation, Southern Oscillation, and Sahel rainfall anomalies. *J. Climate*, 2, 149-172.

Zebiak, S.E., 1993: Air-sea interaction in the equatorial Atlantic region. *J. Climate*, 8, 1567-1586.

Table 2-1 - statistics for annual river series 1950-1995

River	RT	Cross-correlation (%)							
		AC+1	wNile	Niger	Cong	Zamb	Oran	Malw	Seng
<u>Blue Nile</u>	0	9	-4	36	28	33	27	34	47
White Nile	0	78		1	60	35	-6	26	0
<u>Niger</u>	-2.0	49			32	36	-11	7	57
<u>Congo</u>	-0.5	61				56	5	40	22
<u>Zambezi</u>	-1.1	42					19	54	25
Orange	0	19						0	23
<u>Malawi</u>	0	1							-4
Senegal	-1.5	53							

underlined → within index
 22 degrees of freedom, RT = residual trend % pa., AC+1 = auto-correlation in year+1

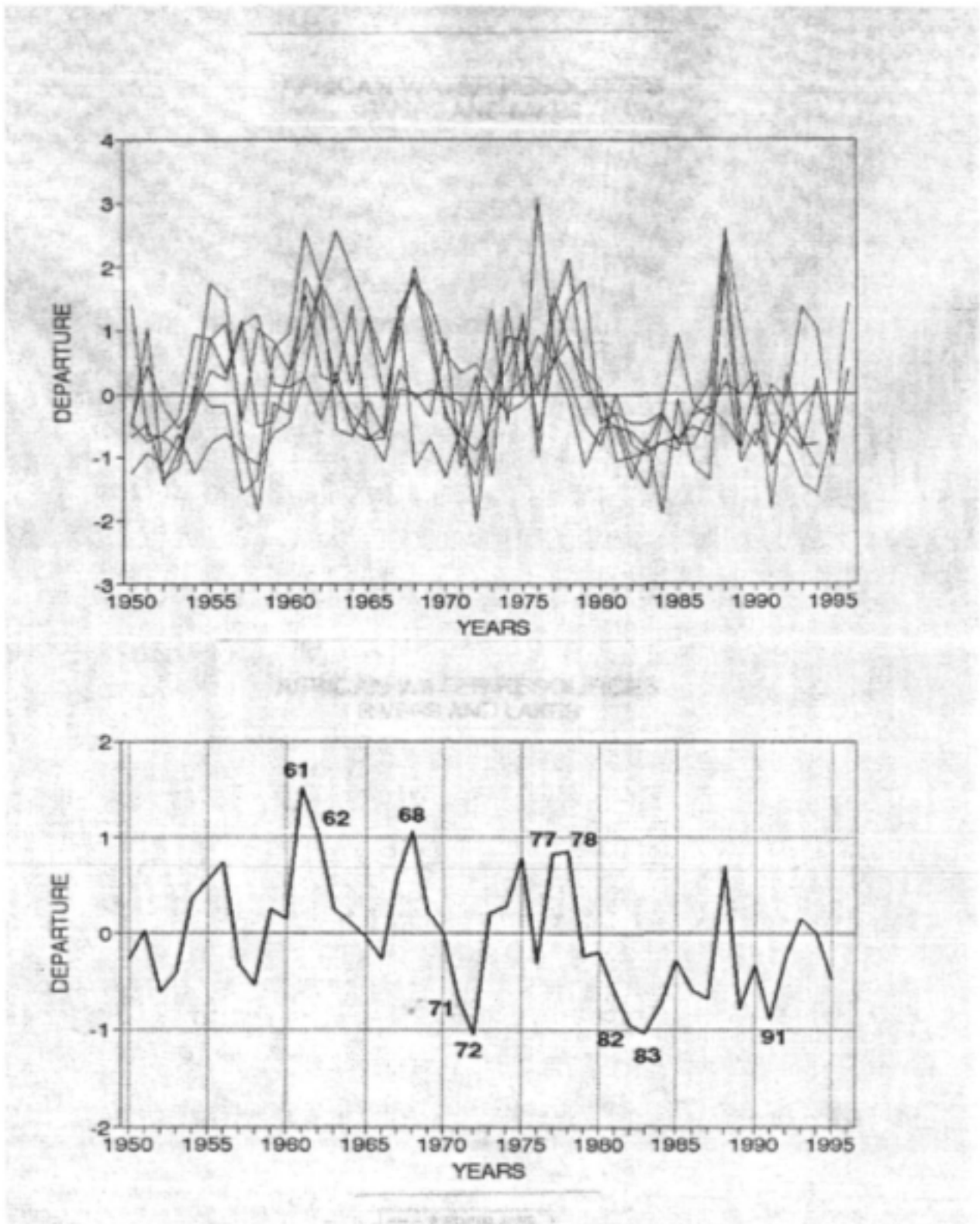


Fig 2-1 – Individual time series (a) of annual flows for the five rivers included in the all-Africa index (b). Identified years are incorporated into the high and low flow composites.

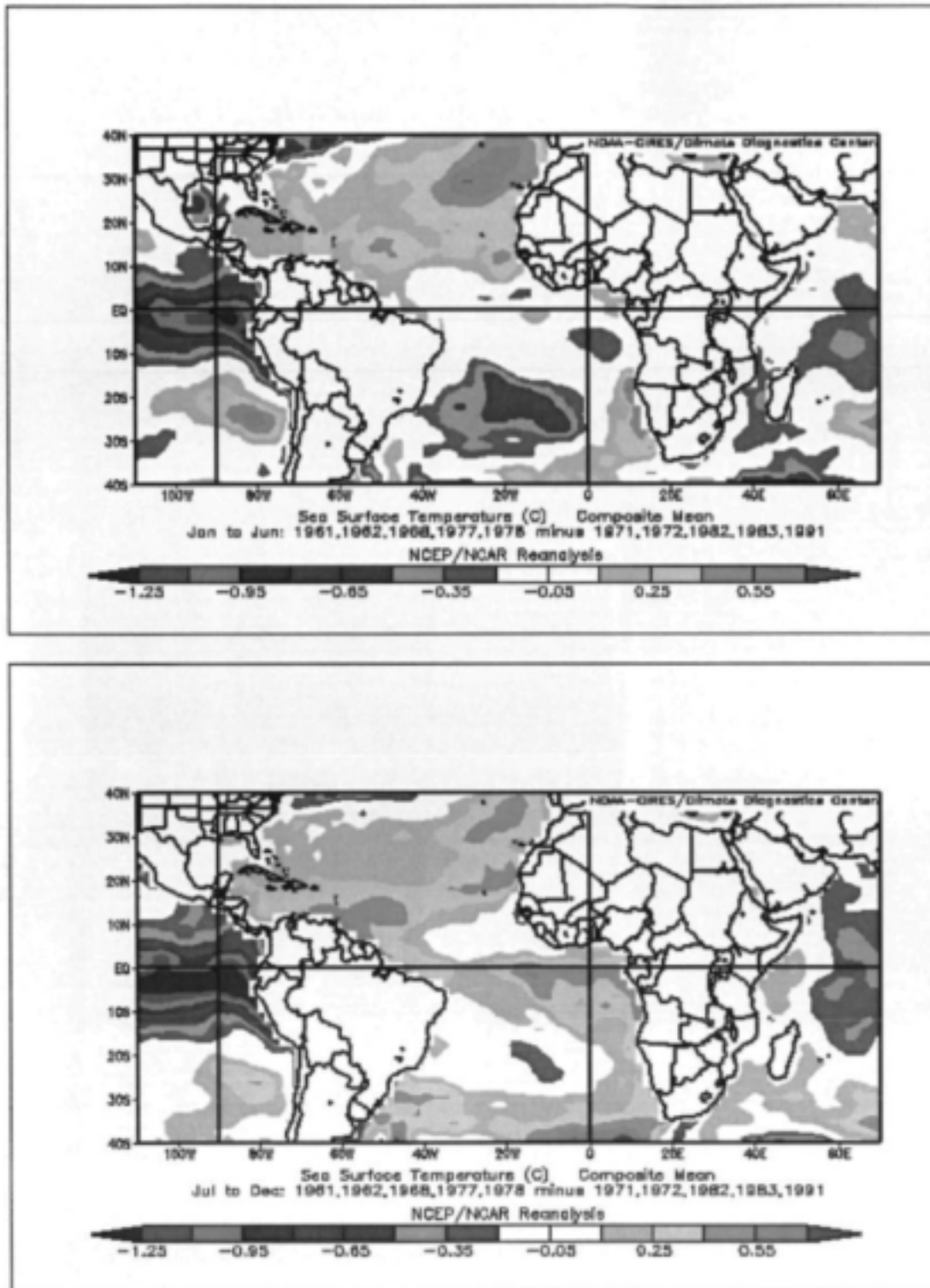


Figure 2-2 – SST differences for the 1st (a) and 2nd (b) half of the composite year. Colour bar lower. Patterns are an average of high flow years minus low flow years.

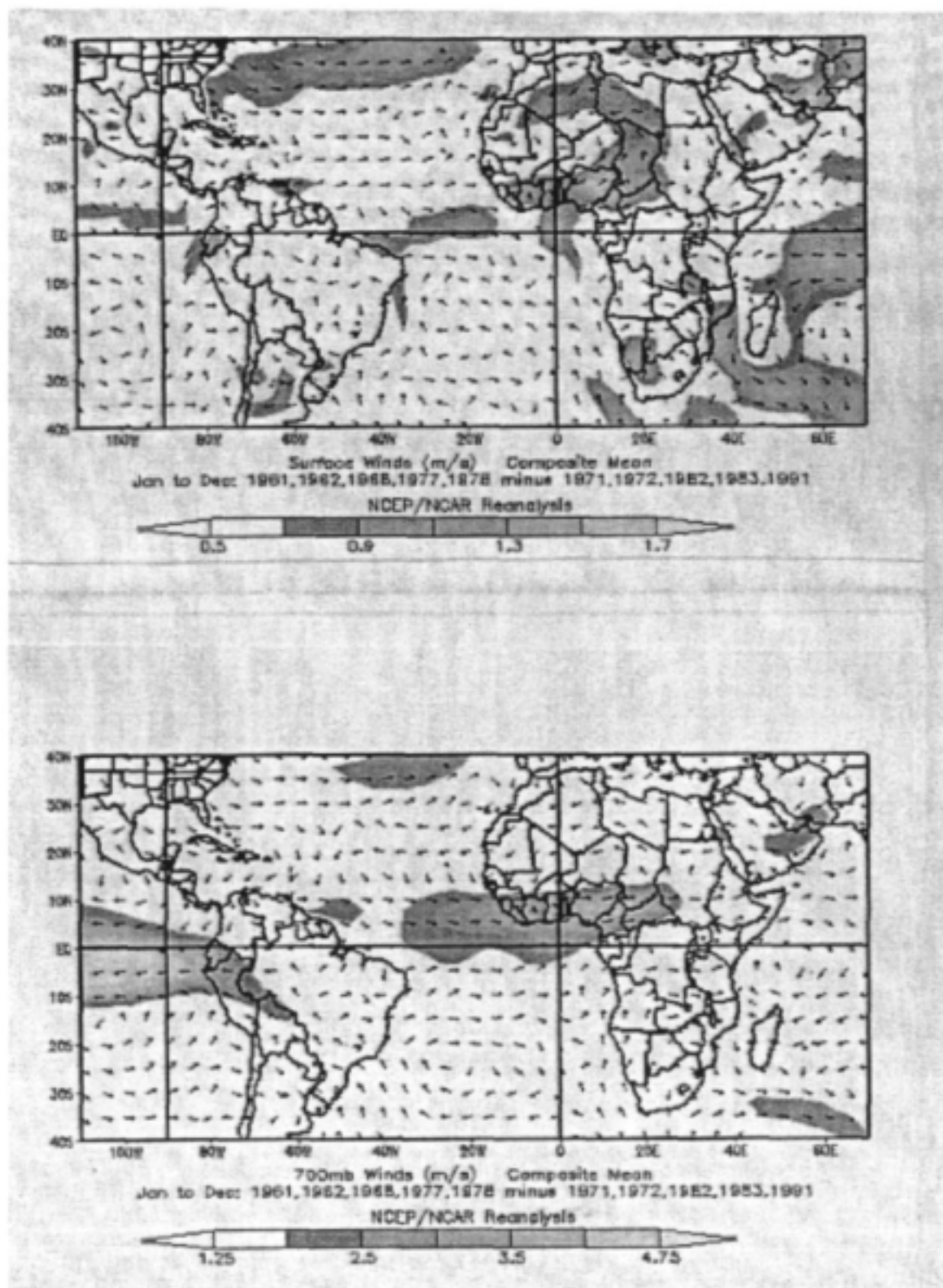


Figure 2-3 – Surface (a) and 700 hPa level (b) vector wind differences for the composite year. Shading refers to areas where circulation differences are significant.

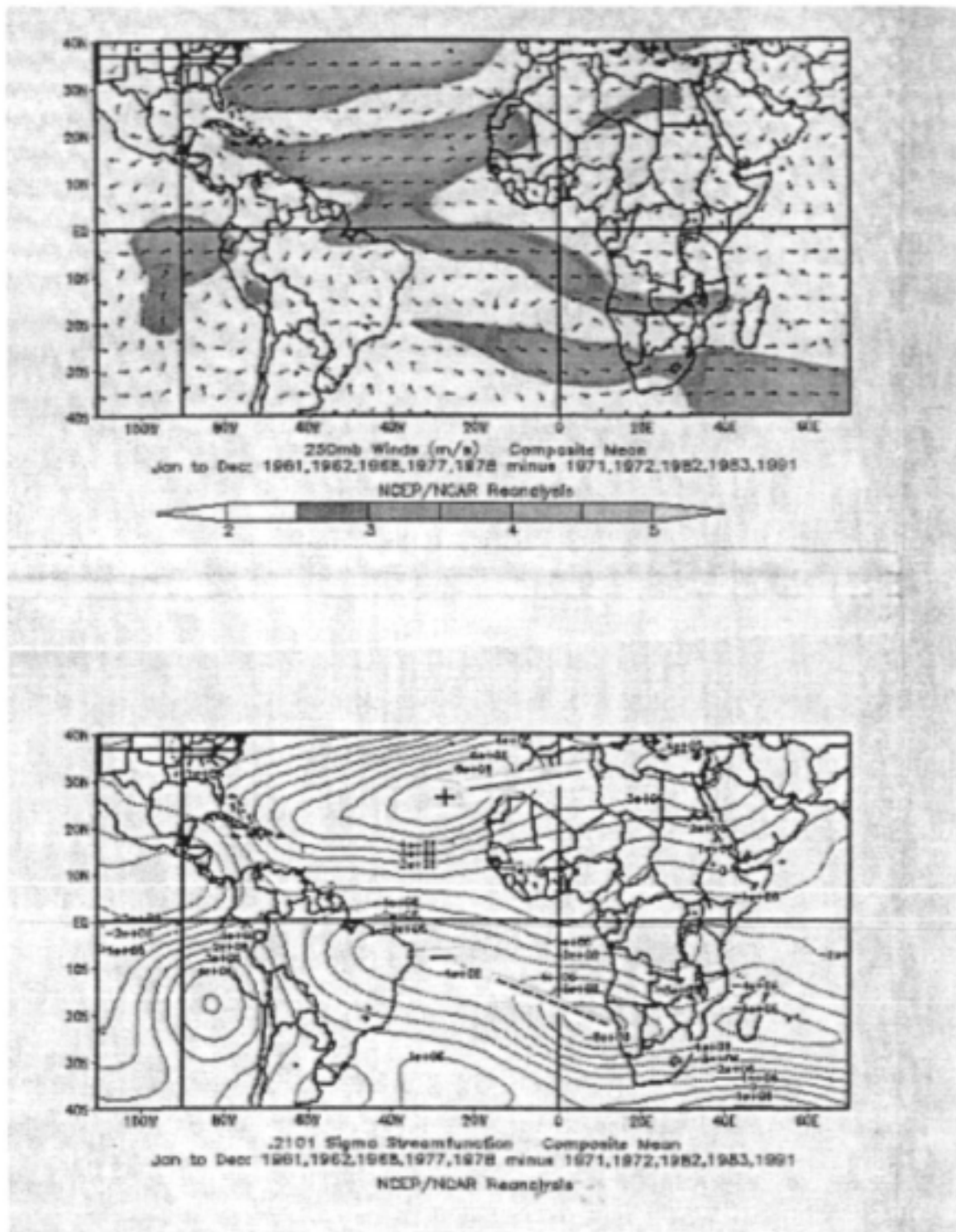


Figure 2-4 – 250 hPa level vector wind differences for the composite year (a), where shaded areas are significant. Upper (~200 hPa) streamfunction composite differences (b), describing the rotational flow contribution.

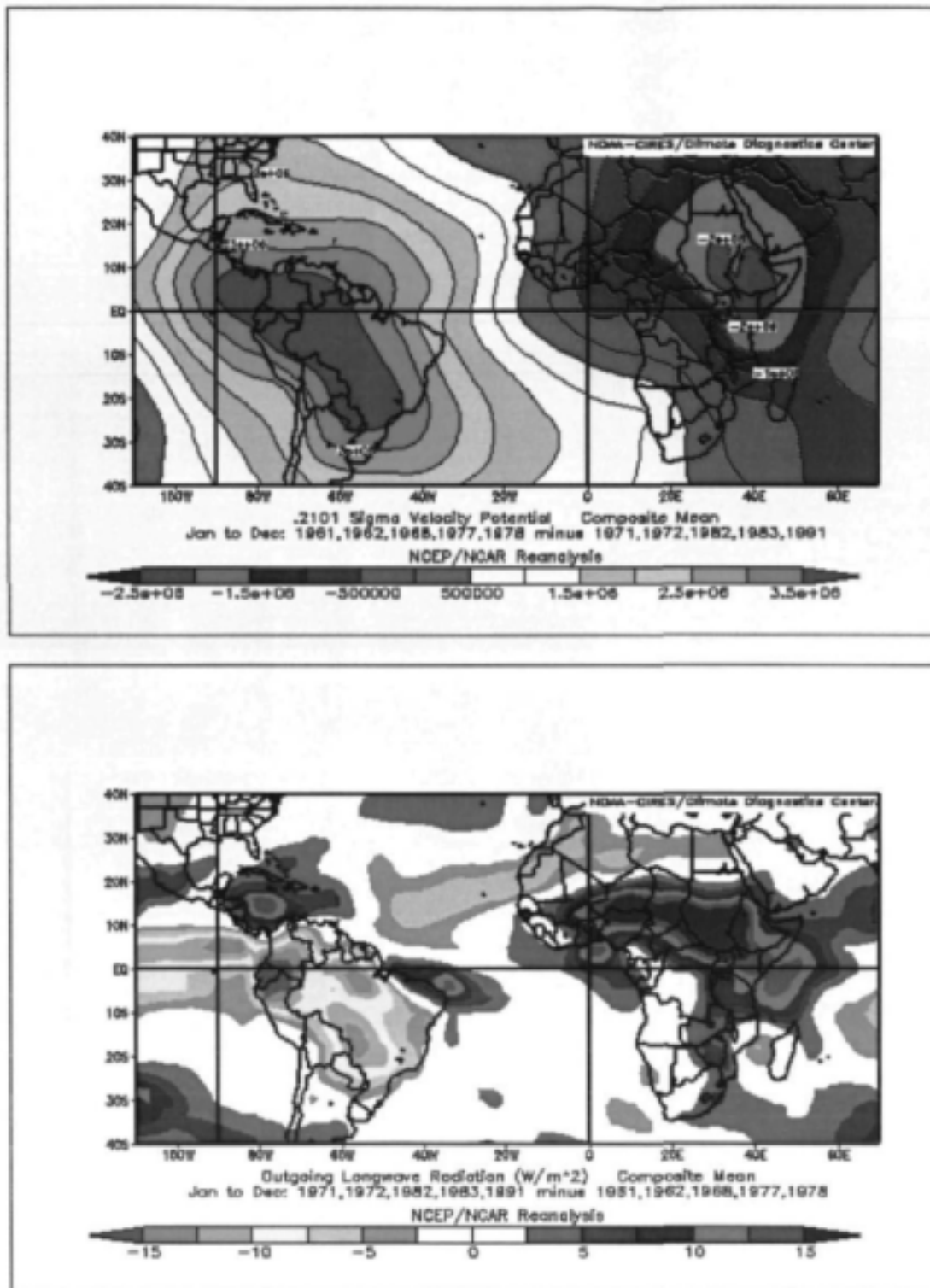


Figure 2-5 – Upper (~200 hPa) velocity potential differences (a) and OLR (b) for the composite year, showing centres of opposing action over Africa and South American. Blue shades = enhanced upper outflow and convection, yellow /orange = subsident dry weather.

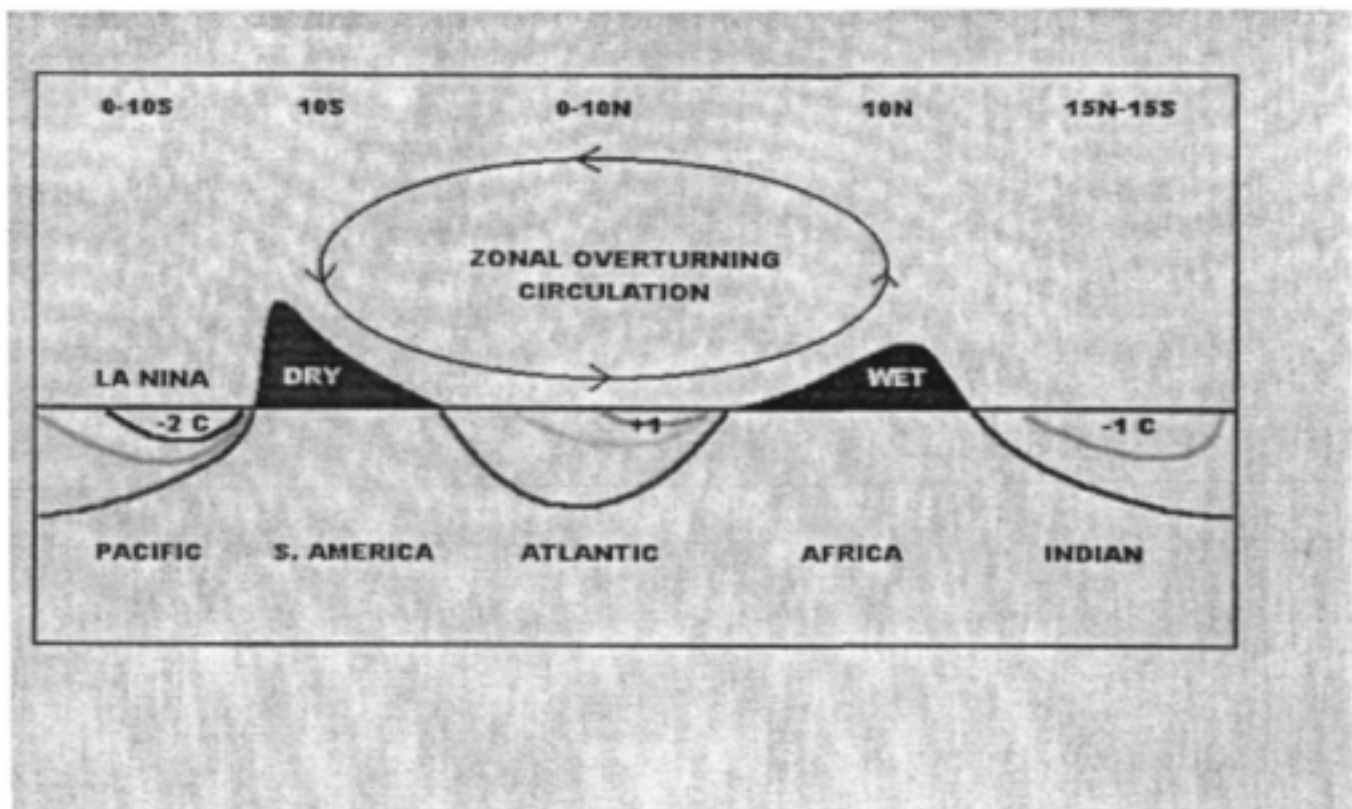


Figure 2-6 – Schematic diagram showing the oceanic anomalies and atmospheric circulation patterns relevant to years with high river flow across Africa.

Chapter 3 – Analysis of long-term data sets – predictability in historical context

In earlier research (Jury et al 1997) used a relatively short period of record in the formulation of predictive models. In this chapter we consider two century-long data sets and assess their temporal behaviour using sophisticated wavelet techniques. This extends the earlier work by placing the local climate variability into historical context.

Introduction

Recent studies of the African climate system suggest that some of the year-to-year variability may be widespread (Jury, 2000a). Ocean-atmosphere coupling over the tropical Atlantic, in response to El Niño (EN) phase, was found to induce common fluctuations of African rivers: the Nile, Congo, Niger and Zambezi. During high flow years, the upper level circulation becomes easterly over Africa, and dry conditions arise over South America (Amarasekara et al. 1997). Here the temporal nature of African climate variability is further explored using long-term data sets in northern (24°N) and southern (30°S) Africa.

Africa's southeastern coast has a dense vegetation cover sustained by intermittent rains produced when humid air is drawn upslope from the nearby warm Agulhas Current (DeJager and Schulze 1977, Walker 1990, Jury et al 1993). Mean annual rainfall is about 1 m at Durban – a large urban centre in South Africa requiring $\sim 10^9$ m³ pa. of water for consumption. Summer rains are produced when anticyclones ridge eastward along the coast, bringing southerly (onshore) winds (Diab et al 1991; Miron and Tyson 1984). Sea surface temperatures east of Durban act as climatic determinants and exhibit quasi-biennial (QB) frequencies Walker (1990).

Some 5000 km to the north of Durban lies the Nile River, draining the Ethiopian highlands (80%) and Sudan (20%). The Nile River flow has been extensively studied and linked with the global El Niño phenomenon (Bliss, 1925; Quinn 1992; Eltahir 1996). The correlation between the Nile flow and the Pacific Niño 3 sea surface temperature (SST) index in the period 1871-1997 is -0.54 at zero lag (Eltahir and Wang, 1999). Warming in the equatorial eastern Pacific causes an indirect circulation and sinking motion over much of Africa, including the source of the Nile, suggesting that climatic influences are widespread.

In this study, we analyse long-term climate records for: intra-seasonal to decadal variability, extreme events and cross-spectral character, and relationships with remote climatic indices. Our aim is to establish the historical context of climate variability in Africa, particularly its temporal character at two select points with long-term records.

Data and Methods

Monthly rainfall data were obtained from the S A Weather Bureau for the period 1872 to 1999 – 128 years at the Durban Botanical Gardens (30°S, 31°E) located near the coast at an elevation of 91 m. Comparisons of monthly rainfall with adjacent stations yielded good agreement (< 10% departure each month) in periods of data overlap. Hence the long-term record could be accepted as accurate. Many features of the Durban data are representative of a wider region according to principal component analysis (PCA) of summer rainfall anomaly maps.

Although much of the rainfall is convective, the Durban results may be applicable to the eastern half of South Africa, encompassing the maize belt.

Monthly rainfall data were subjected to a contingency analysis to identify cases > 200 mm. A more detailed analysis of the temporal character of the Durban rainfall was achieved using the wavelet transform method described below. In addition, streamflow data for the Nile River in the period 1871-1997 was provided by Eltahir and Wang (1999). To characterise the inter-annual variability of the Nile River, monthly streamflow data were obtained for a number of gauges along the river, including: Roseris, Ethiopia, 1914-1989 located at 11°N,35°E; Dongola, Sudan 1912-1973 located at 19°N,31°E, and Aswan, Egypt 1871-1997 (adjusted after 1964, at 24°N,33°E).

The data are based on quality-checked hydrographic records, naturalized for known anthropogenic effects (eg. dams built) based on estimated water use, and published in scientific reports. Following intercomparisons between gauges, peak flow values were retained and the cumulative naturalised flow was calculated for the July to November inflow season each year, to reconstruct the 127 year time series, following procedures adopted by Eltahir and Wang (1999). The time-frequency character of long-term climatic data is investigated using the Continuous Wavelet Transform (CWT) technique (Daubechies 1992, Lau and Weng 1995, Torrence and Compo 1997, Mallat 1998). The CWT is a mathematical tool which allows the decomposition of the signal $x(t)$ in terms of elementary contributions called wavelets, which can be thought of as a packet of sine waves of varying amplitude and wavelength. These wavelets are described from a single function ψ by translations and dilatations:

$$\psi_{b,a}(t) = \frac{1}{a} \psi\left(\frac{t-b}{a}\right) \quad (\text{eq.3-1})$$

where $a > 0$ is the dilatation (scale) parameter and b is the translation (position) parameter. As the CWT is used to both filter and analyse the data, we have normalized by $1/a$ (Delprat et al. 1992). The CWT of the signal $x(t)$ with the analysing wavelet ψ is the convolution of $x(t)$ with a set of dilated and translated wavelets:

$$W_x(b,a) = \frac{1}{a} \int_{-\infty}^{\infty} x(t) \psi^* \left(\frac{t-b}{a} \right) dt \quad (\text{eq.3-2})$$

where $*$ denotes the complex conjugate. The wavelet transform is continuous through variations imposed on a and b . The CWT expands the time series $x(t)$ into two-dimensional parameter space (b,a) and yields a measure of the relative amplitude of local spectral activity at scale a and time b . The choice of wavelet ψ depends on the signal to be analysed. In our case, the signal is relatively well defined in frequency, so we select a wavelet that is localised in frequency space – the continuous complex wavelet devised by Morlet (1983). This wavelet is defined by:

$$\psi(t) = \pi^{-1/4} e^{-t^2/2} e^{i\omega_0 t} \quad (\text{eq.3-3})$$

where $i = \sqrt{-1}$ and $\omega_0 = 5.4$. The wavelet is expressed in terms of modulus and phase, defined by the inverse of scale and frequency. The relation between the scale a and the frequency f is given by (Meyers et al., 1993):

$$f(a) = \frac{\omega(a)}{2\pi} = \frac{1}{4\pi} \left(\frac{\omega_0}{a} + \frac{\sqrt{2 + \omega_0^2}}{\omega_0} \right) \quad (\text{eq.3-4})$$

The wavelet can be interpreted as a bandpass linear filter of weight $1/a$ centered around $\omega = \omega_0/a$. This filter allows extraction of various components of the signal such as its local amplitude and phase in time-frequency space. The CWT is iterative: the original 1-D signal being transformed into a 2-D time-frequency image. Useful information can be extracted from the 'ridges' of the CWT. These ridges are representations of how well the dilated-translated wavelet coincides with the local frequency of the signal. The ridges are the sets of (b,a) for which the relation:

$$\frac{\partial \phi_{b,a}}{\partial b} = \frac{\omega_0}{a} \quad (\text{eq.3-5})$$

is satisfied and where $\phi_{b,a}$ is the phase of $W_x(b,a)$ and ω_0/a is the frequency of the dilated wavelet applied to the time series. This acts to filter out the annual cycle for monthly data records. In the case of the Nile River flow, we make use of annual records, so this is unnecessary.

We investigate relationships between Durban rainfall and two climatic indices over recent decades. A well-known index is the tropical Atlantic dipole (Servain, 1991). It is calculated from the difference between the SST anomaly over the northern tropical Atlantic (5° - 28° N) and over the southern part (5° N- 20° S). The dividing latitude of 5° N can be regarded as the position of the thermal equator and inter-tropical convergence zone (ITCZ). The tropical Atlantic SST dipole is known to couple with the Hadley cell and N – S excursions of the ITCZ over Africa. It exhibits a decadal rhythm. Another well-known climatic index is the Southern Oscillation (SOI, Walker and Bliss, 1932) which is formulated by subtracting the pressure anomaly of Darwin, Australia from that of Tahiti in the eastern Pacific Ocean. We compare a filtered version of the SOI with the Durban rainfall data.

The relationship between two series is investigated in time-frequency domain by computing their cross-wavelet spectrum. $x(t)$ is the low-frequency component of the rainfall series and $y(t)$ the low-frequency SOI. The cross-wavelet spectrum of the two series is then expressed as:

$$W_{xy}(b,a) = W_x(b,a)W_y^*(b,a) \quad (\text{eq.3-6})$$

where $W_x(b,a)$ and $W_y(b,a)$ are the CWT of $x(t)$ and $y(t)$ respectively and where * denotes the complex conjugate. The complex cross-wavelet coefficient $W_{xy}(b,a)$ may be expressed in terms of modulus and phase difference, according to: $x_1 x_2^* = a_1 a_2 e^{j(\theta_1 - \theta_2)}$, where phase is independent of amplitude.

Results

Temporal Variability

The raw time series $x(t)$ of the rainfall data at Durban is displayed in fig 3-1 and 3-2. The series is standardized and its CWT is computed from equation (2). Upward spikes refer to flood events, which are analysed independently. The modulus of the wavelet transform coefficient $W_x(a,b)$ is included for intra-seasonal and inter-annual periods. Largest amplitudes are found from 2 to 5 months – the typical length of rainy spells, around 12 months (the annual cycle) and between 2 to 4 years. Inter-annual amplitudes in the 2.3 – 4 year band are greatest around 1917, 1972, 1983 and 1998 appear to be related to El Niño (EN) events. There are times when a 4 – 5 year cycle is sustained (1930 – 1960), but for most of the historical record cyclical rhythms are short-lived. Decadal amplitudes with periods from 6 to 16 years are stronger from 1880 to 1900 and 1970 to 1995.

The variation of the modulus around 12 months corresponds to the amplitude modulation of the annual cycle. This ‘ridge’ exhibits some decadal variability (not shown). The correlation coefficient between the annual cycle and the series $x(t)$ is $r = 0.57$. So, the annual cycle extracted by the CWT explains 33 % of the rainfall variability. The low-frequency component is obtained by filtering the data in wavelet space. Inter-annual fluctuations account for 10 % of the rainfall variability.

A contingency analysis of flood events, defined as months with rainfall > 200 mm, was made. A bimodal distribution is evident with increased cases in November and March. These are known to be months when ‘cut-off lows’ disturb the stability of the sub-tropical jet stream, causing looping and diffluent patterns, and the undercutting of a continental low by an anticyclone in higher latitudes. The cut-off low is less likely to develop during mid-summer (January) when continental heating diverts the upper westerly flow. Cut-off lows can produce upslope rains near Durban, but the potential for floods depends on an adequate inflow of moisture from the SW Indian Ocean. The moist inflow is supported by the NE monsoon of the tropical west Indian Ocean from November to March. The combination of these two factors leads to the bimodal nature of flood events.

Relations with climatic indices

It is thought that part of the temporal variability in the Durban rainfall may be explained by large-scale climatic patterns governed by slowly varying SST conditions. Comparisons were made between the Atlantic SST dipole index in the period 1964 to 1998 to the amplitude of the annual cycle of the Durban rainfall. Good agreement is found between these two series, with the dipole index leading the rainfall. It can be deduced that the annual cycle is modulated by the meridional gradient of SST over the tropical Atlantic. A proposed mechanism is a more southerly excursion of the ITCZ over southern Africa during years when SSTa in the south Atlantic are positive (north Atlantic is negative).

Filtered values of the SOI index and Durban rainfall for the same period are illustrated in fig 3-3. Close agreement is observed between the two series. The SOI-rainfall relation in the inter-annual (1.5 – 16 yr.) frequency band over the 1935-1999 period is evaluated by cross-

wavelet analysis. Large modulus values are observed around 1972, 1983 and 1998 mainly in the 2.3 and 4 year band. This may reflect a harmonic association between QB and EN teleconnections. From the cross-wavelet spectrum, we estimate the instantaneous phase difference and time delay between the two series. It is observed that when the cross-wavelet spectrum power (modulus) is high, the SOI leads rainfall by a few months. The time delay is quite unstable though. SOI leads rainfall in the 1970s, but 'follows' in the 1950s.

The temporal character of the naturalised Nile River flow is illustrated in the upper panel of fig 3-4. Higher flows and larger fluctuations are found in the period up to 1920. Thereafter the amplitude of inter-annual variability is more confined, with a down-trend apparent in the period 1960-1980. Year-to-year changes in flow increase again in recent years. A cross-wavelet spectral analysis is performed with the Durban summer rainfall data to investigate common temporal fluctuations. The association is similar to that with the SOI. Large modulus values are found in the frequency bands around 2.3 and 4 years from 1890 to 1920, and 1960 to 1990. In recent decades both QB and EN cycles are present, however throughout most of the record, either one or the other is more dominant.

Discussion

Africa's water supplies are reaching sustainable limits. Uncovering scale-interactions in intra-seasonal to decadal climate variability is of value in the management of resource availability. In comparison with Jury (1998), seasonal (2 – 5 month) persistence in Durban rainfall was confirmed by more rigorous CWT analysis over a 128-year record. The annual cycle accounts for 33% of rainfall variance, whilst inter-annual fluctuations explain 10%. The CWT analysis indicates a relatively chaotic temporal character, with cross-spectral energy concentrated in the 2.3 (QB) to 4 year (EN) bands. There is little evidence for long-term trends in the Durban rainfall record, however the naturalised Nile River flow exhibits a downtrend, likely related to land use and a consequent reduction of run-off.

Jury (1998) demonstrated associations between Durban rainfall and meridional winds in the north Indian Ocean and the Southern Oscillation Index. In the longer analysis here, both the SOI and the Atlantic dipole lead Durban rainfall. A mechanism for EN influence is proposed (Jury 2000), whereby warm tropical seas (El Niño) reduce 'waviness' of the subtropical jet stream south of Africa, thereby producing fewer extreme weather events. These circulation anomalies operate near-simultaneously on either side of the equator, as illustrated by the shared spectral energy. Given the widespread nature of inter-annual forcing, our results take on added meaning in efforts to describe, understand and predict climate variations and resource availability over Africa. In the context of this report, knowledge is contributed on the widespread nature of climatic anomalies and techniques to reveal them. Some ambiguities remain as regards the interaction of regional (Indian / Atlantic) and global (ENSO) signals that influence African water resources, and further work is needed to identify leading indicators of this interaction.

References

- Amarasekara, K N, Lee, R F, Williams, E R, Eltahir, E A B, 1997, ENSO and the natural variability in the flow of tropical rivers, *J Hydrology*, 200, 24-39
- Bliss, E W, 1925, The Nile flood and world weather, *Mem. Roy. Meteor. Soc.*, 4, 36, 53-84.
- Daubechies I, 1992, Lectures on wavelet transforms. SIAM, Philadelphia.
- Delprat N., Escuidé B., Guillemain P., Kronland-Martinet R., Tchamitchian P. and B. Torrèsani, 1992, Asymptotic wavelet and Gabor analysis: extraction of instantaneous frequencies. *IEEE Trans. Info. Theory*, 38 (2), 644-664.
- DeJager, J.M. and Schulze, R.E. (1977) The broad geographic distribution in Natal of climatological factors important to agricultural planning, *Agrochemophysica*, 9, 81-91
- Diab, R.D., Preston-Whyte, R.A., and Washington, R. (1991) Distribution of rainfall by synoptic type over Natal, South Africa, *Intl Journal Climatology*, 11, 877-888
- Eltahir, E A B, 1996, El Niño and the natural variability in the flow of the Nile River, *Water Resources Research*, 32, 131-137.
- Eltahir, E A B, and Wang, G, 1999, Nilometers, El Niño and climate variability, *Geophys Res Letters*, 26, 4, 489-492.
- Jury, M.R., Valentine, H., and Lutjeharms, J.R.E. (1993) Influence of the Agulhas Current on summer rainfall along the southeast coast of South Africa, *J Applied Meteorol*: 32, 7, 1282-1287
- Jury, M R, 1998, Statistical analysis and prediction of KwaZulu-Natal climate, *Theoretical Appl. Climatol.*, 60, 1-10
- Jury, M R, 2000a, Inter-annual variability of African river flows and composite climatic structure, *J Hydrology*, in press
- Jury, M R, and Mason, S J, 2000b, Evolution of ENSO influence in the African hemisphere from NCEP reanalysis composites, in prep.
- Lau K.M. and H.Y. Weng (1995). Climate signal detection using wavelet transform: how to make a time series sing. *Bulletion of the American Meteorological Society*, 76, pp. 2391-2402.
- Mallat S. (1998). A wavelet tour of signal processing. Academic Press, San Diego, CA.
- Meyers S.D., Kelley B.G. and J.J. O'Brien (1993). An introduction to wavelet analysis in oceanography and meteorology: with application to the dispersion of Yanai waves. *Monthly Weather Review*, 121, pp. 2858-2866.
- Miron, O. and Tyson, P.D. (1984) Wet and dry conditions and pressure anomaly fields over South Africa and the adjacent oceans 1963-1979, *Monthly Weather Review*: 112, 2127-2132
- Morlet J. (1983). Sampling theory and wave propagation. NATO ASI Series, FI, Springer, pp. 233-261.
- Philipp, A, 1999, Principal component analysis of summer rainfall anomalies over southern Africa, (pers. comm.), Geography Dept, Univ. Wuerzburg, Germany.
- Quinn, W H, 1992, A study of southern oscillation -related climatic activity 622-1990 incorporating Nile river flood data, in *El Niño: Historical and Paleoclimate Aspects of the Southern Oscillation*, ed Diaz, H F, and Markgraf, V, 119-142.

Servain J. (1991). Simple climatic indices for the tropical Atlantic Ocean and applications. *J. Geophys. Res.*, 96 (15), 15137-15146.

Torrence C. and G.P. Compo (1997). A practical guide to wavelet analysis. *Bull. Amer. Meteorol. Soc.*, 79(1) 61-78.

Walker, G.T., and E.W. Bliss, 1932: World Weather V, *Mem. Roy. Meteor. Soc.*, 4, 53-84.

Walker, N.D. (1990) Links between South African summer rainfall and temperature variability of the Agulhas and Benguela Current systems, *J. Geophys. Res.*, 95, 3297-3319

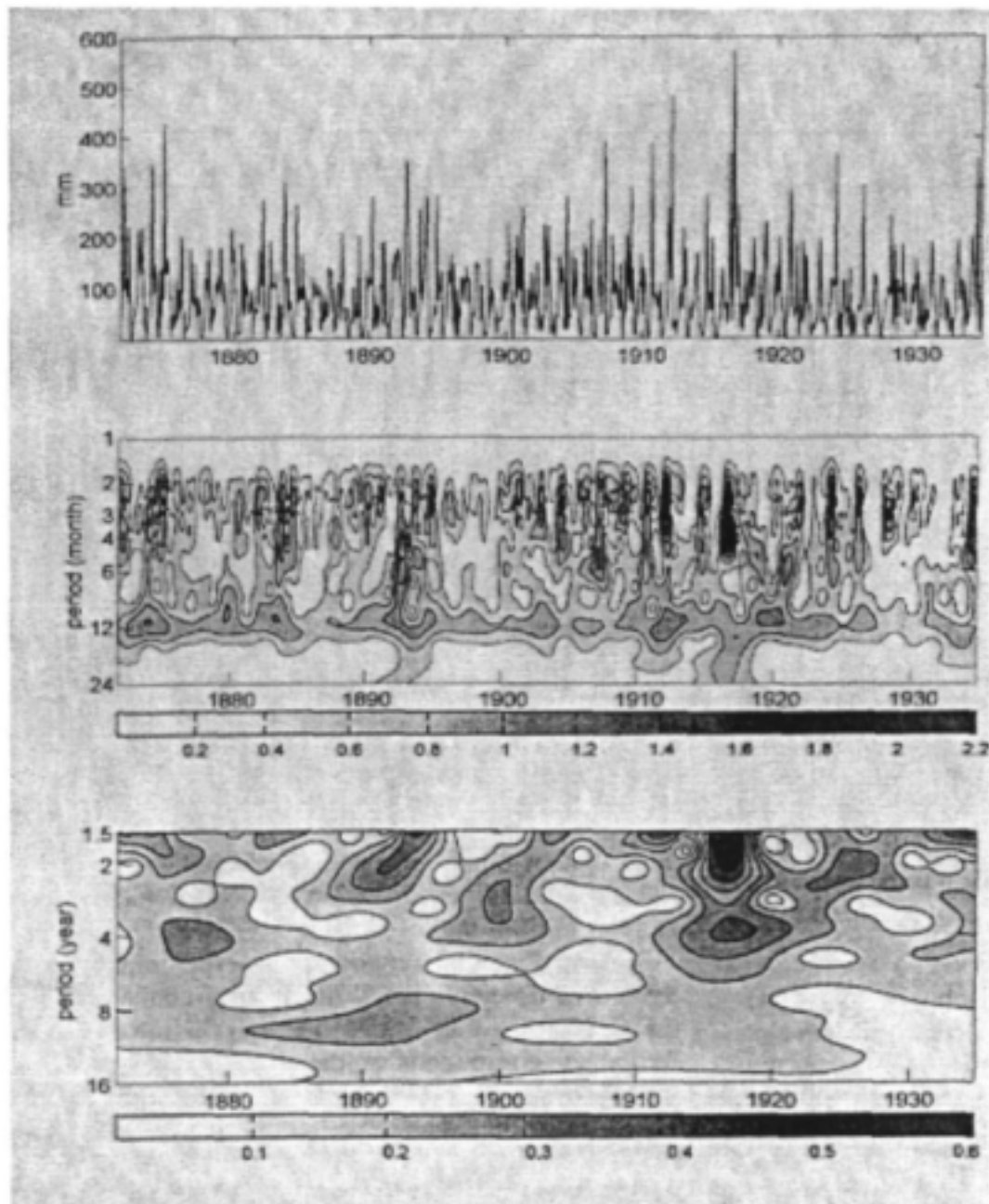


Fig 3-1 – Raw rainfall time series (top), modulus of the wavelet transform coefficient for intra-seasonal (middle) and inter-annual time scales (lower) for the first half of the period 1872-1935.

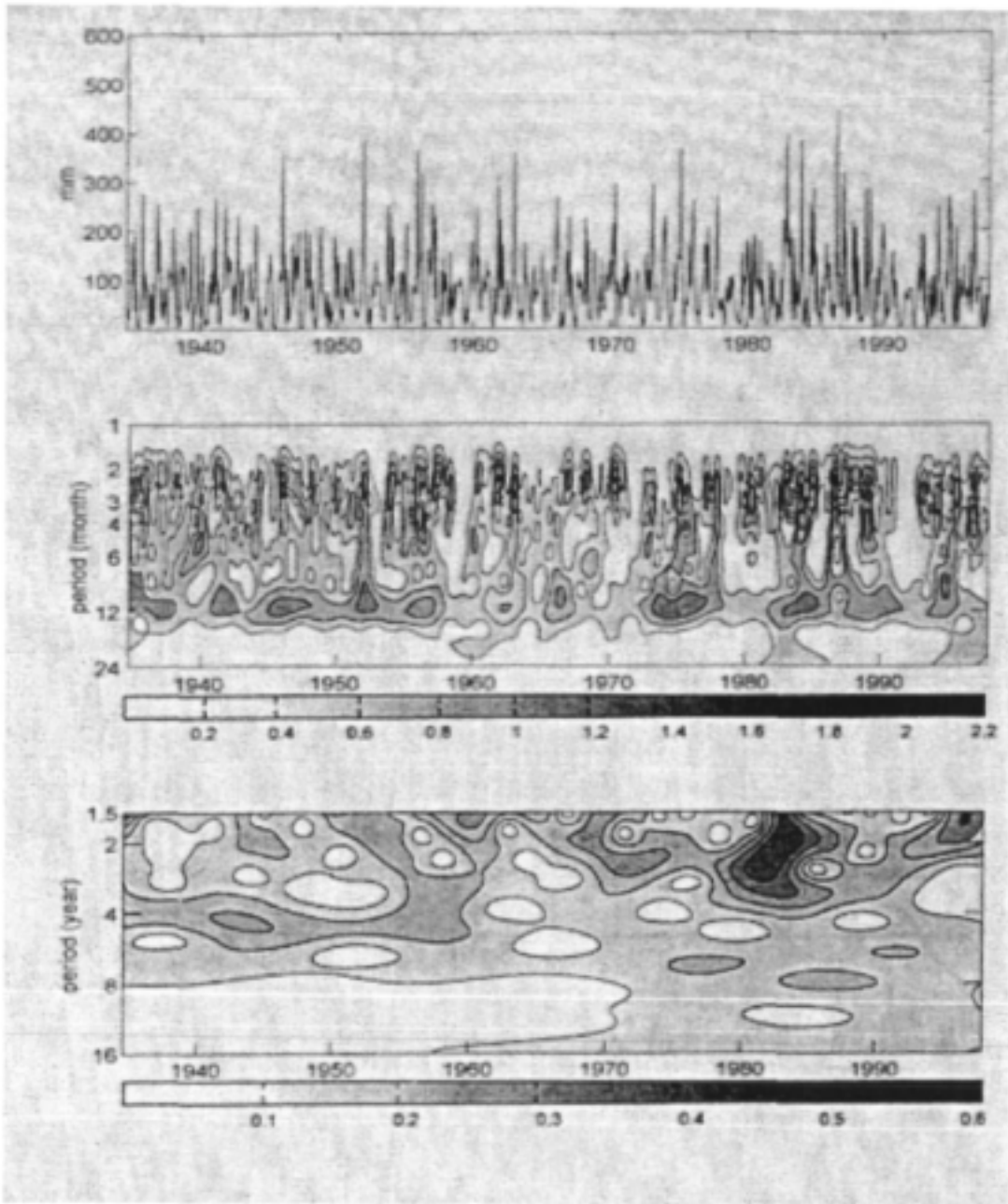


Fig 3-2 – Rainfall time series and modulus of the wavelet transform coefficient for the period 1935-1999.

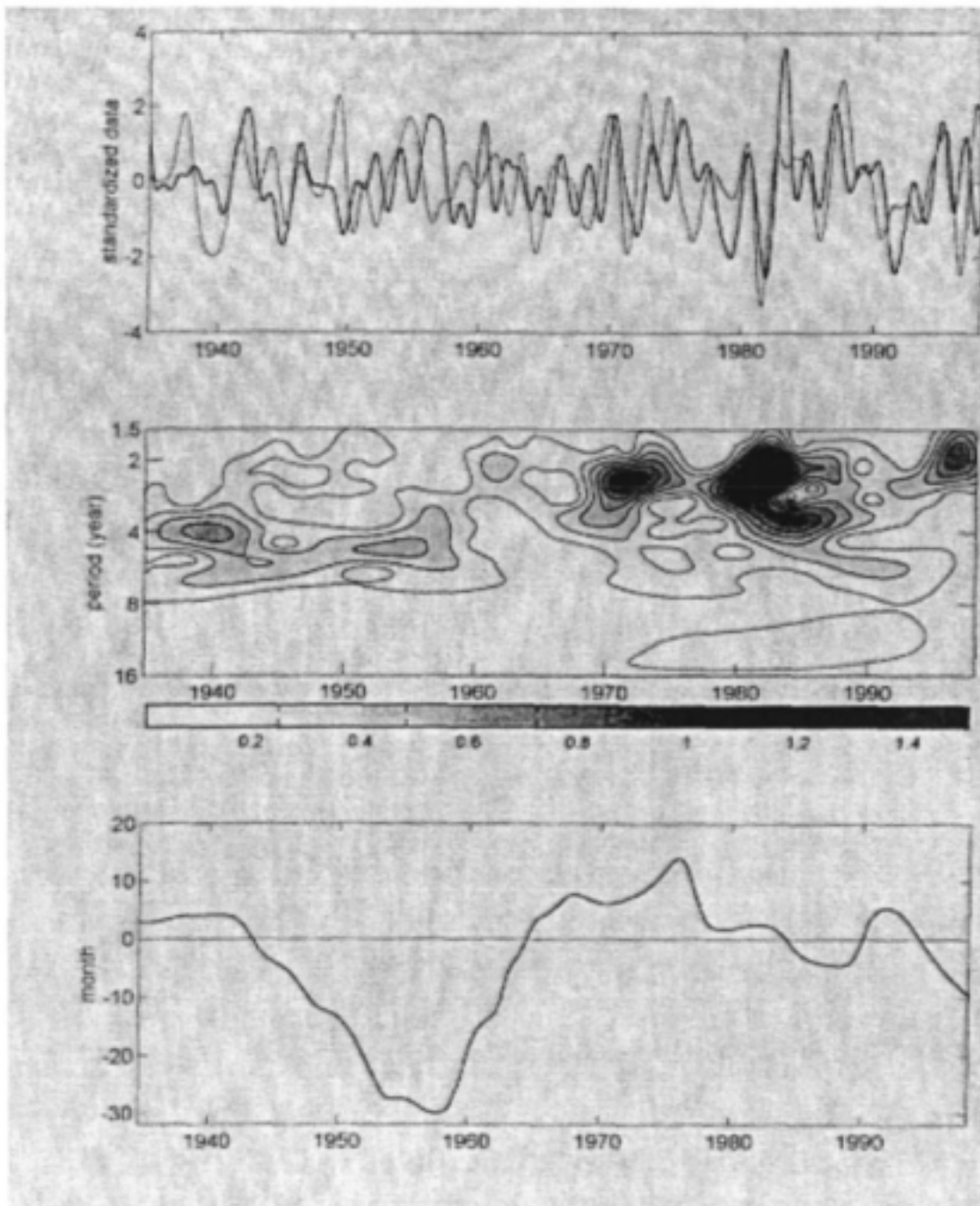


Fig 3-3 - Standardized low-frequency components for rainfall (bold) and SOI (thin) for the second half of the period 1935-1999. Cross-wavelet spectrum, comparing cycles in SOI and rainfall. Time delay between SOI and rainfall (lower), where SOI leading is +.

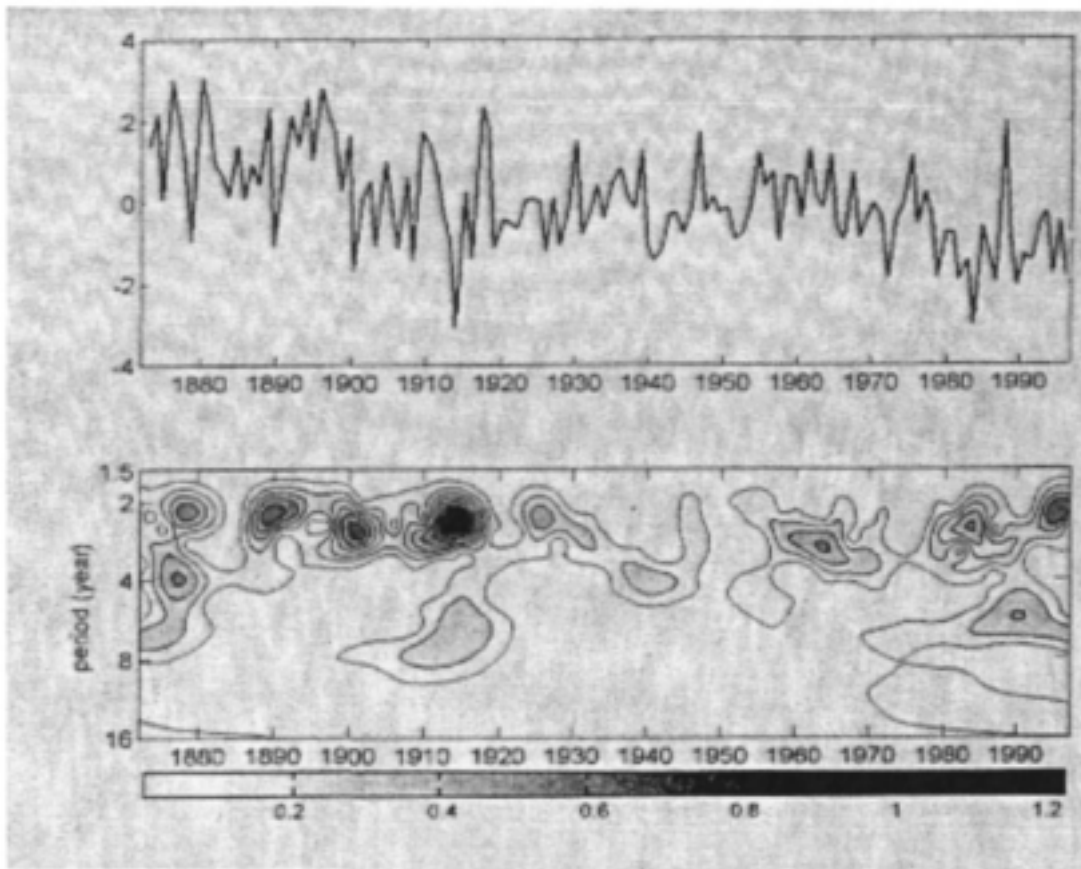


Fig 3-4 - Standardized Nile River flow record for the period 1871-1997 (upper) and cross-wavelet spectrum (lower) comparing Nile flows and Durban rainfall.

Chapter 4 – Indian Ocean circulation and rainfall over southeast Africa

It has been noted in many studies that rainfall over the tropical west Indian Ocean ‘competes’ with rainfall over southern Africa. In this chapter we analyse a composite situation of increased rainfall over southeast Africa coincident with dry conditions over the ocean east of Madagascar.

Introduction

Much of the summer rainfall over Africa south of the Zambezi River ($\sim 15^{\circ}\text{S}$) is produced by quasi-stationary troughs (Harrison, 1986; Levey and Jury, 1996). The convection is often focused along a NW-SE oriented band by a Rossby wave in the subtropical upper westerly flow. Prior to the convective event, a period of low-level easterly flow from the tropical Indian Ocean is necessary to build up moisture (D’Abreton and Lindesay, 1993; D’Abreton and Tyson, 1995). Widespread rainfall occurs over many days at near-monthly intervals during the November to March season (Makarau, 1995; Levey and Jury, 1996). Each convective spell brings ~ 100 mm of rainfall and contributes about 20% of the seasonal total, so an understanding of their coupling to the surrounding monsoon circulations would be useful.

A number of studies have described the meteorological structure of multi-day rainfall events (Taljaard, 1987; Matarira and Jury, 1990; Lindesay and Jury, 1991; Lyons, 1991; D’Abreton and Lindesay, 1993; Jury et al., 1993) based on statistical inferences from model-interpolated weather data. Across southeastern (SE) Africa and the southwestern (SW) Indian Ocean the wet spells appear to be pulsed at frequencies which are consistent with the passage of tropical waves during austral summer (Hayashi and Golder, 1992). Transient waves of the tropical Indian Ocean were studied by Jury et al., (1991) through hovmoller analysis of satellite imagery in the 10° to 20°S band over the period 1970-1984. 50% of years between 1971 and 1984 exhibited westward moving convective disturbances with a mean speed of 2 m s^{-1} and wavelength of 3 500 km giving an average period of 20 days. Other years had quasi-stationary or eastward-moving disturbances. Characteristics of the background circulation with respect to the potential for easterly waves have not been investigated. Here we look specifically at this issue. We investigate whether tropical easterly inflows are sourced from a divergent centre in the Indian Ocean and analyse the regional structure and ocean-atmosphere environment.

Data and methods

Our study considers the principal components analysis of Mulenga (1998) on gridded summer rainfall departures (Hulme and Jones, 1993). In that work, areas with common fluctuations were identified over the period 1950-1992. A significant mode (PC4) occurs over Africa south of 20°S and east of 25°E . This area is agriculturally productive and yields a substantial food grain reserve following wet seasons (Lindesay, 1990). Seasonal rainfall extremes were noted and related to differences in the atmospheric circulation over the west Indian Ocean. Two common circulation patterns were identified based on the NCEP reanalysis zonal 850 hPa wind anomaly in the area 5° to 20°S , 45° to 85°E northeast of Madagascar exceeding \pm one standard deviation. East flow years include: 1961, 66, 69, 76, 77, 79, 81; west

flows are: 1968, 71, 80, 83, 90, 92, and 95; seven of each type. The season considered is December to March and coincides with the NE monsoon season, when the inter-tropical convergence zone (ITCZ) lies south of the equator near 15°S from 25° to 50°E (Ho and Wang 2000). The easterly regime occurred more frequently in the 1960s and 1970s with a cooler tropical Indian Ocean, whilst the westerly regime has been more prominent in the 1980s and early 1990s during repeated El Niño warming events. The easterly regime appears to have become re-established since 1996. Table 4-1 lists the 850 hPa zonal wind anomaly in the area 10 - 15°S, 60 - 70°E. The intra-composite bias is limited according to grid point and field significance tests. Individual years do not significantly affect the composite patterns, according to sensitivity tests conducted by withdrawing more extreme years.

Meteorological differences between easterly and westerly composites are analysed for winds at 850 hPa and at upper levels, geopotential height at 700 hPa, OLR, SST, and velocity potential at lower and upper tropospheric levels. The dry-westerly fields are subtracted from the wet-easterly fields to infer differences between seasons when the tropical inflow is enhanced or suppressed. Zonally propagating circulation systems are analysed using climatological mean low-level meridional winds plotted in Hovmöller fashion in the latitude band 7° - 17°S across the Indian Ocean. Hovmöller plots of zonally propagating convective anomalies based on pentad OLR data for individual years are also considered.

Our analysis makes use of the NCEP reanalysis products available from the NOAA/CIRES/ CDC website on the Internet. The data are at a resolution of 2°, four times a day averaged into monthly means. Kalnay et al. (1996) describe the reanalysis system in detail. Suffice to say that composite differences, consisting of 28 months for each flow regime, should be realistic, despite the known observational discrepancies around tropical Africa.

It is useful to consider the seasonal monsoon circulations of the SW Indian Ocean. Easterly near-surface winds prevail in the austral winter from April to November, according to historical averages. During austral summer, cross-equatorial flow recurves to create westerly winds from 5° to 10°S between December and March. The monsoon flow in this area north of Madagascar extends to a depth of 4 km or 600 hPa and is overlain by easterly winds aloft. This westerly flow, if persistent, can oppose the influx of Indian Ocean moisture to the continent. However, when the monsoon weakens or reverses, tropical moisture can extend across Madagascar and penetrate into SE Africa.

Results

A comparison of area-averaged rainfall for the composite years is given in Table 4-1 together with austral summer values for the southern oscillation index and the quasi-biennial oscillation index (equatorial zonal wind at 30 hPa, U30). There is a distinct and symmetrical difference in rainfall over SE Africa for the easterly and westerly cases. Rainfall in the easterly regime averages about 1 standard deviation above normal, in the westerly regime it is as much below normal. D'Abreton and Tyson (1996) have shown that the area north of Madagascar is a source region for moist inflows to subtropical troughs over southern Africa, so this result is expected. Their results suggest that the inflow maintains a constant elevation, but undergoes an

increase in the moisture content after crossing the east coast of Africa around 15°S. The increase is attributed to evapotranspiration and eddy heat fluxes along the densely forested eastern escarpment. The moist inflow is pulsed at intra-seasonal scales via easterly waves embedded within the mean flow as described in the composites below. Table 4-1 suggests that the relationship with ENSO phase is not well defined. The easterly inflow regime is favoured when equatorial stratospheric (30 hPa) winds are from the west.

Composite patterns

In fig 4-1 the east minus west differences are analysed for 850 hPa winds. The lower level pattern is used to select composite years for inclusion and illustrates a broad band of easterly flow in the area 5° - 20°S, 40° - 90°E to the northeast of Madagascar in the Indian Ocean. An anticyclonic circulation near 25°S, 60°E separates easterly flows in the tropics from westerlies to the south. Analysing the composite differences at higher levels one finds a deep easterly circulation over Madagascar. The lack of an opposing return flow at the upper levels means that the westward flux of mass from the Indian Ocean cannot be conceptualised as a zonal overturning (Walker) circulation. Geopotential differences are positive (anticyclonic) to the east of Madagascar and negative in the equatorial and mid-latitude bands. The anticyclone guides easterly waves westward to Africa, drawing tropical air polewards across SE Africa and cool dry air equatorward over the South Indian Ocean, thereby suppressing tropical cyclone formation there (Jury, 1993).

In fig 4-2 the SST pattern is analysed. Sea surface temperatures play a role in shifting convection toward the continent. Poleward of the easterly wind regime and supporting the anticyclonic gyre, a warm anomaly of magnitude +1.0°C extends from 50 - 80°E along 30°S. Throughout the entire tropics, covering an area $2 \times 10^{13} \text{ m}^2$, SST differences are of order -0.4°C, in agreement with the earlier results of Jury (1996). The meridional gradient of SST is more than 1°C weaker to the east of Madagascar resulting in a reduced thermal wind: $(\partial T / \partial y \sim \partial U / \partial z)$ where T and U are layer-averaged temperature and zonal wind, respectively. The subtropical jet stream is displaced poleward, hence limiting the penetration of westerly shear in the tropics. This mechanism is represented in the GCM study of Reason and Mulenga (1999) wherein a +1°C SST anomaly south of Madagascar induces a 2 - 5 m s⁻¹ easterly wind anomaly at the 200 hPa level in the 5°-25°S latitude band across southeast Africa.

The vertical extent of the anomalous wind response to cooling (warming) of the central (southern) Indian Ocean is significant. Easterly anomalies extend through the troposphere from the surface to 100 hPa (15 km) in the 5°-25°S latitude band over the longitudes east of Madagascar. The zonal wind differences are 2 to 5 m s⁻¹ between east and west years. In the higher latitudes upper westerlies are more intense. The deep layer of easterly wind anomalies over the western tropical Indian Ocean creates a suitable barotropic environment for the westward propagation of convective waves. Fig. 4-3 illustrates the velocity potential (divergent component of the circulation), and reveals an intense centre of low-level inflow / upper level outflow over the south Indian Ocean. Lower at 15°S, 70°E with a radius of $3 \times 10^6 \text{ m}$. This cell dominates the entire Indian hemisphere in this set of composites and can be described as a source

region from which easterly waves advect. Its causes have been discussed by Behera and Yamagata (2001)

SST and circulation patterns for the period August to November (not shown) provide an indication of antecedent conditions. Tropical Indian SSTs are $< -0.3^{\circ}\text{C}$ below normal leading into the easterly flow regime. This is the case everywhere except west of Malaysia (5°S , 100°E) where low-level westerly wind anomalies of $+2\text{ m s}^{-1}$ and associated equatorial downwelling occur - SST differences there are $+0.4^{\circ}\text{C}$. A deep anticyclonic circulation is located east of Madagascar in the precursor season.

Many of the composite differences in the precursor season exceed the historical inter-annual standard deviation, hence prediction of the easterly wave regime may be possible. Consideration of years listed in Table 4-1 suggests a decadal rhythm, with the 1960s and 70s experiencing an upsurge in easterly anomalies, and the 80s and early 90s dominated by the westerly regime. As the ENSO influence is obscure in these analyses, it is not clear what mechanism underlies this low-frequency modulation, also found in the 18 year rainfall cycle over southern Africa (Tyson 1986).

Discussion

A comparison of pentad OLR anomalies for easterly and westerly regimes was made in Jury et al., (1991). In the easterly case, the convective troughs and their attendant ridges propagate westward into SE Africa along 10° - 15°S . The propagation speed across the Indian Ocean from 80° to 20°E is 3.3 to 4.1 m s^{-1} , consistent with the background flow. In the easterly case, the convective anomalies develop further west than usual, and travel along a path that is further equatorward, so sliding past northern Madagascar and into SE Africa along the Zambezi River valley. The intra-seasonal surges enhance the moisture supply over southern Africa and contribute to latent heat release in quasi-stationary troughs over the continent - the main source of rainfall. In the westerly regime, continental moisture is depleted and an eastward propagation of convective weather systems may occur, often coupled to equatorial Kelvin waves as outlined by Vincent et al., (1998).

In this study it is demonstrated that summer rainfall over SE Africa increases when easterly flow is present off northern Madagascar in the tropical Indian Ocean. Our composite reveals deep easterly flow differences in the band 5° - 20°S . Convection is reduced over the South Indian Ocean (0 - 30°S , 60° - 110°E) whilst increased over SE Africa. Differences between wet and dry years are evident in the velocity potential and indicate a centre of subsident outflow at 15°S , 75°E . SST in the latitude band 25° - 35°S . This couples with a deep anticyclonic anomaly in the wind field which transfers moist convection westward to SE Africa. SST in the tropics are below normal, hence the poleward thermal gradient is reduced and the associated subtropical jet stream shifts polewards to 40°S . In the tropics around the latitudes of Madagascar, deep easterly flow anomalies of 2 to 5 m s^{-1} develop when SST increases (decreases) to the south (north). The observational results here correspond well with the numerical modelling study of Reason and Mulenga (1999).

In the precursor season (August - November) SST fields indicate that warming in the subtropics is weak and may lag the atmosphere through air-sea interaction processes as described in Reason (1999). Over the central basin, below normal sea temperatures are found in contrast to warmer conditions off the coast of Malaysia. Westerly 850 hPa wind differences are found over the equatorial band particularly near 90°E. In the upper levels the tropical flow is easterly and at higher latitudes the flow differences are westerly. The easterly anomalies are related to the anticyclone and warmer SST in the south. In this scenario convective surges from the Indian Ocean remain in the 7° - 15°S latitude band and are drawn into the convective bands over SE Africa at ± 20 day intervals. It was the recognition of these patterns during the spring of 1999 that contributed to a correct forecast of the February 2000 flood over northeastern South Africa and southern Mozambique.

References

- Behera, S.K. and Yamagata, H.T., 2001: Subtropical SST dipole events in the southern Indian Ocean. *Geophys. Res. Lett.*, 28, 327-330.
- D'Abreton, P C and Lindesay, J A (1993) Water vapour transport over southern Africa during wet and dry early and late summer months. *Intl. J. Climatol.* 13, 151-170.
- D'Abreton, P C and Tyson, P D (1995) Divergent and non-divergent water vapour transport over southern Africa during wet and dry conditions. *Meteorol. Atmos. Physics* 55, 47-59.
- D'Abreton, P C and Tyson, P D (1996) Three-dimensional kinematic trajectory modelling of water vapour transport over southern Africa. *WaterSA* 22, 297-306.
- Harrison, M S J, (1986) A Synoptic Climatology of South African Rainfall Variability. PhD Thesis, Univ. Witwatersrand, Johannesburg, 341 pp.
- Hayashi, Y and Golder, D G (1992) Tropical 40-50- and 25-30-day oscillations appearing in realistic and idealized GFDL climate models and the ECMWF Dataset. *J. Atmos. Science* 50, 464-494.
- Ho, L, and Wang, B (2000) Southern African Monsoon. *Proc 6th Intl. Conf. S. Hem. Meteorol.*, Santiago, Amer. Meteorol. Society, 6A4 (in press).
- Hulme, M, and Jones, P D (1993) A historical monthly precipitation dataset for global land areas, application for climate monitoring and evaluation. in *Analysis methods of precipitation on global scale*. WMO TD 558, Geneva.
- Jury, M R, Pathack, B, Campbell, G, Wang, B, and Landman, W (1991) Transient convective waves in the tropical SW Indian Ocean. *Meteorol. Atmos. Physics* 47, 27-36
- Jury, M R (1993) A preliminary study of climatological associations and characteristics of tropical cyclones in the SW Indian Ocean. *Meteorol Atmos Physics* 51, 101-115
- Jury, M R, Lindesay, J A, and Wittmeyer, I (1993) Flood episodes in central South Africa from satellite and ECMWF data. *S.Afr.J. Science* 89, 263-269.
- Jury, M R (1996) Regional teleconnection patterns associated with summer rainfall: South Africa, Namibia and Zimbabwe. *Intl. J. Climatol.* 16, 135-153

- Kalnay, E, and co-authors (1996) The NCEP/NCAR 40-year reanalysis project. *Bull. Amer. Meteorol. Soc.* 77, 437-471.
- Levey, K M and Jury, M R (1996) Composite intra-seasonal oscillations of convection over Southern Africa. *J. Climate* 9, 1910-1920.
- Lindesay, C J (1990) Economic and socio-political impacts of rainfall variations. *MBA Thesis*, Univ. Witwatersrand, Johannesburg, 181 pp.
- Lindesay, J A and Jury, M R (1991) Atmospheric circulation controls and characteristics of a flood event in central South Africa, *Intl. J. Climatol.* 11, 609-627.
- Lyons S W (1991) Origins of convective variability over equatorial southern Africa during the austral summer, *J. Climate.* 4 23-39.
- Makarau A (1995) Intra-seasonal oscillatory modes of the southern Africa summer circulation, *PhD. Thesis*, Oceanogr Dept, Univ Cape Town. 324 pp.
- Matarira C H and Jury M R (1990) Contrasting atmospheric structure during wet and dry spells in Zimbabwe, *Intl. J. Climato.* 12, 165-176.
- Mulenga, H M (1998) Southern African climate anomalies, summer rainfall and the Angolan low. *PhD. Thesis*, Oceanogr Dept, Univ Cape Town, 234 pp.
- Reason, C J C (1999) Interannual warm and cool events in the subtropical / mid-latitude south Indian Ocean region. *Geophys Res Lett* 26, 215-218.
- Reason, C J C, and Mulenga, H (1999) Relationships between South African rainfall and SST anomalies in the southwest Indian Ocean. *Intl. J. Climatol.* 19, 1651-1673.
- Taljaard J J (1987) The anomalous climate and weather systems during summer 1976. *SAWB Technical paper 16*, Pretoria, 80 pp.
- Tyson, P D (1986) *Climatic change and variability in southern Africa*. Oxford Univ. Press, Cape Town, 220 pp.
- Vincent, D G, Fink, A, Schrage, J M, and Speth, P (1998) High- and low- frequency intra-seasonal variance of OLR on annual and ENSO time scales. *J. Climate* 11, 968-986.

Table 4-1: Years selected for inclusion in the composite.

year	Rain	SOI	U30	Type	U850 grid pt.
1961	+1.0	+4	-1.0	East	-3.6 m/s
66	+1.4	-1.5	+7	East	-2.4
68	-.8	+3	-1.5	West	+2.2
69	+1.2	-.4	+1.1	East	-2.9
71	-.5	+1.3	-.7	West	+1.1
76	+1.6	+1.8	+5	East	-2.5
77	+1.1	-.2	-.7	East	-1.8
79	+.9	-.3	+3	East	-0.9
80	-.9	-.3	-.5	West	+1.7
81	+.7	-.5	+8	East	-1.9
83	-1.2	-2.5	+1.0	West	+2.1
90	-.9	+3	-.5	West	+2.3
92	-1.2	-1.4	-1.4	West	+3.7
95	-1.0	-.4	+8	West	+1.6
East - West	+2.0	+3	+7 std dep.		

Year refers to December to March season labelled according to the January month, Rain = standardised departure over Africa south of 20°S and east of 25°E, SOI = southern oscillation index, U30 = equatorial zonal wind anomaly at 30 hPa, Type is defined by U 850 hPa zonal wind averaged over the grid box 5 - 15°S, 50 - 75°E.

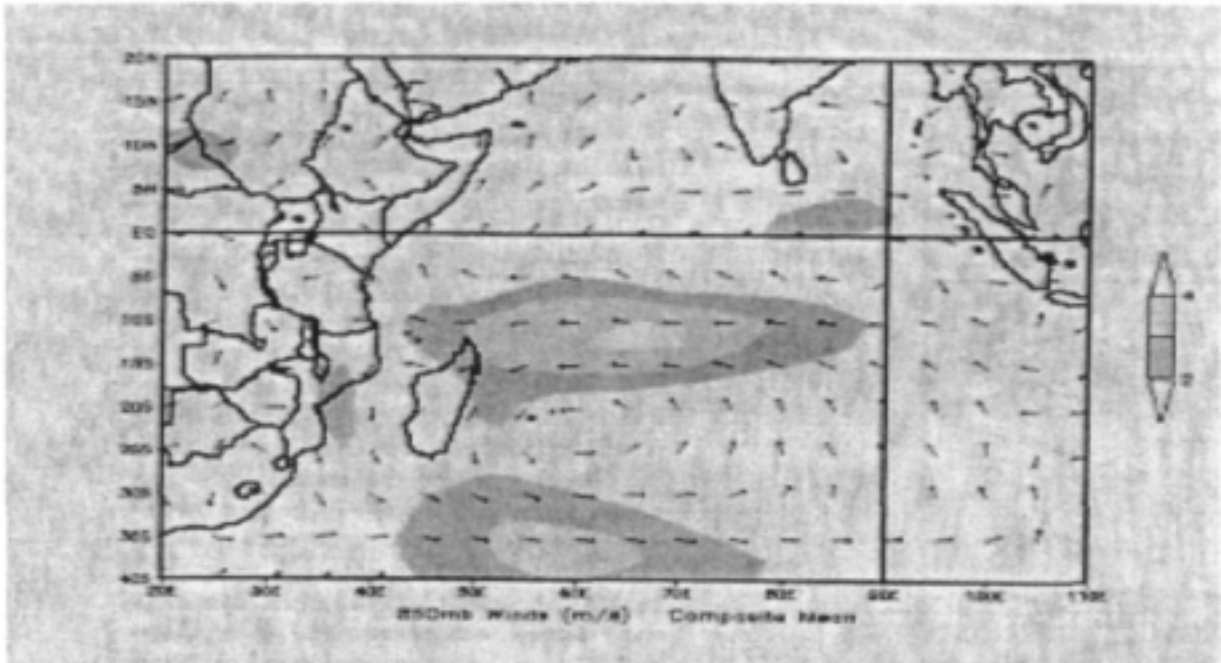


Fig. 4-1 - Composite wet/easterly minus dry/westerly differences over SE Africa and the Indian Ocean for December to March period for winds (m s^{-1}) at 850 hPa

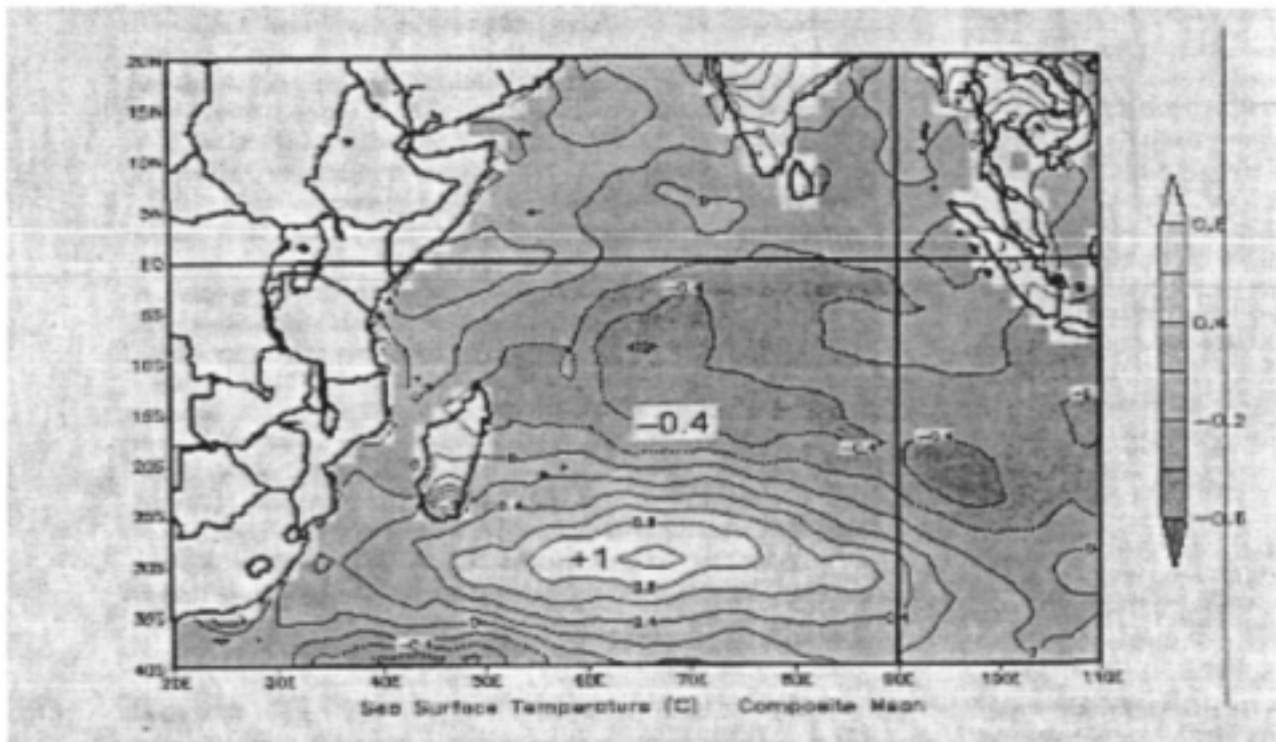


Fig. 4-2 - Composite wet/easterly minus dry/westerly differences as in Fig. 4-1 but for SST $^{\circ}\text{C}$.

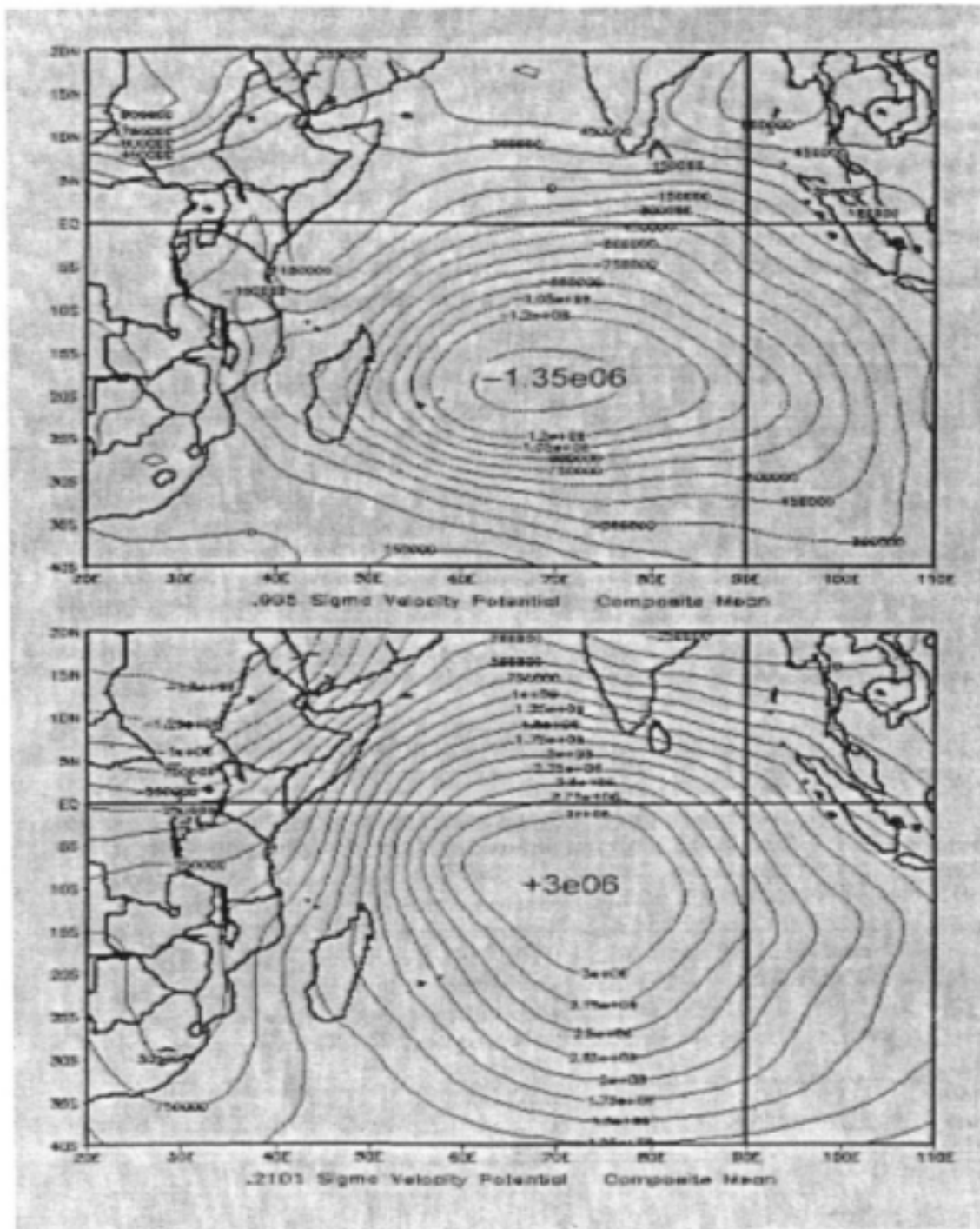


Fig. 4-3 - Composite wet/easterly minus dry/westerly differences as in Fig. 4-1 but for lower and upper velocity potential $10^6 \text{ m}^2 \text{ s}^{-1}$. Such a pattern is consistent with the Indian Ocean 'dipole' uncovered by Behera and Yamagata (2001).

Chapter 5 – Composite wet and dry spells and implications for predictability

In this chapter we apply simple composite techniques to study climate variability over southern Africa. A mathematical framework is established which helps explain the causes of large-scale drought over southeast Africa in the context of warming of the west Indian Ocean. Statistical forecast models are developed. Although much of the work focuses on Malawi due to the origin of the contributing graduate students, its mean rainfall correlates with South African rainfall at 0.52 ($p < 1\%$) during the period 1949-1998, suggesting that results may be generalised for southern Africa.

Introduction to drought analysis

Water is scarce in most of Africa, and economic prosperity depends on rain-fed crops (Jury, 2001). The water supply is highly variable: dry or wet spells can range from months to decades. Therefore understanding the nature and causes of climate variability and exploring its predictability can provide useful guidance to farmers, hydrologists and strategic planners for the sustainable management of resources.

Africa is plagued by recurrent drought, for example from 1982 to 1984 maize yields south of the Zambezi Valley declined to 10% of historical values and about 80% of livestock perished (Makarau, 1995). In the 1992 summer, rainfall was 50% of normal over southeastern Africa and 90% of small inland dams dried up in Botswana, South Africa, Zimbabwe and Namibia. Other spheres of human activity are disrupted by drought: social problems increase with higher unemployment, political instability arises from the economic impacts of high inflation and currency devaluation, and the environment is degraded through overgrazing and widespread fires (Dilley, 1996; Zhakata, 1996).

The variable climate along the margins of the tropics is receiving increased interest from research scientists. International studies are in place to focus attention on climate variability and prediction (CLIVAR). Locally several studies on rainfall variations over southern Africa have looked at spatial and temporal aspects of climatic variations in the rainy summer months - November to March (Mulenga, 1998). Relationships between rainfall and the regional circulation have been uncovered (Harangozo and Harrison, 1983; Harrison, 1986; Lindesay and Jury, 1991) and related to global ENSO phase. Whilst many of these studies have focused on South Africa and its neighbouring countries, very little work has been done on Malawi's climate.

Malawi shares many of the same climatic aberrations as southern Africa. During the drought of 1992 maize production decreased by 50 % (Malawi Ministry of Agriculture, 1993) and food had to be imported. The failure of rains for more than one month in the rainy season adversely affects agriculture and the economy of Malawi. The farming community requires an advance warning of drought, however the oceanic thermodynamic patterns and corresponding atmospheric circulation associated with extreme weather conditions are not well known. Statistical models for the prediction of seasonal rains are unverified. This paper addresses these issues so that the adverse effects of climate fluctuations could be mitigated.

Background

The domain of study is from 20°N to 40°S and 30°W to 90°E but with a focus on Malawi. Located within tropical southern Africa: Malawi covers an area of $118 \times 10^3 \text{ km}^2$ between the latitudes 9-17°S and longitudes 32-36E. Lake Malawi, part of the Great African Rift valley, is a major source of water and its shores draw considerable tourism income. The lake is 571 km long, 470 m above sea level and covers two thirds the length of the country in the east. To the west, Malawi rises to a plateau of 1 500 m with N-S oriented mountains to 2 500 m.

Malawi experiences a mild tropical climate with an austral summer rainy season. The winter is very dry and nocturnal temperatures decline to near 5°C from May to September. The climate of Malawi depends on the inter-tropical convergence zone (ITCZ), the subtropical high pressure belt in the south, and the topography (Torrance 1972). The ITCZ marks the convergence of the northeasterly monsoon and southeasterly trade winds, and during the rainy season it oscillates over the country, often connecting with troughs in the Mozambique Channel. The other main rain bearing system for Malawi is the northwest monsoon, comprised of recurved tropical Atlantic air that reaches Malawi through the Congo basin. This system brings well-distributed rainfall over the country and floods may be experienced in conjunction with the ITCZ. There are times when the country is affected by tropical cyclones from the west Indian Ocean. Depending on their position, cyclones may result in either dry or wet spells over Malawi. Easterly waves originating near Madagascar often penetrate up the Zambezi Valley during summer. Extra tropical westerly waves are thought to be most active at the beginning and end of the rainy season.

Literature on climate variability specifically for Malawi is scarce. Nkhokwe (1996) reported a positive correlation between Malawi and Ethiopian rainfall. Localised associations were found between summer rainfall and the stratospheric quasi-biennial oscillation (QBO) and the Southern Oscillation Index. A multivariate correlation technique was applied to develop statistical models, one for each station. Kamdonyo (1993) studied the cyclical component of rainfall variance and found significant spectral energy in the biennial band.

The ITCZ lies in the 0-10°S band where low frequency ocean-atmosphere coupling is likely. In the sub-tropical band from 10-20°S, convective waves are embedded within an easterly flow from the Indian Ocean, producing wet spells at near-monthly intervals (Jury and Nkosi, 2000). At higher latitudes internal atmospheric variability is high owing to the passage of westerly troughs, and responses to tropical ocean conditions are less easily identified (Mason 1997). At times tropical outflows occur along NW-SE axes (Preston-Whyte and Tyson 1988), producing cloud bands along preferred paths that vary from year-to-year (Harrison, 1986; Jury and Levey, 1997), according to El Nino-Southern Oscillation (ENSO) phase and associated zonal circulations (Lindesay *et al.*, 1986). Typically below normal rainfall is experienced over southern Africa during an El Nino year (Nicholson and Entekhabi, 1986) as upper westerly winds strengthen and the ascending branch of the Walker Cell shifts to the west Indian Ocean.

Some studies have related stratospheric QBO phase to African rainfall variability. The QBO refers to a zonal wind in the equatorial stratosphere which changes direction from easterly

to westerly with a period of ± 28 months (Naujokat, 1986). The QBO enhances the likelihood of drought when it is in easterly phase (Mason and Tyson, 1992). Ogallo et al (1994) and Jury *et al* (1994) have reported a significant correlation between African rainfall and the QBO. Mukherjee, *et al.* (1985) indicate that easterly phase QBO is associated with a weak monsoon over India. However no clear mechanism has been found to explain the interaction of the QBO, the tropospheric circulation and convection over Africa.

Many studies have related African rainfall variability to sea surface temperature (SST) over the Atlantic, Indian and Pacific Oceans. Nyenzi (1988) looked into the relationship between east Africa rainfall variability and SST over the Atlantic and Indian Oceans. It was observed that fluctuations of SST off Angola were often out of phase with the west Indian Ocean, and together corresponded with ENSO phase and rainfall. Walker (1989) found that South African rainfall is suppressed when SST in the Agulhas Current to the southeast of Africa is below normal. Mason (1992) identified links between warmer SST across the west Indian Ocean and rainfall deficits over southern Africa. In further studies, SST over the west Indian Ocean ($5^{\circ}\text{N} - 10^{\circ}\text{S}$, $55 - 80^{\circ}\text{E}$) was found to be correlated at -0.6 with southern African summer rainfall three months in advance (Rocha, 1992; Pathack, 1993; Jury, 1996). The statistical associations suggest that warmer SSTs and strengthened convection over the west Indian Ocean precede drought over southern Africa. However, recent results indicate that the relationship changes phase over time (Jury et al 2001).

In our study of climate variability a number of hypotheses are addressed:

- (i) Thermodynamic and circulation patterns around southern Africa are significantly different before a dry (or wet) season
- (ii) Climate variations over Malawi are similar to those of the south.
- (iii) Predictability of summer rainfall hinges on the regional expression of global ENSO phase.

Data and methods

The analysis is underpinned by conventional surface data obtained from the Malawi Meteorological Services over the period 1962 -1995. Monthly rainfall data are quality checked to WMO standards and 21 stations spread over the country are utilised. After inspection of the annual cycle, totals are averaged into a November to April mean value each year. Cross-correlations between station data are significant, so a single index is composed from the average of all 21 stations. A two-tier approach is used to identify 'dry' seasons. First, an objective threshold of -0.5 standardised departure is applied to the rainfall series. Secondly, the regional environmental anomalies are plotted and years with 'outlier' patterns are subjectively eliminated (Mwafulirwa, 1999). The dry summers that are retained include: 1968, 1970, 1983, 1992, and 1995. NCEP reanalysis data are analysed via the Climate Diagnostic Centre website as composites for dry years for 500 hPa vector winds, SST and precipitable water fields. The historical 40-year mean is subtracted to produce anomalies.

SST, sea level pressure (SLP), zonal (U) and meridional (V) winds are extracted from the COADS marine data set in $10^{\circ} \times 10^{\circ}$ grid cells in the area $20^{\circ}\text{N} - 40^{\circ}\text{S}$, $20^{\circ}\text{W} - 90^{\circ}\text{E}$. Although the observational inputs are confined to ship tracks, there is a relatively consistent density of

observations around Africa in the period 1962 -1995. The field data are grouped into three-month seasons for analysis with respect to seasonal rainfall. Each of the time series are reduced to a standardised departure, subtracting the mean and dividing by the standard deviation. NOAA satellite outgoing longwave radiation (OLR) data are similarly analysed over the shorter period 1975–1995. Although the degrees of freedom for most environmental variables is 32, for satellite-based OLR it is only 20, and 95 % significance is achieved at a correlation of 42 %.

To guide the choice of climate ‘predictors’, cross-correlations are mapped with respect to the Malawi summer rainfall index for the environmental fields of: SST, OLR, SLP and surface winds at lags –6 and –3 months (JAS,SON). Wind correlations are represented as vectors after re-constituting the U and V values. Statistically significant ‘key areas’ are isolated and extracted for further analysis, together with global indices such as the SOI, Nino3 SST and the QBO. Pair-wise correlations are performed with a view to obtaining a limited set (12) of candidate predictors.

Predictive models are developed using the step-wise, multivariate regression technique. Variables for the JAS period are entered with the aim of obtaining a model with a high degree of fit to the rainfall series. A maximum of three predictors are allowed in the model, providing they are correlated with adjacent predictors at a value $< |0.2|$. The predictive models are then tested for reliability by excluding the first or last eight years and predicting the outcome based on a model for the remaining years, as suggested by Mason (1998). Further tests are performed on residual errors using the Durbin-Watson statistic. Similar methods for statistical model development have been employed for South African rainfall (Hastenrath et al, 1995; Jury et al, 1999).

Results

Temporal analysis

Fluctuations of the Malawi summer rainfall index at inter-annual scale are investigated to establish historical relationships, from which predictability can be investigated. The seasonal cycle and anomaly series is illustrated in figure 5-1. Rainfall increases rapidly to a plateau of 200 mm/month between December and March. November and April are drier transition months. The high summer rainfall indicates the presence of deep convection contributed by the ITCZ. Even in ‘dry’ years, the area-averaged rainfall is 700 mm. The anomaly series exhibits low values in the late 1960s and early 1970s, from 1979 to 1984, and after 1989. A notable biennial fluctuation is apparent. This anomaly series is employed in all subsequent analyses.

Spectral analysis of the rainfall index gives evidence of cycles at 3.8, 2.4 and 11.1 years, suggesting links with the ENSO, QBO and solar cycle, respectively. These cycles are inherent in rainfall records over Zimbabwe and South Africa (Makarau and Jury (1997). Given the significant ENSO influence, correlations for individual stations were computed. Values are stronger in the south and become weaker near the northern border with Tanzania. It is suggested that northern Malawi lies in the transition zone between a dipole of ENSO influence, with opposing centres of action in southern and east Africa (Goddard and Graham 1999).

Correlation mapping

The field correlation analyses at -6 and -3 month lags (JAS, SON) are illustrated in figures 5-2 for SST, OLR, SLP, and surface winds, respectively. For SST, positive values are found southeast of Madagascar and in the tropical Atlantic. Negative correlations are observed over the west Indian Ocean, particularly in the region 0 - 10°S, 60 - 70°E. The southwest monsoon usually curves around this area, thereby creating wind stress curl and vertical motions in the ocean interior (Gill 1982). A N-S gradient is apparent in the sub-tropical west Indian Ocean. The contrast generates enhanced thermal winds in the upper troposphere, as will be shown later.

The OLR correlation pattern is dominated by positive values over the tropical west Indian Ocean (fig 5-3) and weaker values over the tropical east Atlantic. A significant negative correlated area extends NW-SE across the Mozambique Channel during SON season, a precursor to meridional cloud bands, which link sub-tropical standing Rossby waves with the ITCZ over Malawi. The correlation maps indicate that decreased convection (+OLR) northeast of Madagascar is associated with wet summers over Malawi.

SLP field correlations with respect to the rainfall index at -6 and -3 month lags are illustrated in fig 5-4. Values are generally negative over the tropical oceans around Africa during JAS, but become positive over the west Indian Ocean by SON season. A strong E-W gradient is noted with significant negative values in the east Indian Ocean. The wind vector correlation map (fig 5-5) illustrates the pattern of circulation w.r.t. the rainfall index. Larger (significant) vectors are found in the southeast Atlantic and exhibit a southwesterly anticyclonic flow. The Indian Ocean circulation during the JAS season is somewhat vague. However by SON a pronounced cyclonic circulation is found, comprised of southerly flow near Mauritius curving to westerly flow in the eastern tropics. This pattern is related to global ENSO conditions (Mason and Jury 2001). From a perspective of rainfall prediction, the delayed onset of this circulation pattern is problematical.

Given the correlation maps for SST, OLR, SLP, and wind it appears that a number of useful candidate predictors could be extracted for further consideration. From the SST pattern it is noted that two key areas (east Atlantic and Agulhas) are sympathetic and another is inverse (west Indian). The SST exhibits a NW-SE orientation consistent with the area of -OLR correlation in SON. When the Atlantic-Agulhas region is cool, and the west Indian is warm, we suggest that meridional cloud bands tend to link with the ITCZ in the Madagascar-Mauritius sector, leaving southern Africa dry. We represent the strength of this feature through a three-area SST index (3 AI). Similarly, other key area indices, such as the east Indian Ocean pressure, are isolated for further consideration.

Key area associations

The pair-wise cross-correlation of the summer rainfall index with key environmental variables for JAS season in the period 1962 -1995 is listed below in descending order:

Predictor	Key area	Correlation
3 AI (SST)	SST 5°S,5°E + SST 25°S,45°E – SST 5°S,65°E	52 %
SOI	Tahiti – Darwin pressure anomaly	47 %
Nino3	SST 5°N-5°S,150°-90°W	44 %
Atl SST	SST 0°-10°S, 10°W-10°E	43 %
E I P	SLP 10°N-10°S, 70°-90°E	43 %
QBO ₋₁	Zonal wind at 30 hPa (prev. year)	33 %
Atlw ₂₀₀	Zonal wind at 200 hPa over central Atlantic	29 %
W I U	Zonal wind over west Indian Ocean	-28 %
W I V	Meridional wind over west Indian	26 %
Maur P	SLP Mauritius region 15°-25°S, 55°-70°E	-25 %
N I U	Zonal wind over north Indian Ocean	-25 %
C I SST	SST 5°N-10°S, 55°-70°E	-19 %

The correlations at three-month lead time represent a suitable period for advance warning in the context of agricultural planning and mitigating actions. The most influential predictors include the regional variables: 3 area-index SST, tropical Atlantic SST (a subset of 3 AI), and east Indian Ocean pressure; and ENSO variables: SOI and Nino3. In total 12 predictors are utilised in subsequent model development.

Predictive modelling

In this section the model to predict seasonal rains over Malawi is formulated based on historical relationships with environmental predictors. The step-wise multivariate linear regression approach is adopted and a 3-predictor JAS model is developed in a 34 year training period: 1962 -1995. Predictors are screened to reduce co-linearity and the model is validated using an independent test period consisting of the first or last eight years of the record. The model for Malawi summer rainfall achieves an adjusted r^2 fit of 55% and a Durbin-Watson statistic of ~1.9.

$$\text{Malawi rain} = +0.48(3AI) - 0.32(EIP) - 0.26(QBO_{-1})$$

The resulting output is shown in fig 5-6. The 3-area SST index has the strongest influence, and contributes positively to rainfall when the east Atlantic and Agulhas are warm and the west Indian Ocean cool. The second-most influential predictor is the air pressure in the east Indian Ocean. The least influential predictor is the QBO, exhibiting a negative relation in the previous SON, hence westerly phase in the target season. Model validation tests achieve adequate results, although at times the model-predicted amplitude is too small. The performance is similar in early and late test periods. Models were also generated for early (NDJ) and late (FMA) summer periods, but will not be considered here.

Conceptual discussion

In this section we briefly investigate the anomaly structure of mid-tropospheric circulation based on a composite of the five driest summers in Malawi. The dry minus 40-year-

mean pattern of 500 hPa winds is shown in fig 5-7. A narrow axis of accelerated westerly flow is evident in the west Indian Ocean along 15°S, in response to warmer (cooler) SSTs to the north (south) and the steeper geopotential gradient (thermal wind). Upstream over Africa the axis of westerly flow is located along 35° S. A northward swing of the sub-tropical jet occurs over Africa's eastern escarpment. The large-scale equatorward flow obtains a sinking component according to the equation:

$$f \int d\omega = \int \mathbf{V} \cdot \nabla (\zeta + f) dp.$$

Integrating between 700 and 300 hPa and substituting values for: $f = 10^{-4} \text{ s}^{-1}$, $df = -.53(10^{-6} \text{ s}^{-1})$, $dy = 2(10^6 \text{ m})$ and $\zeta = -10^{-5} \text{ s}^{-1}$; and observed values for the V anomaly of 2 m s^{-1} , and $dp = 4 \cdot 10^4 \text{ Pa}$. Solving the equation we find $\omega = 0.2 \text{ Pa s}^{-1}$ and the vertical motion anomaly (w) is $-2 \cdot 10^{-3} \text{ m s}^{-1}$, in agreement with composite observations. Sinking motions (over southern Africa) prevail on the back of the standing rossby wave, whilst a convective trough occurs near the apex at 55°E in the west Indian Ocean.

The key determinant of climatic anomalies over southern Africa (and Malawi) is the standing rossby wave, its links to the ITCZ, and the way it responds to regional SST patterns. The dry composite SST and precipitable water patterns, which reflect these features, are illustrated in fig 5-8. Negative values are noted in the higher latitudes of the Atlantic and Indian Oceans, and in the tropical Atlantic around 10°S, 0°E. A large area of positive SST anomalies is located in the west Indian Ocean with a centre of action at 10°S, 70°E. For precipitable water, negative values are found in the Mozambique Channel (25°S, 40°E), extending into Africa with a NW orientation. Positive values are found over the western Congo, extending SE to a centre of action in the west Indian Ocean at 20°S, 70°E. The half-wavelength is 3000 km, and the orientation is 300°-120°.

We propose the following conceptual model. A global El Nino finds regional expression around Africa through a warming of the tropical west Indian Ocean and a concurrent cooling of the tropical east Atlantic and the subtropical Agulhas region (Jury and Mason, 2001). A large-scale rossby wave train along 20°S interacts with the SST pattern during austral spring and summer to become anchored with a wavelength of $\sim 70^\circ$. Local centres of opposing action occur in the Mozambique Channel extending northwest across southern Africa and Malawi, and in the south Indian Ocean extending northwest toward east Africa and Kenya.

We suggest that the atmospheric circulation is coupled with standing rossby waves across the tropical ocean basins. Prior to and during El Nino conditions, the 'heave' of the thermocline is westward in both the Indian and Atlantic Oceans (Zebiak, 1993; Tourre, et al. 1999; Jury and Mason, 2001). Hence an axis of convection occurs east of Madagascar, whilst an axis of subsidence occurs over southern Africa, linked with cooler SST near Angola. Because this ocean-atmosphere coupling commences at least one season in advance, a degree of predictability is available for exploitation as demonstrated here.

Summary

Our study of climate variability over Malawi has revealed a sympathetic response with southern Africa and significant associations with ENSO and QBO phase in the period 1962 -

1995. Composite anomaly patterns with respect to dry seasons illustrate a mid-tropospheric ridge – trough pattern on 20°E and 55°E, respectively. The meandering of the sub-tropical jet stream around the standing rossby wave contributes to subsidence over southern Africa. We argue that this atmospheric circulation system is anchored to the SST pattern, which during dry years is comprised of positive anomalies over the west tropical Indian Ocean, and negative anomalies in the Agulhas region and in the tropical east Atlantic.

Precursor patterns are recognised through extraction of key area indices, and a predictive model is developed at three-month lead-time, which explains 55 % of variance in the 34-year period 1962 -1995. Residual errors are acceptable in the independent test periods, eg. forecasts are produced within the observed tercile 'bins' 10 of 16 years (62 %). Further work could include the updating of models to present, an analysis of the stability of association between rainfall and leading predictors, and numerical modelling experiments that seek to refine the concept of ocean-atmosphere coupling of standing rossby waves around Africa.

References

- Dilley, M, 1986, Usefulness of climate forecast information for drought mitigation and response from a donors' standpoint, Proceedings of a workshop on 'Reducing climate-related vulnerability in southern Africa', Zimbabwe, 30-37.
- Gill, A E, 1982, Atmosphere-Ocean Dynamics, Academic Press, Hague, 380 pp
- Goddard, L, and Graham, N E, 1999, The importance of the Indian Ocean for simulating rainfall anomalies over eastern and southern Africa. *J. Geophys. Res.*, 104, 19099-19116.
- Harangozo, S A, and Harrison, M S J, 1983, On the use of synoptic data in indicating the presence of cloud bands over southern Africa, *South African Journal of Science*, 79, 413-414
- Harrison, M S J, 1986, A synoptic climatology of southern African rainfall variability, PhD Thesis, Univ Witwatersrand, Johannesburg, 341 pp
- Hastenrath, S, Greishar, L, and VanHeerden, J, 1995, Prediction of summer rainfall over South Africa, *Journal of Climate*, 8, 1511-1518
- Jury, M R, 1996, Regional teleconnection patterns associated with summer rainfall over South Africa, Namibia, and Zimbabwe, *International Journal of Climatology*, 16, 135-153.
- Jury, M R, McQueen, C, and Levey, K, 1994, SOI and QBO signals in the African region, *Theoretical and Applied Climatology*, 50, 103-115
- Jury, M R, and Levey, K M, 1997, Vertical structure of wet spells over southern Africa, *Water S A*, 23, 51-55
- Jury, M R, Mulenga, H M, and Mason, S J, 1999, Exploratory long-range models to estimate summer climate variability over southern Africa, *J Climate*, 12, 1892-1899
- Jury, M R, and Nkosi, S E, 2000, Easterly flow in the tropical Indian Ocean and climate variability over south-east Africa, *Water SA*, 26, 147-152
- Jury, M R, 2001, Economic impacts of climate variability in South Africa and development of resource prediction models, (submitted to *Journal of Applied Meteorology*)

- Jury, M R, Melice, Jean-Luc, and Enfield, D B, 2001, Tropical monsoon indices around Africa: stability of ENSO associations and links with continental rainfall, (submitted to *Journal of Geophysical Research*)
- Jury, M R, and S J Mason, 2001, Evolution of ENSO teleconnections around southern Africa, (submitted to *Journal of Climate*)
- Kamdonyo, D, 1993, Use of percentiles in delineating the spatial and temporal extent of Malawi's drought, *Proceedings of 4th Conference on Land and Water Management in the SADC*, Windhoek, Namibia
- Lindesay, J A, and Harrison, M S J, 1986, The southern oscillation and South African rainfall, *South African Journal of Science*, 82, 196-198
- Lindesay, J A, and Jury, M R, 1991, Atmospheric circulation controls and characteristics of floods events in central South Africa, *International Journal of Climatology*, 11, 609-627
- Makarau, A, 1995, Intra-seasonal oscillatory modes of southern African summer circulation, PhD Thesis, University of Cape Town, 263 pp
- Makarau, A, and Jury, M R, 1997, Seasonal cycle of convective spells over southern African during austral summer, *International Journal of Climatology*, 17, 1317-1332.
- Malawi Ministry of Agriculture Report, 1993, The food situation in Malawi, Internal Government Report, Blantyre
- Mason, S J, 1992, Sea surface temperature and South African rainfall variability, PhD Thesis, Univ of Witwatersrand, 235 pp.
- Mason, S J, and Tyson, P D, 1992, The modulation of sea surface temperature and rainfall associations over Southern Africa with solar activity and the Quasi-biennial oscillation, *Journal of Geophysics Research*, 97, 5847-5356
- Mason, S J, 1997, A review of recent developments in seasonal forecasting of rainfall, *Water SA*, 23, 57-62
- Mason, S J, 1998, Seasonal forecasting of South African rainfall using a non-linear discriminant analysis model, *International Journal of Climatology*, 18, 147-164
- Mukherjee, B, Indira, K, Reddy, S R, and Murty, R, 1985, Quasi-biennial oscillation of stratospheric zonal wind and Indian summer monsoon, *Monthly Weather Review*, 113, 1421-1424.
- Mulenga, H A, 1998, Southern African climatic anomalies, summer rainfall and the Angola, low, PhD Thesis, University of Cape Town, 283 pp.
- Mwafulirwa, N D, 1999, Climate variability and predictability in tropical southern Africa with a focus on dry spells over Malawi, MSc Thesis, Univ. Zululand, 234 pp
- Naujokat, B, 1986, An update of the observed quasi-biennial oscillation of stratospheric winds over the tropics, *Journal of Atmospheric Science*, 43, 1873-1877
- Nicholson, S E, and Entekhabi, D, 1986, The quasi-periodic behaviour of rainfall variability in Africa and its relationship to the southern oscillation, *Archive for meteorology, geophysics and bio-climatology*, A34, 311-348

- Nkhokwe, J L, 1996, Predictability of inter-annual rainfall variability in Malawi, Internal report, Malawi Meteorological Service, Lilongwe
- Nyenzi, B S, 1988, Mechanisms of east African rainfall variability, PhD Thesis, Florida State Univ, 184 pp
- Ogallo, L J, Okolla, R E, and Wanjohi, D N, 1994, Characteristics of quasi-biennial oscillation over Kenya and predictability potential for seasonal rainfall, *Mausam*, 45, 57-62.
- Pathack, B, 1993, Modulation of summer rainfall over South Africa by global climatic processes, PhD Thesis, Univ Cape Town, 326 pp
- Preston-Whyte, R A and Tyson, P D, 1988, The atmosphere and weather of Southern Africa, Oxford University Press, Cape Town, 374 pp
- Rocha, A, 1992, The influence of global SSTs on the southern African summer climate, PhD Thesis, Univ Melbourne, Australia
- Torrance, J D, 1972, Malawi, Rhodesia, and Zambia, *in* *Climates of Africa*, ed. Griffiths, J F, *World Survey of Climatology*, 10, Elsevier, Amsterdam, 409-460
- Tourre Y. M, Rajagopalan, B and Kushnir, Y, 1999: Dominant Patterns of Climate Variability in the Atlantic Ocean Region During the Last 136 Years. *Journal of Climate*, 12, 2285-2299.
- Walker, N D, 1989, Sea surface temperature – rainfall relationships and associated atmosphere coupling mechanisms in the southern Africa region, PhD Thesis, Univ.Cape Town, South Africa
- Zebiak, S.E., 1993: Air-sea interaction in the equatorial Atlantic region. *Journal of Climate*, 8, 1567-1586.
- Zhakata, W, 1996, Impacts of climate variability and forecasting on agriculture, Proceedings of a workshop on 'Reducing climate-related vulnerability in southern Africa', Zimbabwe

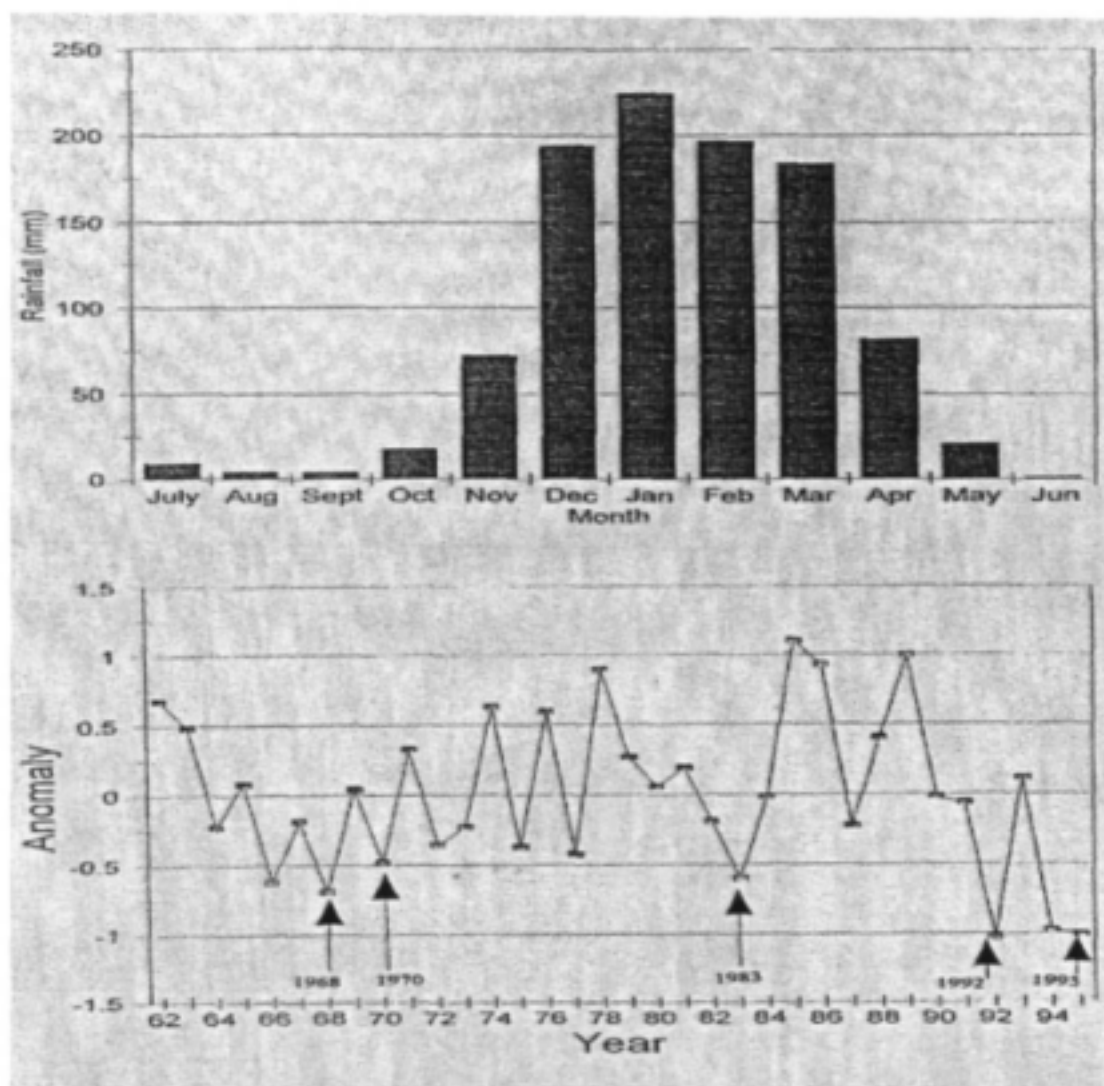


Fig 5-1 – Rainfall time series (a) long term mean monthly rainfall illustrating the seasonal cycle, and (b) standardised anomalies for the November to April period of each year.

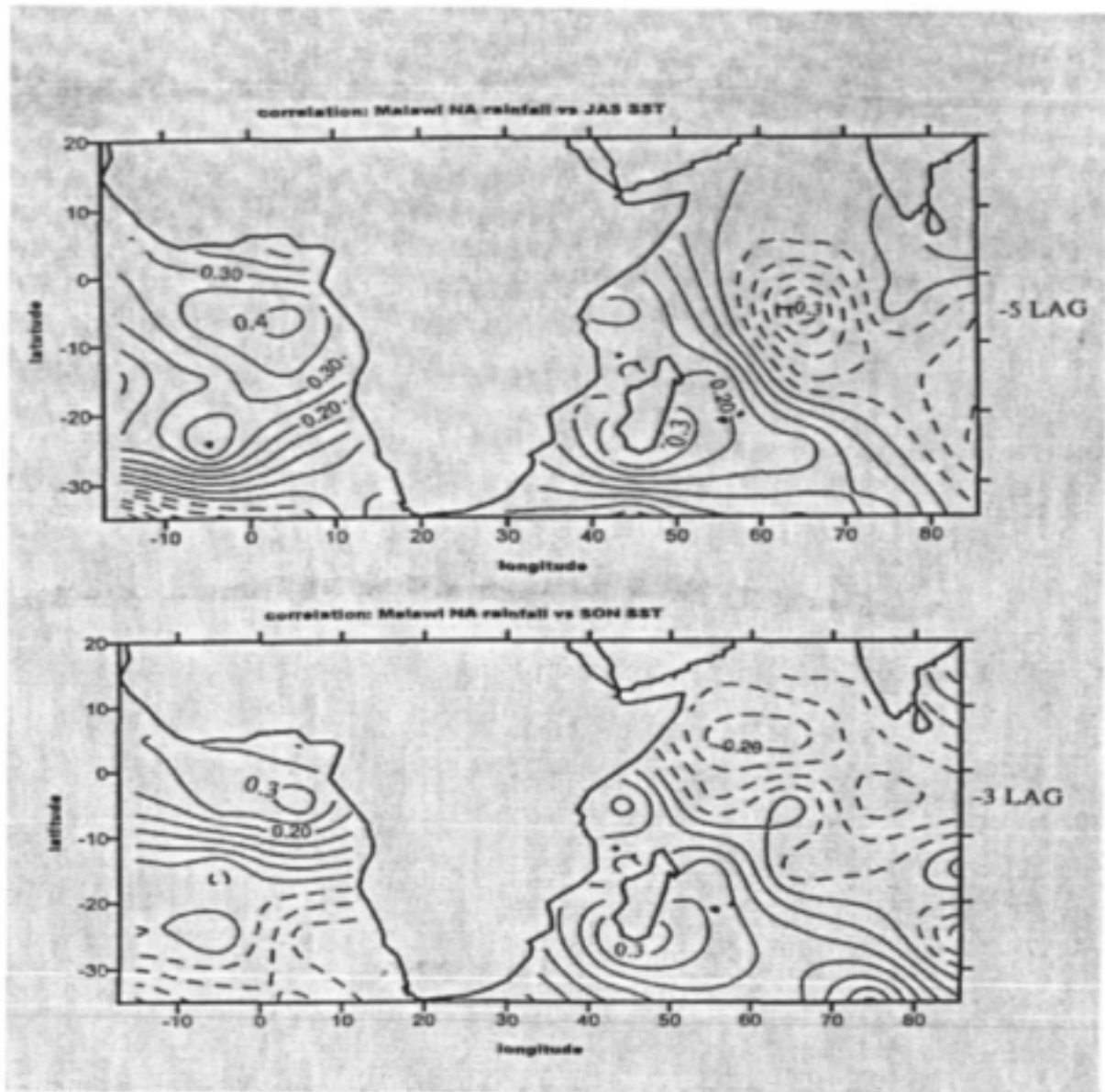


Fig 5-2 – Correlation maps for JAS and SON seasons for the COADS-based SST with respect to the Malawi summer rainfall index. Negative values are dashed. Values $> \pm 0.3$ are significant at 95% confidence limit.

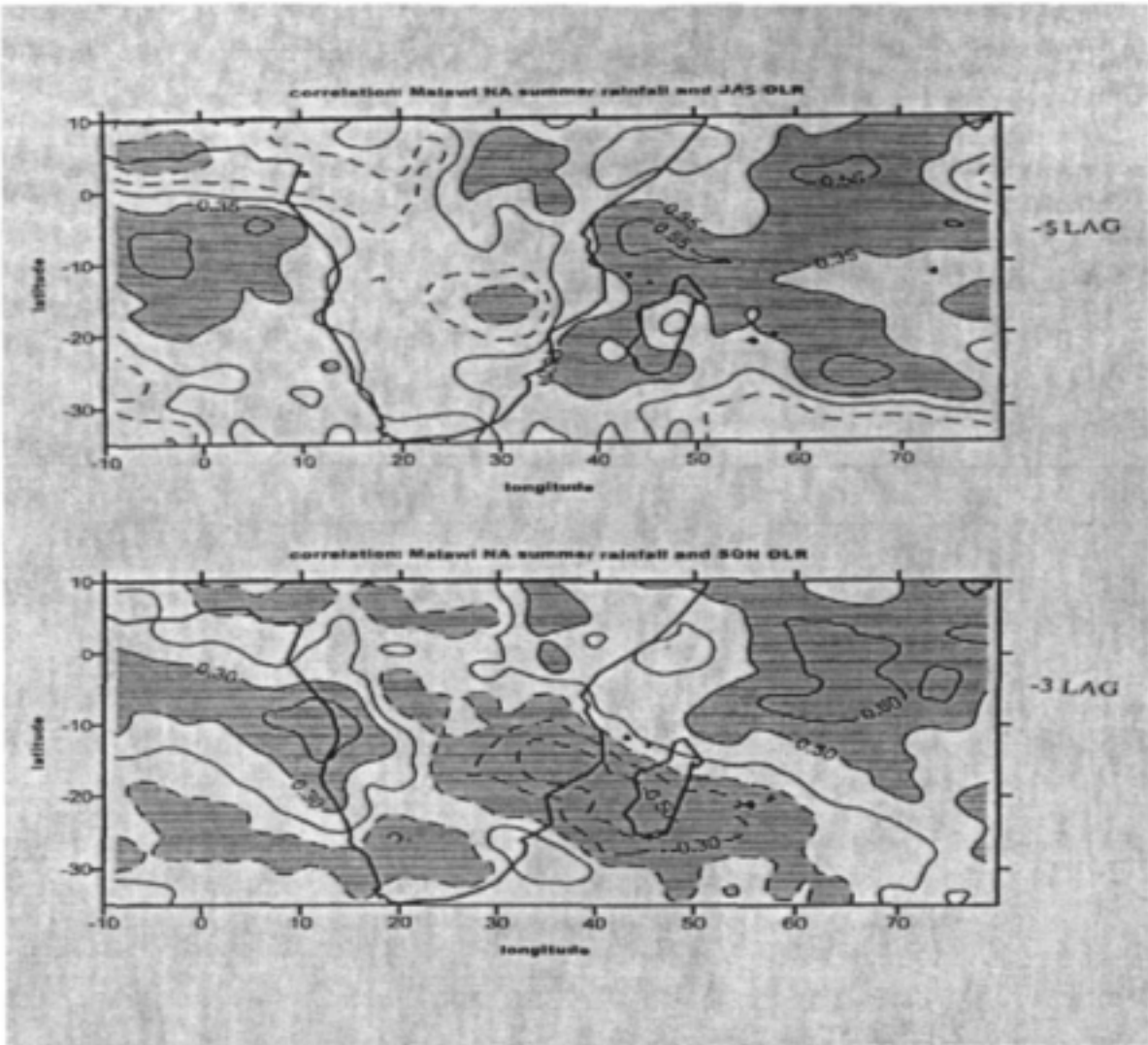


Fig 5-3 – Correlation maps for JAS and SON seasons for the NOAA satellite OLR field with respect to the Malawi summer rainfall index, as in figure 5-2. Values > 0.42 are significant at 95 %.

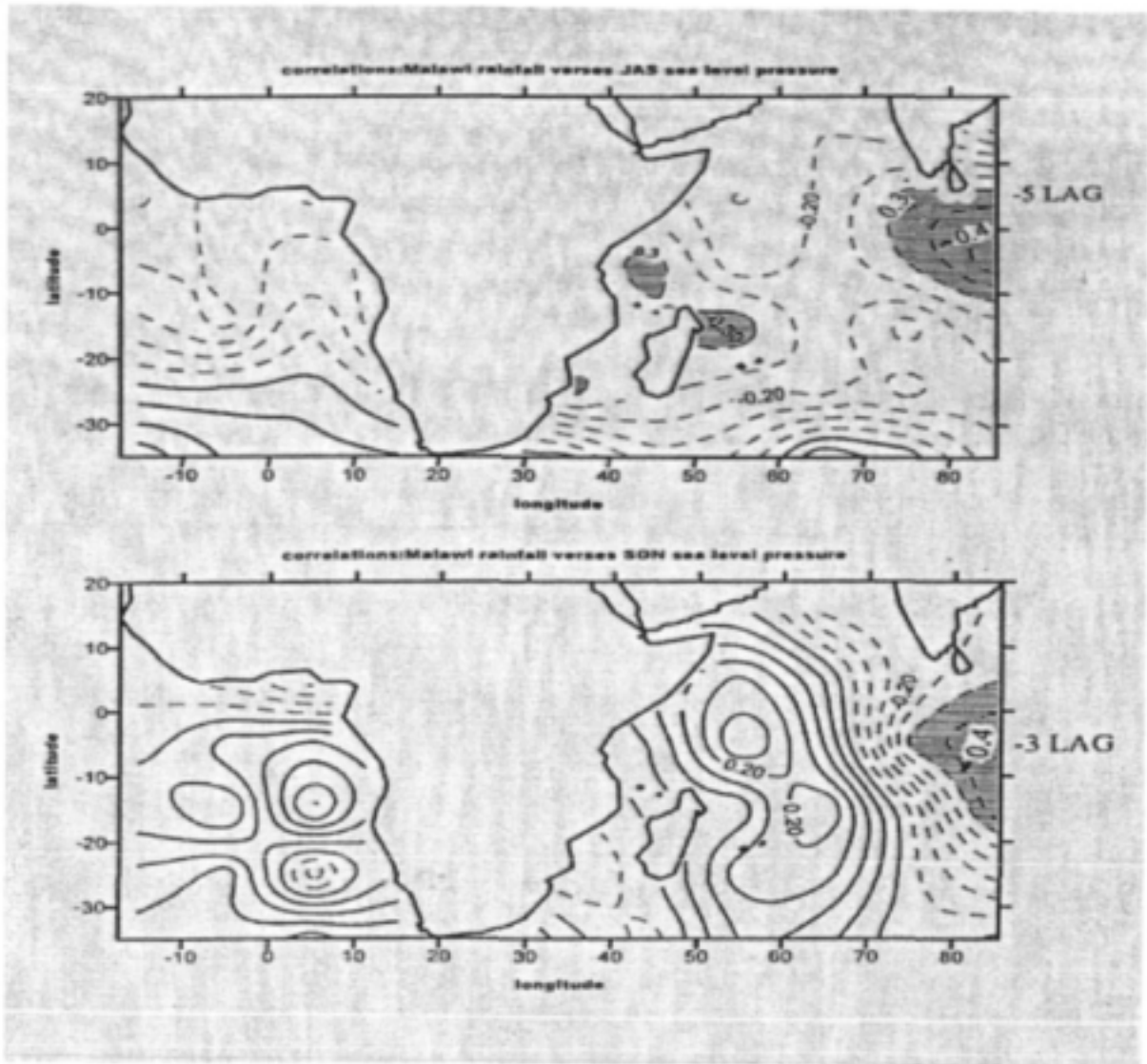


Fig 5-4 – Correlation maps for JAS and SON seasons for the COADS-based SLP field with respect to the Malawi summer rainfall index as in figure 5-2.

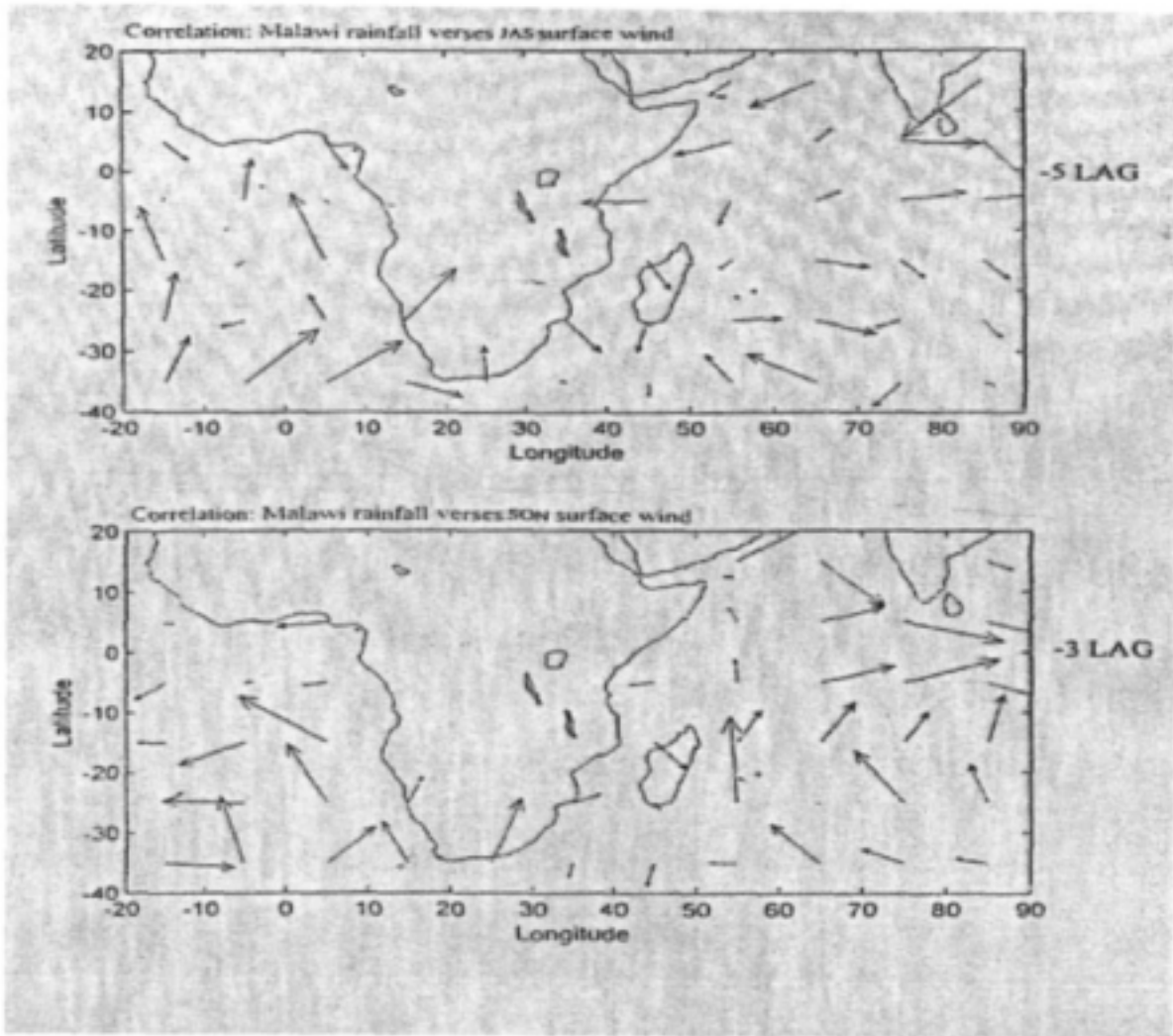


Fig 5-5 – Correlation maps for JAS and SON seasons for the COADS-based vector wind field with respect of the Malawi summer rainfall index, as in figure 5-2. Vector lengths correspond to significance level and directions are reconstructed from U and V values.

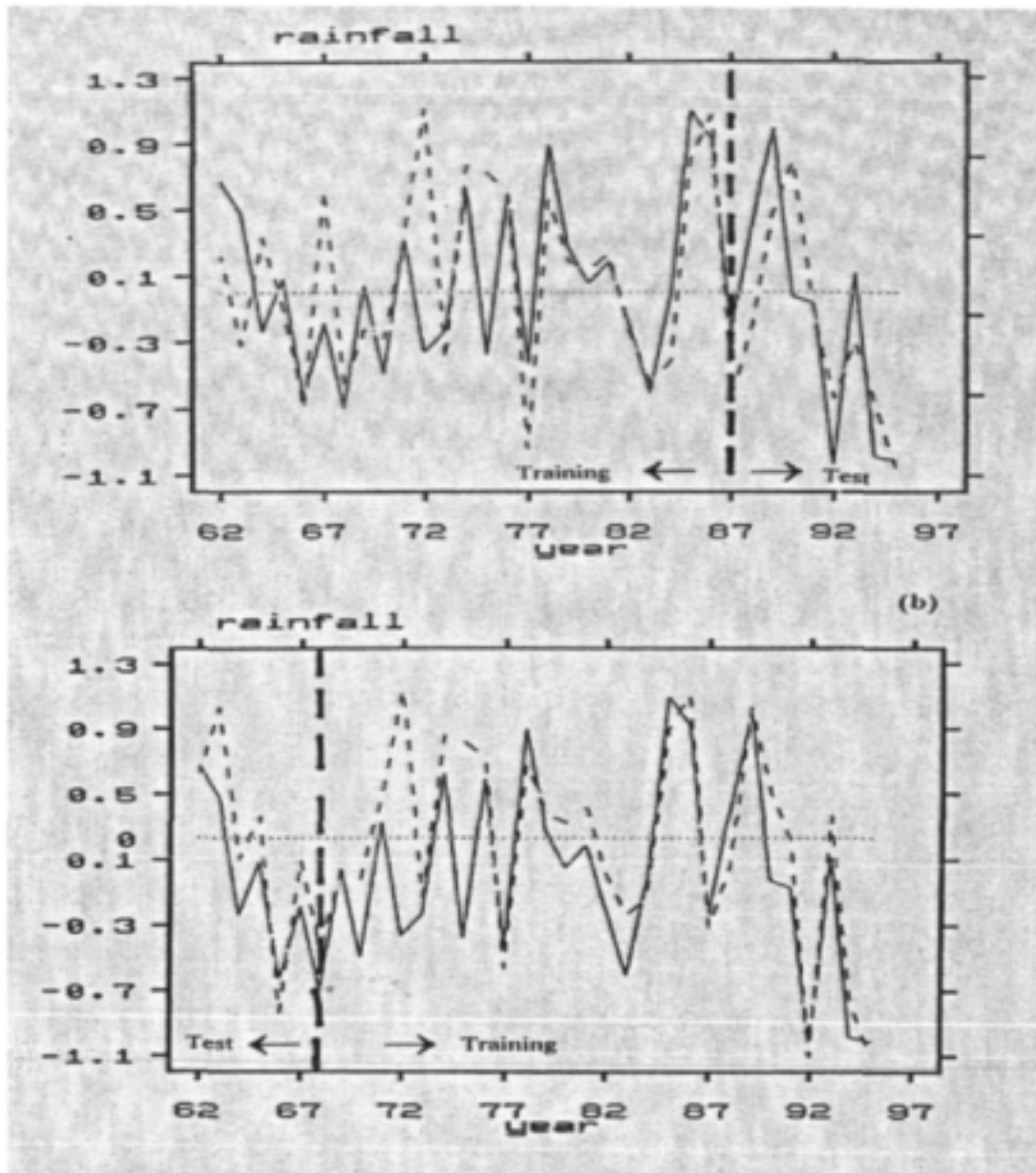


Fig 5-6 – Predictive model output (dashed) compared with the observed summer rainfall index (solid) illustrating a reasonable fit at 3 month lead time. In (a) the test period is the last eight years, in (b) the first eight.

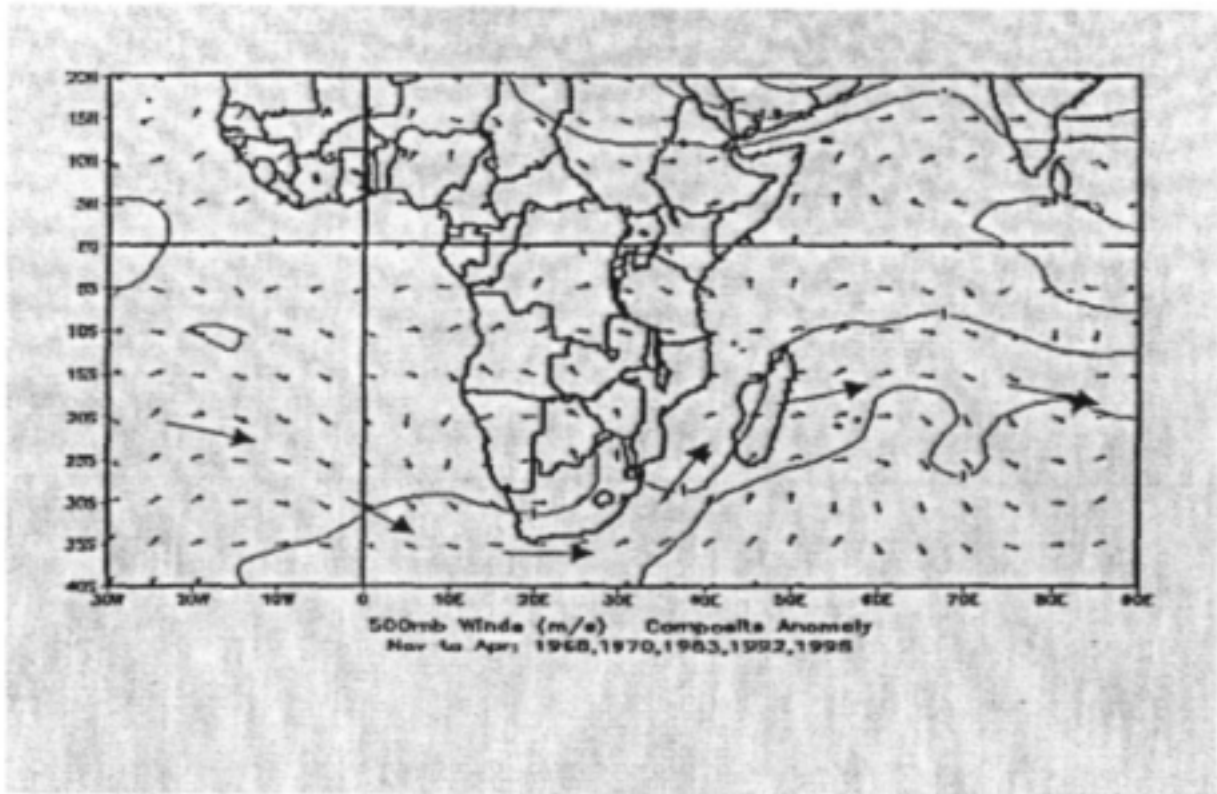


Fig 5-7 – Composite analysis, illustrating 500 hPa winds during dry summers. A meandering axis of westerly flow anomalies is noted over southeast Africa.

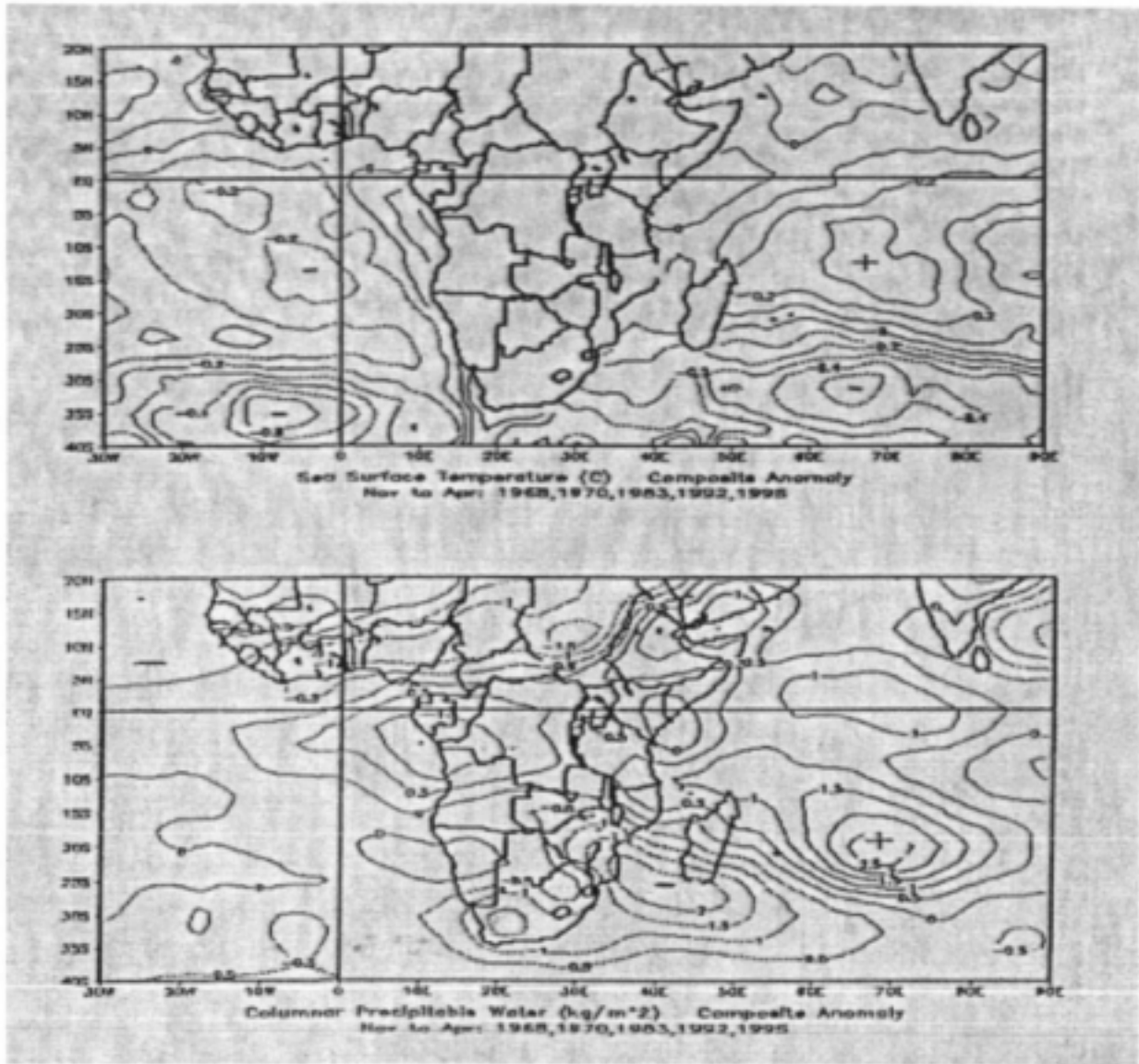


Fig 5-8 – Composite analysis, illustrating (a) SST and (b) precipitable water during dry summers as in figure 5-7. The standing rossby wave is reflected in alternating NW-SE axes of warm (moist), cool (dry) SST (atmospheric conditions). This is a coupled ocean-atmosphere system.

Introduction to Lake variations study

Lakes and rivers in tropical southern Africa provide much needed water resources, but the supply varies from year to year depending on prevailing climatic conditions. Summer rainfall is the main recharging system, contributed by the inter-tropical convergence zone (ITCZ) and cloud bands connecting equatorial convection with temperate troughs (Harrison 1986). Variations in rainfall create a range of economic impacts, and recent observations suggest that tropical southern Africa is prone to widespread drought and flood events (Jury et al 1992). Although many studies have focussed on the climate of the region, few have addressed the hydrologic responses. There is recent evidence for changes in the climate of Africa based on variations in the levels of inland lakes (Maidment 1993). Lake levels respond to rainfall and to human interference and consumption, so care is needed in relating water levels directly to climate.

Water supplies in southern Africa are relatively under-exploited for human use either by agriculture through irrigation or for consumption through damming. Water resources of economic importance include Lake Malawi, Lake Kariba, the Zambezi River, the Orange River, and a number of smaller rivers over a 5 M km² area of tropical southern Africa (Fig 5-9). The Zambezi stretches a distance of 2660 km across five countries (9-20°S, 17-36°E), with a drainage area of 1.3 10⁶ km², a mean discharge of 2.5 10³ m³ s⁻¹, and a hydro-electricity capacity near 10⁴ Mw (Gandolfi and Salewicz 1991). The Zambezi River divides the wet tropics in the north from the arid sub-tropics to the south. The mean annual rainfall over its catchment is about 1000 mm, and the potential evaporation is 870 mm. The rainfall / run-off coefficient is 13 % averaged over the basin and at Victoria Falls the mean annual run-off is 24 km³ (Liebaert 1997).

Lake Malawi lies at 474 m above sea level in the African rift valley, with a surface area of 2.8 10⁴ km², a volume of 8 10³ km³, a land catchment area of 9.6 10⁴ km², a length of 550 km and a breadth of 15-80 km, and borders three countries. Six small rivers create an annual inflow of ~ 360 m³ s⁻¹ to the lake, and one river (Shire) drains southward over a weir to the Zambezi. The vegetative cover across this region is woodland (*Brachystegia*, etc) interspersed with dense savanna, some of which is cleared for cultivation to feed ~ 20 M people. The catchment experiences potential evaporation rates around 1600 mm (Mandeville and Batchelor 1990). The mean annual rainfall around Lake Malawi ranges from 600 mm to 2500 mm and its variability is the primary factor affecting inflows. In 1949-50, 1972, 1967 and 1992 low rainfall resulted in declining lake levels, whilst in 1961-63, 1978-80, and 1989, high rainfall produced elevated levels. The peak flood of 1979 resulted in many lakeshore developments being inundated.

To establish the water balance, the rate of change of lake volume with time is related to the water input and output rates: $dV / dt = (R+P) - (D+E)$, where R is runoff, P is precipitation, D is discharge rate, and E is surface evaporation. The equilibrium lake level is given by: $L = (R+A(P - E))$ where A is area, and D is neglected. Evaporative losses are controlled by the available surface energy, and dependent on temperature, humidity and wind speed. Run-off is computed by dividing the inflow by the catchment area. Estimates for water balance in Lake Malawi according to Kidd (1983) include: R = +1100 mm, P = +1414 mm, E = -2264, G (Shire outflow) -418 mm, leaving a net storage of +12 mm. Departures from mean conditions are

generated by cumulative effects from previous years and by fluctuations in the intensity of run-off during the rainy season. These can be decomposed into trends, quasi-cyclic variations, stochastic auto-regressive properties and chaotic or random behaviour.

The regional climate is influenced by the topography and surface fluxes, and the manner in which the prevailing moisture transport is organised by weather systems (Torrance 1972). In the winter season from May to August, a high pressure system dominates the area and divergent southeast trade winds induce persistently dry conditions. Mean temperatures in spring (September-October) exceed 30 C and windy conditions enhance evaporative losses then. By summer the ITCZ shifts southward to 10°-15°S and air masses from the Congo basin and the west Indian Ocean meet over Malawi, causing heavy rainfall at times. The terrestrial moisture flux is governed by monsoon responses over the adjacent Atlantic and Indian Oceans. A strengthening of upper easterly flow during El Nino Southern Oscillation (ENSO) cool phase and a concomitant increase in the sea-to-land temperature gradient results in an enhanced supply of moisture over tropical southern Africa (Hastenrath et al 1993) and a replenishment of water resources.

In this study we analyse variations in the level of Lake Malawi and the flow of the Zambezi River at Victoria Falls, and establish the nature and context of water resource variability in terms of regional climate. Our objective is to study climatic patterns contributing to flood events and to develop forecast models for hydrological resources over tropical southern Africa.

Data and Methods

Monthly lake level data were obtained from the Malawi Water Resources Dept. for the period 1916-1995 for three stations along Lake Malawi. Levels are measured above a reference, the Shire Weir Datum. Although water level records started then, the period prior to 1937 exhibits a linear upward trend as the lake filled to the weir level. Thereafter a more cyclical, climate-impacted behaviour is noted. In our analysis an inflow index is computed from the difference in the level from the month with the lowest data for the year (~ November) to the month with the highest level (usually May). The data are then standardised to produce anomalies by subtracting the long-term mean from each year and dividing by the standard deviation. Annual stream flow totals for the Zambezi at Victoria Falls were obtained from the Namibian Dept. of Hydrology for the period 1915-1996. Annual standardised departures for a matching period were computed. From conventional surface weather data, monthly rainfall was obtained for a group of stations along the shores of Lake Malawi. Monthly potential evaporation was computed using the Penman formulae.

The lake level time series is analysed for variability using various techniques: auto-correlation for persistence, linear regression for trends, and spectral analysis for cyclic behaviour. The remaining variance is assumed to have both stochastic and chaotic components. The lake inflow index is cross-correlated with various environmental indices to determine what part of the variability is predictable and linked with global and regional climate at one season lead-time.

To investigate regional climate patterns contributing to lake inflows, National Centre for Environmental Prediction (NCEP) reanalysis data are utilised to derive composite fields of wind

and precipitable water. The data are at 2.5° resolution and suitable for use in describing the regional climate over tropical southern Africa. Years for inclusion in the composite analysis are selected by ranking the inflow index time series. On consideration of the composite and correlation results, a group of candidate 'predictors' is extracted for comparison with the lake inflow index. A multi-variate model is developed using step-wise insertion to forecast changes in lake inflow at one season lead-time.

Results

Time variability of water resources

The seasonal cycle of inflows and inter-annual variability for Lake Malawi is illustrated in fig 5-10 over the 1937-1995 period. The 58-year mean incremental increase in lake level is typically +0.17 m in January, and +0.24 m in each of the three months: February, March and April. December and May exhibit small increases, whilst lake levels fall during winter and spring, June through November, peaking at -0.21 m in July. The inter-annual variability exhibits a biennial oscillation (2.0-2.6 years) and a weaker oscillation around 5.6 years in the period 1937-1995. Lake inflows were at a minimum in 1949 and a maximum in 1979. The years with highest lake inflows, in the period of data overlap with NCEP, include 1962, 1963, 1974, 1978, and 1989. A frequency distribution of inflow years (not shown) indicates a prevalence of cases in the 0 to -1 sigma range, and a smaller group of cases in the +1 to +2 sigma range. The auto-correlation of the inflow time series at +1 year lag is near zero, indicating that persistence is limited by biennial oscillations and the intervening dry winter season. Comparing an average of all lakeside summer rainfall data with the inflow index, a correlation of +0.77 is achieved. The degrees of freedom is 56, so the r-value is significant at the 99% confidence limit. The strong relationship indicates that lake inflows are useful in gauging climate variability in the region. The lake acts as a raingauge, when incremental changes are considered. Incremental decreases in lake level and outflows via the Shire River were similarly analysed, but for the sake of brevity will not be reported here. In summary, Lake Malawi has a 'short memory' and is quite sensitive to inter-annual rainfall variability. The relation of Shire outflows to absolute lake levels is high due to hydraulic pressure, but is relatively low with the inflow index, as expected.

The temporal nature of Zambezi River streamflow is illustrated in fig 5-11. Farquharson and Sutcliffe (1998) suggests that its high amplitude of variability is attributable to erratic rainfall and high evaporation, owing to warm temperatures and the elevated topography. Flows decline as low as 14 B m^3 in 1915 and peak at 73 B m^3 in 1958. 1958 appears as an inflection point, with a rising trend before and a decline thereafter. A 80-100 year cycle is found in proxy data for the Zambezi and other African rivers (Nicholson and Yin 1998, Tyson 2000). Our 1958 inflection point appears to be a part of this low frequency cycle. The histogram of Zambezi streamflows is skewed toward the 0 to -1 sigma range, and flood events above +2 sigma are rare. Spectral analysis of the time series of annual streamflows reveals weak cycles at 2.5, 5.8 and 9.7 yrs. Relationships with Zambezi basin-averaged rainfall are strong with an r-value of +0.74. The cross-correlation of Zambezi streamflow with Lake Malawi inflow is relatively high at +0.53, suggesting that hydrological impacts occur on continental scales, in agreement with Sutcliffe and

Knot (1987). The Zambezi's higher degree of persistence (auto-correlation at +1 year lag = +0.42) is distinct from that found for Lake Malawi. We attribute the persistence to the larger basin scale and to inflow from Angola being partially governed by Atlantic decadal variability (Tourre et al 1999).

Composite analysis of high lake inflow years

A composite analysis is conducted using NCEP reanalysis data for the 'wet' summers (DJF): 1962, 1963, 1974, 1978, 1979, and 1989. The historical mean is subtracted to produce anomaly fields for precipitable water and winds over the domain 10°N – 40°S, 30°W – 90°E. It should be noted that the composite sea surface temperature anomaly pattern is relatively weak around Africa. The precipitable water pattern for wet summers is shown in fig 5-12 and illustrates a broad moist tongue extending from east to southern Africa. Its axis of orientation is along the eastern escarpment and NE monsoon flow. Within this moist anomaly, a smaller NW-SE-oriented positive axis is observed over Mozambique around 25°S, 35°E. This 'Mozambican trough' extends toward Zimbabwe and Malawi, and is a regular feature of the summer climate of southern Africa (Washington and Todd, 1999). The precipitable water composite results suggest that wet summers are contributed by steady monsoonal inflows triggered by a sub-tropical standing wave.

The wet composite circulation patterns are described using 3 and 12 km level data. Composite winds at the 700 hPa level (Fig 5-12) reveal a low pressure cell in a clockwise circulation over the central plateau (Botswana). Northerly flow on its eastward flank corresponds with the Mozambican trough axis. A westerly flow anomaly occurs along 10°S, whilst easterlies are found at higher latitudes. Together these zonal flows create cyclonic vorticity in the lower troposphere over tropical southern Africa. At the upper level (Fig 5-12), an axis of easterly winds occurs along 20°S, with an outflow channel branching poleward over South Africa. The easterly axis extends into the tropical Atlantic and is indicative of ENSO cool phase conditions (Jury and Mason 2001).

Vertical sections of the composite circulation anomaly are given in fig 5-13. The E-W zonal wind section reveals a deep layer of westerly flow over tropical southern Africa and a shallow layer of easterlies aloft. The zonal overturning appears connected to the Atlantic, where precipitable water anomalies are negative. The N-S meridional wind section illustrates poleward flow induced by the Mozambican trough. Maximum negative values occur around 25°S in the 300-500 hPa layer. V-wind anomalies are weak elsewhere and suggest that the Hadley circulation is a lower order determinant of wet summers.

Development of predictive models

With increasing concern about climate variability in tropical southern Africa, regional climatic factors underlying the temporal fluctuations have been assessed with respect to key hydrological resources. Changes in the level of Lake Malawi and Zambezi River streamflows, driven by basin-averaged rainfall, exhibit spectral energy in 2-10 year periods consistent with cycles found in the stratospheric quasi-biennial oscillation (QBO), the global ENSO phenomenon, and the solar cycle. Incremental inflows in Lake Malawi are offset by evaporation

during the dry season. Biennial fluctuations ensure that each rainy season commences with little residual effect from previous years. Based on a suite of six cases, composite NCEP reanalysis fields provide a number of clues to climatic conditions underlying wet summers. Foremost amongst these is a tropical circulation pattern comprised of low level westerlies, upper easterlies and a moist trough over Mozambique. The climatic patterns are tracked to the precursor spring season, and variables are extracted for inclusion in multivariate forecast models, designed to 'fit' changes in Lake Malawi inflows. Following a careful screening process from analysis of precursor season (JAS) environmental fields (Gwazantini 1999), candidate predictors are extracted: swAst, eAst, eAp, cAu₂₀₀, elp, swlp, clu, clst, slst; where the 1st letter refers to position, the second to ocean, and the 3rd to parameter. In addition global indices: SOI, QBO and nino3 (Pacific SST) are utilised. These are combined into regression formulae using a forward step-wise insertion technique (Jury et al 1999). A set of rules are applied in the formulation process:

- Statistical models should be developed for 'large' area-averages (catchments) e.g. > 3 deg². Regionalisation (eg. rotated principal component analysis, etc) should be performed on continental and ocean-basin scale.
- Predictors should be drawn from 'large' areas e.g. > 10 deg² and confined to the tropics (< 15 lat.) where convective responses are exponential. Predictors other than SST may be used, e.g. SLP, U / V winds, global indices, etc.
- Target and predictor data should be filtered to three-month averages to remove intra-seasonal oscillations. The lead-time preferred by users is three months, e.g. JAS for summer (DJF).
- The training period should exceed 30 years and the number of candidate predictors should be less than half this (eg. 15), to minimise artificial skill.
- The number of predictors in the algorithm can not exceed three and may not be cross-correlated such that $r^2 > 20\%$.
- A hindcast r^2 fit > 40 % should be achieved. If the model falls below this level, then confidence in its use must be limited.
- Independent validation tests are conducted by 'blanking out' a number of years and predicting those based on the remainder. Performance is judged by tercile categories 'hit'.

Applying these rules to our set of predictors, two JAS-season algorithms are produced:

$$Lm = -.34(nino3) + .34(slst) - .29(swlp) \quad (1)$$

$$Lm = -.50(cAu2) - .47(eAp) + .35(swAst) \quad (2)$$

Model 1. obtains a r^2 fit of 43% and a Durbin-Watson value of 2.2 in the period 1958-1993. The predictors in order of appearance include the nino3 SST in the eastern Pacific, southern Indian Ocean SST and SW Indian Ocean surface pressure. The sign of the coefficient indicates how the predictor contributes to increased lake levels (eg. cooler Pacific, warmer south Indian Ocean and lower pressure over the SW Indian Ocean). Performing an independent test on the last 18 years (fig 5-14), model 1. produces a high r^2 fit of 70%. Model 2 obtains a r^2 value of 53%, but its fit during an independent test period is not as good at 60%. The variables in model 2 include the

central Atlantic upper zonal wind, east Atlantic surface pressure and the southwest Atlantic SST. Increased lake levels correspond with upper easterly winds over the tropical Atlantic, lower pressure over the east Atlantic, and higher SST in the SW Atlantic. Interestingly, all predictors in model 1. are from the Indo-Pacific domain, whilst all predictors in model 2. are from the Atlantic.

Summary

In this chapter we have analysed variations in key water resources in tropical southern Africa. Close relationships were found for lake inflows, river streamflows and catchment rainfall as expected. Inflows to Lake Malawi exhibited little persistence and weak cyclical behaviour at periods of 2-10 years. Hydrological resources were found to be sensitive to interannual variations of climate and the regional structure of moisture and circulation. Wet years were examined and found to be characterised by an influx of moist monsoonal air from the NE, a zonal overturning cell connected to the tropical south Atlantic, and a subtropical trough over Mozambique. Predictor indices were extracted from environmental fields exhibiting precursor signals at one season lead-time. An outcome was the development of predictive models to forecast changes in the level of Lake Malawi. A more general outcome, particularly in the context of this WRC report, was the generation of meaningful information on the relative influence of climatic fluctuations on water resources across tropical southern Africa.

Many issues raised in this study deserve further examination. For example, a detailed analysis of flood events, coupled with an objective technique to pinpoint climatic signals and refine statistical models would be of benefit. Such research would improve the uptake of forecasts by hydrological managers. In addition to further statistical analyses, conceptual and numerical modelling of hydrological variability is a necessity in tropical southern Africa, where less than 10% of rainfall is converted to run-off and where water demand by a growing population will result in shortages in a few decades.

References

- Farquharson, F, and Sutcliffe, J V, 1998, Regional variations of African river flows, in *Proceedings on Water Resources Variability in Africa*, ed. Servat et al, IAHS 252, Abidjan, 161-170
- Gandolfi, C, and Salewicz, K A, 1991, *Water resources management in the Zambezi Valley*, IAHS publication 201, 13-24
- Gwanzantini, M E, 1999, *An evaluation of lake and river levels as indicators of climate variability in tropical southern Africa*, MSc thesis, 104 pp.
- Harrison, M J, 1986, *A synoptic climatology of South African rainfall variability*, PhD Thesis, University of Witwatersrand, 341 pp.
- Hastenrath, S, Nicklis, A, and Greisher, L, 1993, Atmosphere-hydrosphere mechanisms of climate anomalies in the western equatorial Indian Ocean, *Journal of Geophysical Research*, 98, 20219-20235.

- Jury, M R, Pathack, B M, and Sohn, B J, 1992, Spatial structure and interannual variability of summer convection over southern Africa and the SW Indian Ocean, *South African Journal of Science*, 88, 275-280
- Jury, M R, Mulenga, H M, and Mason, S J, 1999, Exploratory long-range models to estimate summer climate variability over southern Africa, *Journal of Climate*, 12, 1892-1899
- Jury, M R, and S J Mason, 2001, Evolution of ENSO teleconnections around southern Africa, (submitted to *Journal of Climate*)
- Kidd, C H, 1983, Advancement of hydrological services in Malawi – a water resources evaluation of Lake Malawi and the Shire River, WMO report, Geneva
- Liebaert, B, 1997, Sharing resources in the SADC, *The Courier ACP-EU publication* 161, 1-4
- Maidment, D R, 1993, *Handbook of Hydrology*, McGraw-Hill Publ, New York, 133 pp.
- Mandeville, A N, and Batchelor, C H, 1990, Estimation of evapo-transpiration in Malawi, Report 110, Institute of Hydrology, London.
- Nicholson, S, and Yin, X, 1998, Variation of African lakes during the last two centuries, , in *Proceedings on Water Resources Variability in Africa*, ed. Servat et al, IAHS 252, Abidjan, 181-187
- Sutcliffe, J V, and Knot, D G, 1987, Historical variations in African water resources, *Hydrological Sciences*, 463-475
- Torrance, J D, 1972, Malawi, Rhodesia and Zambia, in *World Survey of Climatology*, 10, 409-460
- Tourre Y. M, Rajagopalan, B and Kushnir, Y, 1999: Dominant Patterns of Climate Variability in the Atlantic Ocean Region During the Last 136 Years. *Journal of Climate*, 12, 2285-2299.
- Tyson, P D, Washington, R and Cooper, G, 2000, Centennial variability of climate in southern Africa, *Proceedings of the SASAS conference*, Pretoria.
- Washington, R and Todd, M C, 1999, Tropical temperate links in southern African and southwest Indian Ocean daily rainfall, *International Journal of Climatology*, 19, 1601-1616.

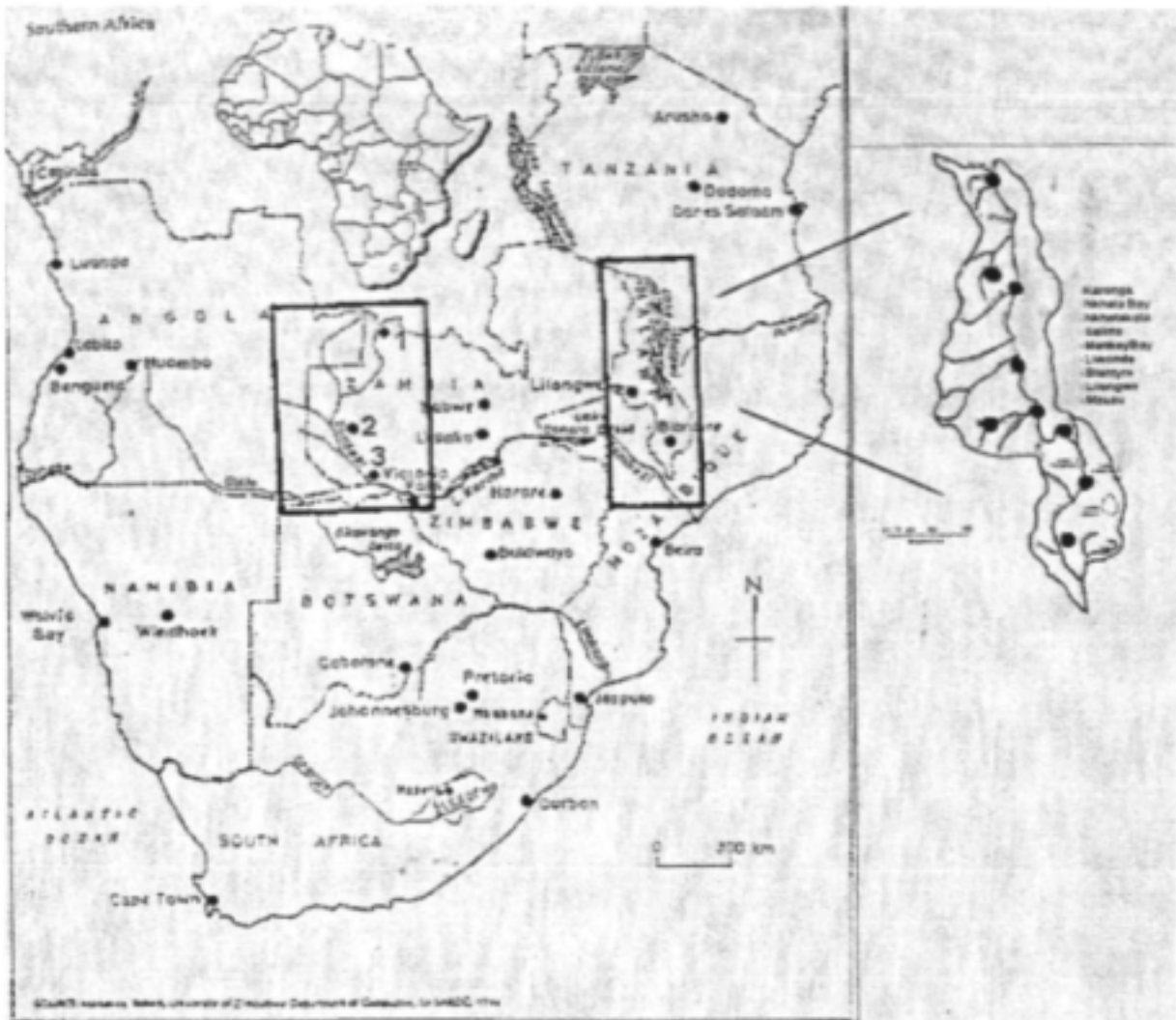


Fig 5-9 – Location map of key hydrological resources over tropical southern Africa

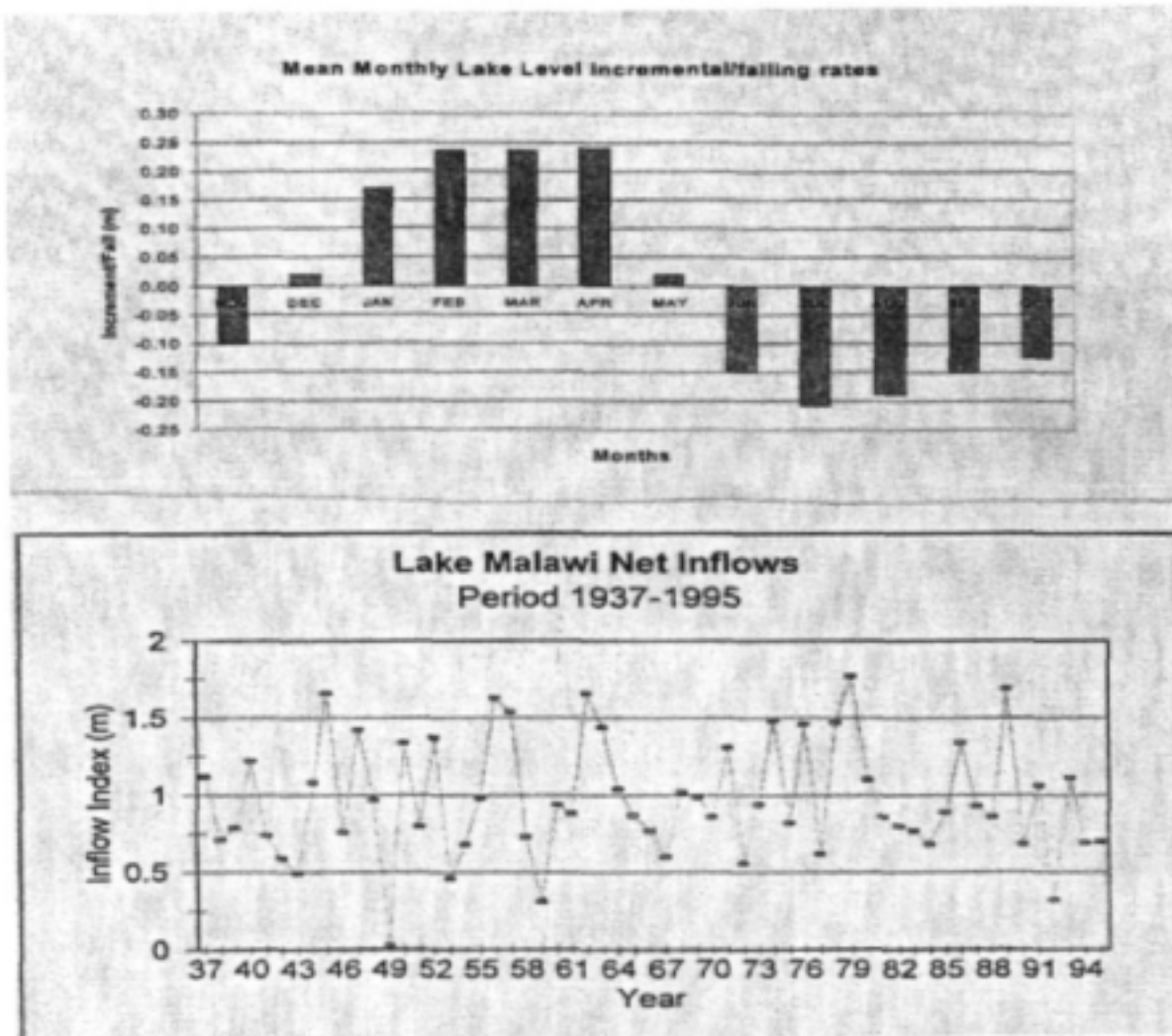


Fig 5-10 – Mean monthly incremental changes in Lake Malawi (top) and summer inflows in the period 1937-1995.

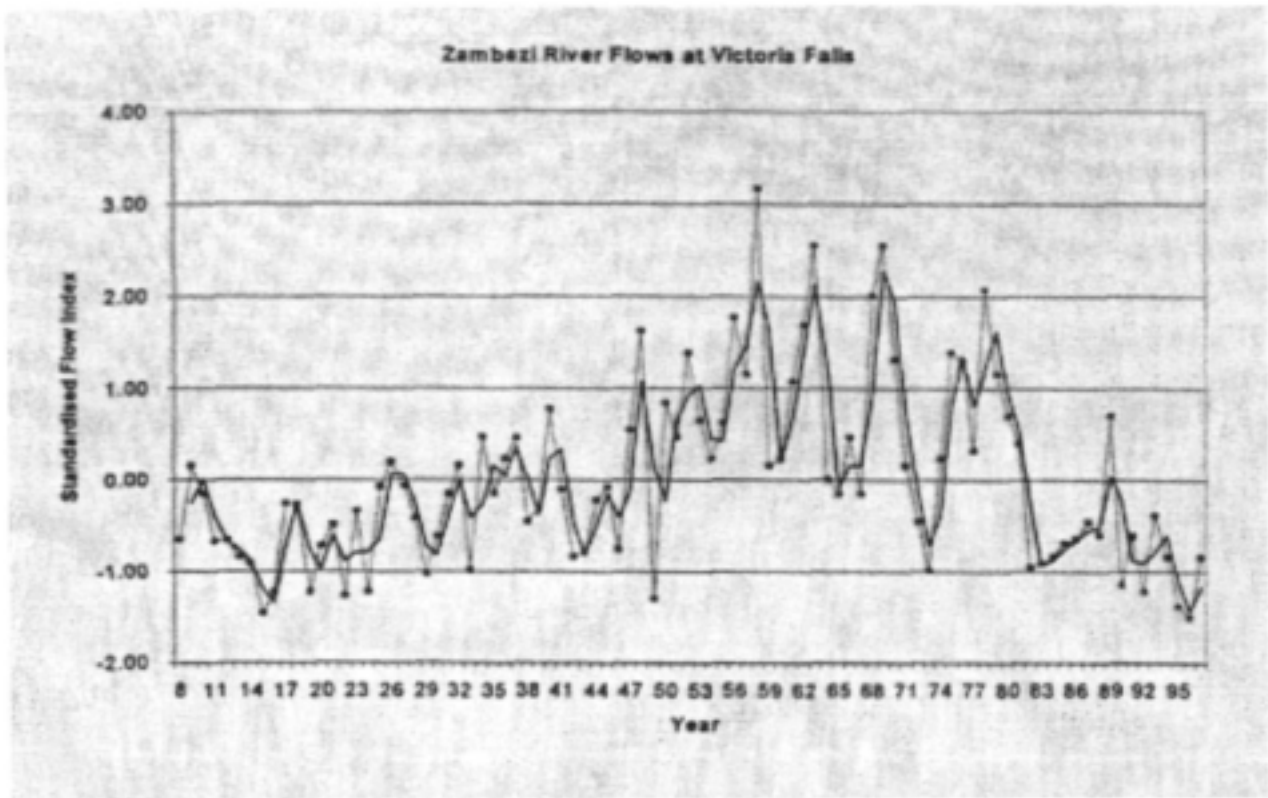


Fig 5-11 – Zambezi River annual streamflows at Victoria Falls (thin) and filtered with 3 pt running mean (thick). The flow data are normalised by the mean and standard deviation.

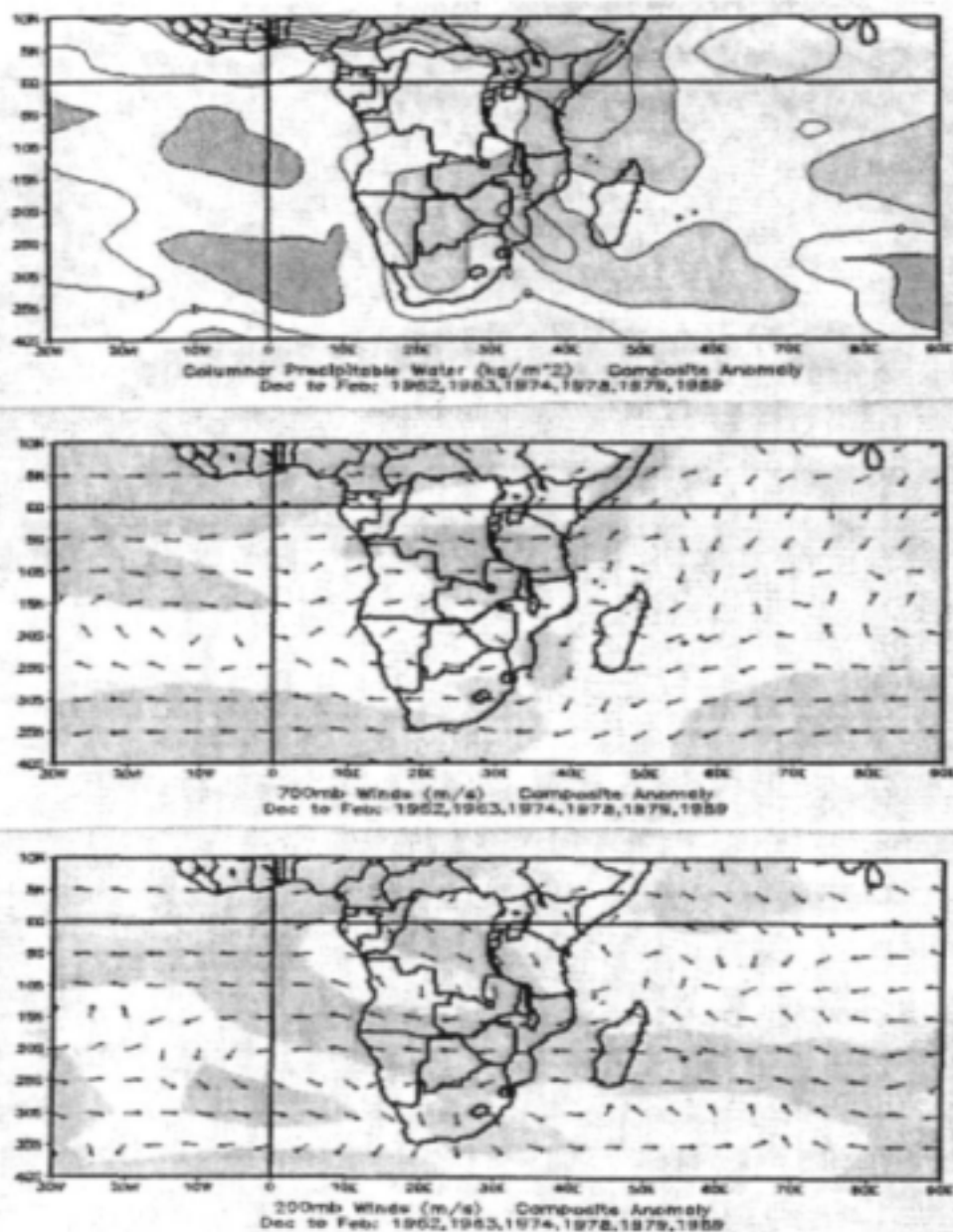


Fig 5-12 – NCEP composite anomalies for wet years for a) precipitable water), b) 700 hPa winds, and c) 200 hPa winds. Light shading in a) represents positive anomalies, dark = negative, contour interval is 1 mm. Light shading in b) and c) refers to wind anomalies $> 1 \text{ m s}^{-1}$.

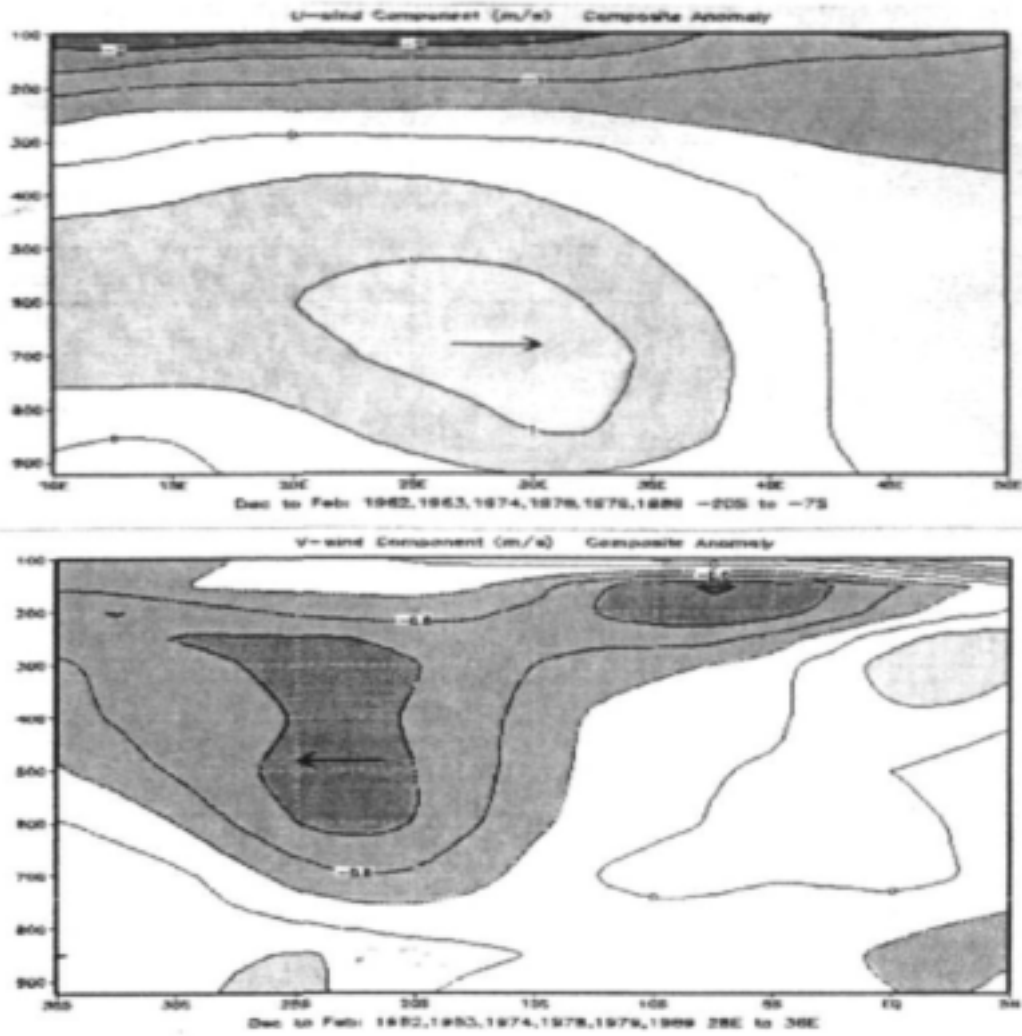


Fig 5-13 – E-W (top) and N-S vertical sections of zonal and meridional winds, respectively, indicating Walker-type overturning and trough activity. Contour interval is 0.5 and 0.4 m s^{-1} respectively.

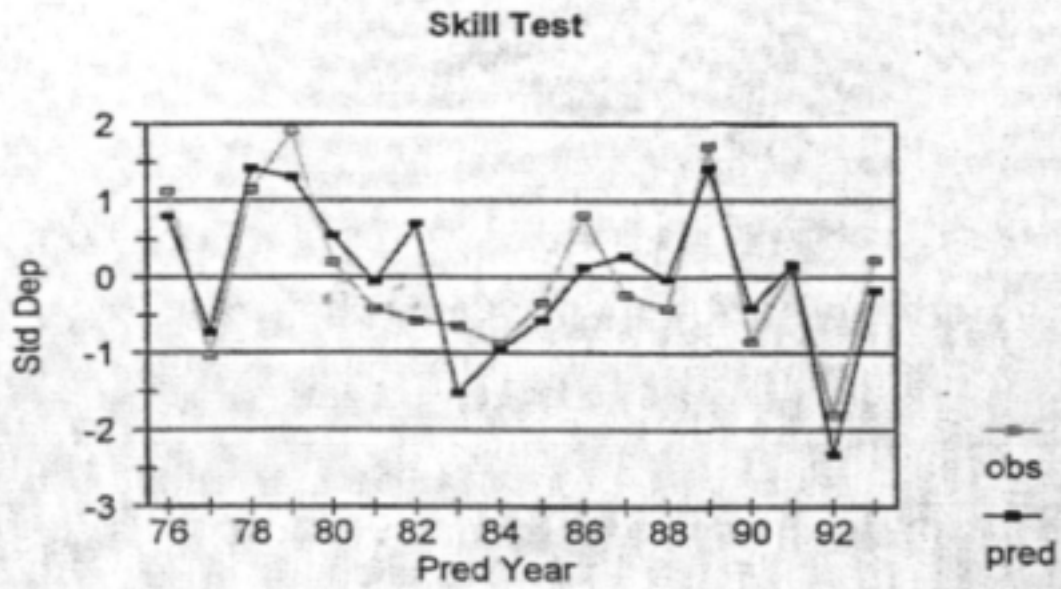


Fig 5-14 – Validation test for model (1) predicting inflows to Lake Malawi at one-season lead-time. The test is a jack-knife type given the length of record. In this method, one year at a time is removed and then predicted based on the remainder.

Chapter 6 – Analyses of monsoon indices and ENSO stability using NCEP data

Consequent to the above studies, a detailed understanding of the value of regional predictors in forecast models for southern African climate is gained. However little is known on their stability of association with ENSO. Furthermore, interactions between the monsoons of the east Atlantic and west Indian Ocean are unexplored. Here these aspects are analysed with the help of wavelet techniques, to elucidate the time-varying nature of our regional climate.

Introduction

The tropical east Atlantic and west Indian Ocean exhibit seasonal monsoon circulations of varying extent and intensity, dependent on north-south contrasts in temperature induced by the landmasses of Africa and Asia. Inter-hemispheric flow from the south intensifies from May to September, bringing convective rains to the northern tropics, from India to the African Sahel. The weaker northeast monsoon flowing out of Asia in the months November to March, extends convective rains into the southern tropics from Madagascar to Angola. The depth and orientation of the shallow monsoon circulation and its embedded weather systems depend on the upstream character of ocean-atmosphere interactions. Surface heat fluxes result in cooling of the tropical oceans, leading to an increase in the north-south thermal gradient, a strengthened Hadley cell and an amplified seasonal cycle. Zonal circulation cells extending toward Africa interact with the monsoon circulations and remote El Niño–Southern Oscillation (ENSO) and contribute to inter-annual fluctuations of climate, our focus here. It is generally accepted that the Indian Ocean behaves differently than the Atlantic and Pacific. Equatorial upwelling is not well-defined and the zonal slope of the thermocline is weak. Thus our analysis needs to account for these differences, whilst seeking to explain some of the monsoon – ENSO interactions around Africa.

Africa experiences climatic extremes lasting from seasons to decades. Persistent dry and wet spells have a proportionately large influence on economic output because more than half of African GDP is derived from subsistence agriculture (Rwelamira and Kleynhans, 1996). Runoff averages 16% of rainfall across the continent of Africa (Peixoto 1993) and river flows have exhibited declining trends in the past 50 years (Jury 2001). Rainfall over the western Sahel has shown a steady decline in recent decades in association with significant multi-decadal to centennial variability. These trends and variations together with rain-dependent economic structures make the continent particularly vulnerable to cycles of drought and flood. Many authors have studied the extent, patterns and temporal nature of rainfall fluctuations in Africa (Nicholson 1986, Janowiak 1988) and have identified three coherent regions:

- Sahelian belt of west Africa,
- sub-tropical southern Africa, and
- equatorial east Africa.

Each has a unique seasonal character and different assimilation of remote teleconnections from surrounding monsoons resident over the tropical east Atlantic and west Indian Oceans. The Sahel rainy season is from June to September, during which time easterly waves travel along defined latitude bands, fed by the Guinea monsoon (Long et al 1998). East Africa experiences

bimodal rains peaking in November and April associated with passage of the ITCZ and attendant Hadley circulations. Interannual rainfall variability is often attributed to zonal circulations of the Indian Ocean (Hastenrath et al 1993, Hastenrath 2001, Mpeta and Jury 2001), particularly with regard to an east-west dipole in climatic anomalies (Webster et al 1999). Over southern Africa rains occur from November to March in the form of meridional bands – positioned according to standing waves of the subtropical westerlies (Harrison 1986). A common factor throughout Africa is the intensity and length of the intervening dry season. Rainfall is absent up to 7 months of the year and springtime temperatures $> 40^{\circ}\text{C}$ are common.

Here, we explore climate variability in the African hemisphere guided by well known determinants: the El Niño Southern Oscillation, a north-south gradient of SST in the tropical Atlantic (Servain et al 1998) and an east-west gradient of SST in the Indian Ocean (Saji et al 2001). Pacific El Niño conditions are associated with warming of the west-central Indian Ocean (Cadet, 1985, Latif and Barnett, 1995; Nicholson; 1997; Reason et al., 2000) and increased upper level westerly winds over Africa (Harrison 1986, Jury et al 1999). Such conditions induce drought across much of the continent (Jury et al 1994; Rocha and Simmonds 1997), except for the eastern tropics (Mutai et al 1998, Goddard and Graham 1999). To further investigate ENSO influence in the Indian Ocean, a composite analysis of air-sea interactions is performed.

The global ENSO often elicits a lagged or opposing response in the tropical Atlantic (Hirst and Hastenrath 1983, Nicholson and Nyenzi 1990, Zebiak 1993, Nicholson 1997). Prior to the development of El Niño conditions in the eastern Pacific, the tropical eastern Atlantic Ocean begins to cool. A zonal overturning (direct) circulation arises (Hastenrath 2001) with upper westerly/lower easterly flow linking subsidence over central Africa with uplift over central South America. Such a pattern contributes to a decrease of river flows across the African continent (Jury 2001) through a sustained interaction between the convective systems and regional circulations (Druyan and Hall 1996, Ward et al 1999). In this manner the tropical Atlantic plays an important role in the transmission of ENSO throughout the African region.

In this chapter we investigate the temporal stability of monsoon indices and ENSO associations around Africa, through statistical analysis of observed data for key areas over the period 1958-1998. The nature of ocean-atmosphere coupling is assessed with a focus on the circulation over the equatorial Atlantic and air-sea interactions of the Indian Ocean. Varying contributions are evaluated for the surface heat fluxes, radiative balance and wind-forced ocean uplift in the development of warm and cold events. We then relate the monsoon indices to time series of continental rainfall via multivariate regression.

Data and Methods

Monthly rainfall data across Africa for the period 1958-1988 is available from the French National Centre for Scientific Research (Richard 1994; Camberlin 1995). Uneven station densities can influence statistical analyses, so some stations were excluded in high-density areas to create a more uniform spatial coverage. 466 stations having complete records were retained. A Varimax rotated principal component (rPC) analysis was carried out on de-seasoned departures of monthly rainfall (Bigot et al 1995). The first 7 rPCs explained over half of variance. Here we

make use of three modes, the 'west' African region comprising Sahel and Guinea areas (21% of variance), the 'southern' African region comprising Zambezi and Kalahari areas (15.5%), and the 'east' African region extending over Kenya, Tanzania and Lake Victoria (explaining 7% of variance). The rainfall time series, based on the rPC scores, are shown in fig 6-1 and spatial loading patterns are schematically represented in figure 6-2.

We investigate relationships between the environmental variables and regional rainfall indices at 0 and 6 month lag using multiple regression models, with predictors inserted in a forward step-wise manner as outlined by Jury et al (1999). The rainfall time series are decomposed into seasons to study the influence of key predictors. Our purpose in regressing rainfall onto the environmental indices is to assess the interaction of ocean monsoons and terrestrial climate. All variables are wavelet-filtered to remove 6 and 12 month cycles, normalized by their standard deviation and smoothed with a 3-month running mean to reduce noise due to observational bias and intra-seasonal fluctuations.

In assessing the significance of statistical fit, we estimate the degrees of freedom (DF) as the sample size minus the number of predictors (three) divided by a measure of persistence. The autocorrelation function declines below the 95% significance level in the case of west African rainfall at 10 months and in southern and east Africa at 7 months. With a total sample of 372 months, the DF for the persistent west African rainfall series is ~ 37 . The persistence is attributable to 'slower' variations of SST in the tropical Atlantic (Enfield et al 1999). For southern and east Africa the DF is ~ 53 .

The selection of monsoon indices to describe the large-scale environment around Africa reflects an extensive body of research (eg. Rocha and Simmonds 1997; Enfield and Mayer 1997, Jury et al 1999; Reason et al. 2000). They include key areas in the tropical Atlantic and Indian Oceans and correspond geographically to zonal circulation systems, regional monsoon flows, known SST responses to ENSO, and internal Atlantic (non-ENSO) variability. Tropical wind indices which anticipate changes in basin-scale SST are found in the east Indian (Rocha and Simmonds 1997) and central Atlantic Oceans (Zebiak, 1993). SST data for key areas were extracted from the Reynolds 2x2 degree reconstructed SST data set (Reynolds and Smith 1994), whilst other atmospheric variables were extracted from the 1958-98 NCEP/NCAR reanalysis climate data assimilation system (CDAS) archives (Kalnay et al 1996). The monsoon indices are used in both the cross-wavelet and regression analysis.

Variables 1 and 5 describe monsoon circulations either side of Africa. The zonal wind components are part of the zonal direct circulation that include the ocean-driving low-level easterlies at the surface, whilst the meridional wind reflects the inter-hemispheric monsoon flow. Variables 1, 8 and 9 are indices known to vary with ENSO phase (Jury et al 1994, Jury et al 1999). Variables 5 and 6 describe the Indian Ocean response to ENSO (Jury and Pathack 1993). Variable 7 is known to modulate southern African climate (Reason and Mulenga, 1999). Variable 2 represents the meridional SST gradient across the Atlantic (Enfield et al. 1999), which is known to influence west African climate (Servain 1991). A total of 13 variables are considered

in 10 key areas. The Niño3 SST (10) is utilized as a reference for ENSO teleconnections from the Pacific sector.

We investigate interactions between environmental variables in the time-frequency domain, with the continuous wavelet transform (CWT) technique (Lau and Weng 1995, Torrence and Compo 1997, Mallat 1998). The CWT is first applied to filter out the seasonal cycle embedded in the data. We then explore relationships within the environmental variables and terrestrial rainfall using the cross-wavelet spectrum. Meyers et al. (1993) has applied this type of analysis to evaluate ocean and atmospheric wave propagation. From this technique, we develop a method that allows estimation of the cross-wavelet amplitude and phase (or time delay) between the signals, localized in time. Its mathematical framework is given in the appendix. There are 'edge' effects in this type of analysis dependent on the spectral character of the signal. Here, the time delay is ambiguous for the first and last 3 – 4 years of the record (1958-62 and 1995-98), while elsewhere the delay may be unreliable when the cross-wavelet amplitude is small. The strongest justification for using wavelet methods is that they localize relationships in time as well as frequency and enable us to examine how the amplitude and time delay at interannual frequencies varies through the record. Correlation analysis, spectral analysis and other record-length methods cannot do this. e.g., correlation analysis can show a single correlation value to characterize the relationship between two variables, with no indication of whether that reflects recurrent associations throughout the record or only a few strong events in part of the record; or whether it reflects primarily high or low frequencies, or even an unresolved trend.

An additional problem is the non-stationary density of observations feeding the NCEP climate data assimilation system, which is likely to be worse in the early part of the records. Conventional observations over the oceans around Africa reach acceptable levels after the mid-1960s. In recent decades satellite observations supplement and improve our knowledge of SST and atmospheric circulation fields.

With consecutive monthly data, it is necessary to remove the seasonal cycle whilst maintaining residual signals. This is accomplished via the CWT ridge procedure described by Delprat et al. (1992). The filtering process successfully removes the seasonal cycle and retains the inter-annual residual of interest.

A brief analysis of subsurface thermal structure in the tropical Atlantic and Indian Oceans is conducted using data assimilated by the ocean model of J. Carton (Univ. Maryland-Delaware) available on the International Research Institute for Climate Prediction's Lamont Doherty Earth Observatory (IRI-LDEO) website. The model is an assimilation of available subsurface T and S observations, and surface wind fields (and calculated fluxes) on a 1 x 1 degree global grid, monthly in the period 1950 to 1998. The model horizontal resolution is 2 degrees longitude by 1-2 degrees latitude (more dense near the equator). The vertical resolution is 20 m near the surface, and increases with depth. The departure in the depth of the 20 degree isotherm from the long-term mean (dZ_{20}/dx anomaly) is evaluated on the equator at 0° and 30°W, and at 60° and 90°E for various seasons. The analysis is carried out for composite ENSO years using two criteria: Niño3 SST and southern African rainfall in accordance with Jury and Mason (2001). We assess

the extent to which the thermocline in both oceans 'heaves' westward during Pacific El Niño conditions, when dry weather is experienced across much of Africa.

In our tropical Atlantic analysis, key variables are combined into an index for comparison with Atlantic hurricane activity, based on information supplied by Landsea (pers comm.). A '3-way index' is calculated from standardized departures by subtracting the 200 hPa zonal winds in the central Atlantic from the surface winds, and adding the tropical north Atlantic SST. This index increases as SST increases and tropospheric wind shear decreases, both of which favor greater hurricane development in the tropical North Atlantic (Gray 1984, Goldenberg and Shapiro 1996, Landsea et al 1999). The hurricane activity index is the number of storm days with winds $> 33 \text{ m s}^{-1}$ in the Atlantic basin $10 - 40^\circ\text{N}$, $40 - 100^\circ\text{W}$.

In our study of the tropical west Indian Ocean the heat budget is assessed using variables 5 and 6, together with the estimated shortwave (Q_s) and longwave radiation (Q_l) and the sensible heat flux (Q_h). All data are extracted from NCEP reanalysis archives in the area $10^\circ\text{N} - 15^\circ\text{S}$, $50 - 80^\circ\text{E}$.

Results

Temporal stability of monsoon - ENSO relationships 1958-1998

In this section, we analyze the statistical association between key environmental variables over the 41- year study period. We first explore the relationship between the Niño3 SST and the central Atlantic upper zonal winds (Fig. 6-3) with the cross-wavelet spectrum technique (see appendix). The modulus (amplitude) of the cross-wavelet spectrum of the two signals is displayed in Fig. 6-3. In analogy with a Fourier spectrum, the modulus corresponds to the cross-spectral energy, except that it varies with frequency and time. The region under the bold line in Fig. 6-3 indicates the area where 'edge' effects are important, and results should be disregarded there. Largest amplitudes are concentrated in the 1.5 to 5 year interval. The relationship between the signals is temporally variant, eg. fading in and out. 'Surges' in the cross-wavelet modulus can be clearly seen centered on ENSO-related features: the El Niño events of 1969-70, 1972-73 and 1997-98, and the El Niño/La Niña oscillation of 1982-1989. The time series in Fig. 6-3 indicates a close coupling between Pacific ENSO and zonal circulation anomalies over the Atlantic. The 200 mb anomalies modulate the climatological mean Atlantic Walker cell, which is comprised of easterlies near the surface and westerly flow aloft that connects upper level outflow over the Amazon convective region with convergence aloft over West Africa. Some of this variability may be associated with the eastward propagating ENSO wave outlined by White and Cayan (2000).

We further investigate this relationship by calculating the time-varying instantaneous lag between the time series in the range 1 – 8 years, using the procedure described in the appendix. The instantaneous time lag between the Atlantic upper zonal wind and the Niño3 SST is displayed in Fig. 6-3. Its mean value is near zero. However, we observe that when the cross-wavelet spectral amplitude is large, the Atlantic upper wind leads Niño3 SST by 1 – 2 months. The correlation between the wind and SST signals, continuously shifted in time by the instantaneous lag is 0.542, whilst the maximum correlation between the signals using the

conventional approach is 0.461 at a lag of 1 month (winds leading). The higher correlation for the fluctuating lag between signals demonstrates the advantage of this approach. Why should the upper zonal flow over the equatorial Atlantic precede the Pacific Niño3 SST index? We believe it is because the tropospheric direct circulation (anomalous zonal overturning) reacts more quickly to eastward-shifted convection in the Pacific than do east Pacific SSTs, which depend on the comparatively slow eastward propagation of ocean anomalies. In other words, both the NINO3 and the Atlantic winds are responding to atmospheric convective forcing in the western Pacific, but NINO3 responds slowly (oceanic response) and the Atlantic winds quickly (through the tropospheric Walker Circulation).

The upper tropospheric zonal wind anomaly is easterly (westerly) prior to (after) the late 1970s. This is consistent with a strengthening of the zonal direct circulation over the equatorial Atlantic during the DJF season, and is associated with a large scale climate shift that occurred around 1978 (Mestas-Núñez and Enfield, 2001). The accelerated 200 hPa flow is part of a pattern that links greater Amazon convection and 200 hPa outflow over northern South America with increased subsidence and inflow over west Africa and the Gulf of Guinea. A conspicuous feature is an increase of outflow over the west-central Indian Ocean, possibly related to a warming trend in SST.

Relationships between upper and surface zonal winds over the central Atlantic are considered. The cross-wavelet modulus and the instantaneous lag (mean = 3.4 months) between the upper and surface winds is analysed. When calculated with a fluctuating lag, the correlation coefficient between the signals is -0.82. The conventional lagged correlation is -0.72 at 2 months (upper winds leading). The instantaneous lag shows small but probably insignificant fluctuations about this value, while the large lags at the beginning of the record are unreliable due to edge effects and because the cross wavelet modulus is small. In the earlier part of the record sustained lower (upper) westerly (easterly) anomalies are associated with greater rainfall over west Africa. The subsequent decrease in west African rainfall, and the Sahel drought, are consistent with the acceleration of the direct circulation (Mestas-Núñez and Enfield 2001). More regular interannual fluctuations are seen after 1980 when Africa experienced drier conditions. The stable anti-phase association suggests a prominent zonal direct circulation in agreement with Hastenrath (2001). Janicot et al. (1998) described and simulated the interannual coupling between the zonal direct circulation in the Atlantic and equatorial SST in the Pacific.

The African-Atlantic climate relationships include an association with the frequency of major hurricane development near 10°N, south and west of the Cape Verde Islands. Gray (1984), Goldenberg and Shapiro (1996) and Landsea et al (1999) describe how ENSO phase modulates Atlantic hurricane activity in this region through local SST and vertical shear anomalies. To create a single index that reflects the environment affecting hurricanes, we subtract the surface wind from the upper zonal wind and add the tropical North Atlantic SST, normalizing all variables. Although located south of the hurricane development region, our equatorial Atlantic vertical wind shear anomalies (200hPa minus surface winds) appear to directly affect the development process. This 3-way index closely tracks western Atlantic hurricane activity as

shown in Fig. 6-4. The peak in the early 1960s is followed by a long trend of declining tropical cyclone days culminating in the 1983 El Niño event. Thereafter a gradual recovery occurs with upper easterly winds, lower westerly winds and a warmer north tropical Atlantic enhancing hurricane activity. These features are consistent with the findings of past hurricane studies and suggest that our 3-way index captures key aspects of the large scale environment (wind shear and SST) affecting the development of Atlantic hurricanes; eg. increased upper easterlies / lower westerlies with respect to La Nina conditions, occur on the equatorward flank of the hurricane development axis and impart cyclonic vorticity.

The Niño3 association with equatorial SST differences on either side of Africa (eg. west-central Indian Ocean minus east Atlantic) is illustrated in Fig. 6-5. The cross-wavelet modulus and the instantaneous lag (mean = -1.5 months) is plotted in Fig. 6-5. The lag is computed for the 1 – 8 year range as before. The instantaneous lag correlation is 0.67, while the conventional correlation is 0.55 at 2 month lag (Pacific leading). The coupling shown by the cross-wavelet modulus is relatively stable with the Pacific ENSO being contemporaneous with Indian-Atlantic SST over most of the period except for 1961-1970 when Niño3 leads. The same ENSO-related features discussed for Fig. 6-3 are also seen in Fig. 6-5. During El Niño years, when the east Atlantic SST is cool and west-central Indian Ocean is warm, African rainfall decreases over much of Africa (Jury 2001). Hence, this relationship is opposite to that of Atlantic minus Pacific SST differences with respect to Caribbean and Central American climates (Enfield and Alfaro, 1999; Giannini et al., 2000), which are wetter when the North Atlantic is warm and the eastern Pacific is cool. The anti-phase relationship between the southeast Atlantic and west-central Indian Ocean SST is significant during the period 1969-1990 (coincident with strong ENSO oscillations), and is more quiescent in the early 1990s and early 1960s when ENSO activity was also weak. Where it exists, the relationship suggests that cool tongue conditions in the equatorial Atlantic precede west-central Indian Ocean warming ($r = 0.33$ at 9 months). Our results therefore suggest that the equatorial thermocline ‘heaves’ toward the west in both oceans during ENSO phase transitions in a manner consistent with the SST changes.

To test this concept, composite dZ_{20}/dx anomalies are analyzed from the Carton ocean data assimilation model. Atlantic thermocline slope anomalies (0-30°W) prior to El Niño cases (Africa - dry) are upward to the east at $+1.7 \cdot 10^{-6}$, yielding an increase in the normal eastward upslope, and thus are consistent with a cooler eastern Atlantic. Prior to La Niña cases (Africa - wet) the slope anomalies are downward to the east at $-1.6 \cdot 10^{-6}$ (warmer eastern Atlantic). Composite Z_{20} slope anomalies in the Indian Ocean (60-90°E) during dry El Niño cases are upward to the east at $+5.9 \cdot 10^{-6}$, and during wet La Niña cases slope anomalies are downward to the east at $-5.1 \cdot 10^{-6}$. The subsurface thermal structure is consistent with the anti-phase expression of SSTa either side of Africa, as expected. The Atlantic ‘leads’ the Pacific, whilst the Indian Ocean follows. The amplitude of dZ_{20}/dx variability is three-times higher in the Indian Ocean in January than in the Atlantic Ocean in the preceding July. For the west equatorial Indian Ocean, the Z_{20} depth averages 95 m during cool events and 115 m in warm events. For the east equatorial

Atlantic the Z_{20} depth is 35 m before La Nina and 25 m before El Nino events. The concept that the thermocline heaves westward during onset and mature phases of El Niño is supported.

The relationship between west-central Indian Ocean SST and surface winds over the east Indian Ocean is investigated in Fig. 6-6. The instantaneous lag correlation is -0.66 and the mean delay is -2.2 months (winds leading). A significant portion of the variability is related to Pacific Niño3 SST. Hence, easterly wind anomalies occur in the eastern Indian Ocean, producing upwelling west of Sumatra and an increase in the zonal slope of the thermocline at the onset of El Niño. SSTs rise to the west as the thermocline deepens there. This is consistent with equatorial ocean dynamics: a westward wind stress anomaly over the equator must be balanced by an eastward pressure gradient anomaly (increased thermocline slope). This ENSO-modulated E-W dipole is consistent with the findings of Saji et al (2001), and Webster et al (1999), and Huang and Kinter (2001) who study its evolution using extended EOF analysis applied to heat content anomalies.

Atmospheric forcing of composite events in the west-central Indian Ocean

The above analysis, as also that of Reason et al. (2000), confirms that much of the ENSO influence on the monsoonal processes relevant to African rainfall is mediated by Indian Ocean SST. Hence, we are interested to inquire as to how warm and cool years in the Indian Ocean are forced. A number of numerical models of the Indian Ocean, and global general circulation models, have successfully simulated the seasonal circulation of the Indian Ocean (Woodberry et al. 1989; McCreary et al. 1993; Schiller et al. 1999). Other research indicates that much of the variability is related to Pacific ENSO fluctuations (e.g., Chambers et al. 1999). However, SST variability has been less successfully simulated because of its greater dependence on sea surface fluxes that are poorly estimated (Schiller 1999). McCreary et al. (1993) showed that advection is important for SST in the boundary regions where upwelling cyclically produces large horizontal gradients of mixed layer temperature, but that elsewhere a multi-layered model that includes a realistic mixed layer will fail to simulate mixed layer temperature when parameters needed for surface fluxes are suppressed. Their work suggests that over a large interior region where SST anomalies can mediate monsoon effects, the mixed layer heat budget may be dominated by a balance between surface fluxes and entrainment across the mixed layer base. It is with this in mind that we now explore the possible role of such a balance over a large interior region of the west-central Indian Ocean straddling the equator (Fig. 6-2).

ENSO - monsoon interactions over the west-central Indian Ocean cover a wide area $\sim 10^{13} \text{ m}^2$ and significantly affect the climate of surrounding countries (Jury et al 2001). Composite events in the Indian Ocean (10°N - 15°S , 50° - 80°E), are analyzed in figures 6-7 and 6-8 through estimation of the heat budget imparted by surface fluxes and vertical motion induced by winds. We identify a group of warm cases (1970, 1993, 1983, 1987, 1992, 1998) and cool cases (1965, 1972, 1974, 1976, 2989, 1997) based on the SST anomaly (variable 5 above) exceeding one sigma during austral spring and summer (Sept-Feb). The predicted SSTa ($T_0 + dT$) based on the net heat flux anomalies and flux plus entrainment anomalies is compared with the observed SSTa

over the west-central Indian Ocean. In this analysis ocean-atmosphere interactions are assumed to be uniform over the domain.

Ocean-atmosphere coupling is explored based on the assumption that cooler SST will derive from increased evaporation (Q_e), entrainment cooling from below through isotherm uplift (cyclonic wind stress curl), and reduced shortwave radiation. Whilst variables derived from the wind fields (eg. flux and entrainment) are interpolated from observed data, radiative anomalies are derived in the NCEP model and vary according to estimated cloud cover. To calculate the change of temperature in the mixed layer, the equation used is: $dT = Q dt / \rho C_p dz$, where Q is the net surface heat flux (eg. $Q_s - Q_l - Q_h - Q_e =$ short-wave, long-wave, heat and evaporative components respectively), dt is time (one month), ρ is density, C_p is heat capacity, and dz is an average mixed layer depth (~15 m). Enfield (1986) used similar methods to obtain Q and dT estimates for the equatorial Pacific. All components of Q are obtained from the NCEP reanalysis model as departures from the mean with units $W m^{-2}$. Fasullo and Webster (1999) suggest that monthly net heat fluxes from the NCEP model are useful in determining the inter-annual variability of SST.

In situ measurements of surface fluxes and upper ocean structure (Majodina et al 2001) reveal lifting of the thermocline in the 0-10°S band from 50-90°E. The uplift of cooler waters is attributable to cyclonic curl in the surface wind field, which is sustained for much of the year south of the equator (McCreary et al 1993). There are a number of assumptions involved in relating curl to dT via vertical entrainment, so a conservative approach is adopted. We determine the percentage departure from the mean curl based on monthly NCEP wind data and calculate vertical motion anomalies using $W = \tau_{curl} / \rho f$, from which we obtain $dT = W (dT/dz) dt$. The influence on mixed layer temperature is estimated using an average dT/dz of order $10^{-1} C m^{-1}$ from the Levitus climatology (IRI/LDEO website). A scale analysis of the equation for vertical motion using typical (dimensionless) values yields: $\tau_{curl} = 10^{-7}$, $\rho = 10^3$, $f = 10^{-5}$, and $W = 10^{-5}$. An order of magnitude departure of τ_{curl} (1σ) can generate a monthly uplift of 10 m and a dT (monthly change of SST) of order $0.1^\circ C$. Because this approach relies on a climatological value for mixed layer stratification, departures may lead to errors in our estimate of entrainment influence. With west-central Indian Ocean SST near the convective threshold $\sim 28^\circ C$, small changes in SST can result in significant changes in thermodynamic energy conversion (eg. latent heating of the troposphere), so altering the surrounding climate.

Warm events start with a near zero SST anomaly and rise gradually to a minor plateau in months 4-7 (April-July) of the onset year. During this time the wind field exhibits an increasing anticyclonic curl which deepens the oceanic thermocline south of the equator. Evaporative flux anomalies remain near zero early in the event. A steep increase of SST occurs in months 8-10 as the evaporative flux declines and the curl continues an anticyclonic trend. The estimated shortwave radiation exhibits a negative tendency and plays a minor role until months 11-13 (Nov to Jan+1) when positive values occur. The anticyclonic curl and evaporative flux anomalies weaken at the mature stage of the warm event. The warm SST anomaly reaches a value of $+0.4 C$ from months 11 to 17 (Oct to May+1), a lengthy spell coinciding with the NE monsoon.

Anticyclonic wind curl provides a warming influence in months 16-18 (April to June+1) and the estimated shortwave radiation increases thereafter, inhibiting dissipation of the warm event, despite a positive heat flux anomaly. Finally SST anomalies remain positive whilst the flux and curl influence contribute to cooling after January. The predicted SST based on both fluxes and curl are consistent with the composite observed values from months 5 to 12, and suggest that ocean-atmosphere interactions can account for the build-up of the warm event rather well. In the decay stage, significant differences between observed and predicted values may be attributable to warm advection by ocean currents and thermal inertia.

The cool event is somewhat different in character, suggesting a degree of non-linear behavior for ocean-atmosphere coupling. SST declines to a minimum more symmetrically in months 11-15 (Nov to Mar+1). The onset phase displays a weak plateau for SST in the months 6-8, following a sharp increase in evaporative flux in month 5 (May). The curl influence is minimal through the onset and mature stages of the cool event. Composite fluxes do not generate 'sufficient' cooling in the initial stages of the event. However by months 9-11 evaporation strengthens considerably. The estimated shortwave radiation exhibits a sharp decline from month 8 to 11 (Nov) and remains below normal through much of the cold event (to month 22). SST anomalies begin to rise rapidly in months 16-20 (Apr to Aug+1) as the southwest monsoon prevails. The monsoon circulation yields an anticyclonic curl influence from months 17-19 (May to July+1) which rapidly dissipates the cool event. In general, SSTs are over-predicted by the composite net flux plus curl components during the OND season.

Contrasts between the composite events can be found in the slow decay of the warm event and its greater amplitude. The estimated shortwave radiation follows the SST anomaly, and supports the wind influence (eg. flux and curl). This is unexpected: an increase of SST should result in locally increased cloud and reduced radiative energy, hence negative feedback. Here the evaporative flux, wind curl and solar radiation are constructively engaged. The τ_{curl} leads the warm events and predicted - observed residuals are small from months 6 - 12. However neither the surface fluxes nor curl (vertical motion) explain the onset of cool events, so it is presumed that cooling is initiated through oceanic advection associated with basin-scale wave propagation, as outlined by Huang and Kinter (2001). The influences are quite seasonal: in both cases the surface heat fluxes are strong in the OND season, whilst the τ_{curl} contributes in the JAS season preceding the warm event, a useful result for predictive purposes.

Associations between monsoon indices and continental rainfall 1958-1988

In this section we apply the monsoon indices to inter-annual fluctuations of continental rainfall over a 31 year period. Our aim is to determine how well the ENSO-monsoon interactions explain the rainfall fluctuations at concurrent and 6-month lead time. By separately considering the three highest correlated predictors for each rainfall series, a number of interesting features can be noted. Correlation values are higher for a wider selection of indices in the case of west African rainfall owing to its larger persistence (serial correlation). The central Atlantic upper and lower zonal winds (cAu_2 cAu) are influential at concurrent times, whilst pressure over the Arabian Sea ($nwIp$) is closely associated with west African rainfall at 6 month lead time. For

southern African rainfall, meridional flow over the west Indian Ocean (wlv) and SST in the SW Indian Ocean are important, whilst zonal winds over the east Indian Ocean are related at 6 month lead. Zonal winds in the east Indian Ocean (elu) are quite influential to East African rainfall, whilst zonal winds over the central Atlantic are also associated.

The regression models are formulated using a forward step-wise regression technique up to a maximum of three predictors as outlined in Jury et al (1999). The resultant predictors are screened to reduce co-linearity below a r^2 threshold of 20%. A useful level of hindcast fit is achieved when the multiple r^2 value exceeds 30% for west Africa and 27% for southern and east Africa, including the artificial skill imposed by a candidate pool of 13 predictors over a training period of 31 years. With the time series normalized, the regression coefficients may be assessed to determine the degree of influence of the various monsoon indices on African climate. The multivariate models (Table 6-1) often differ from pair-wise assessments (Table 2). Within our 31-year record, decadal signals and model stability may not be resolved.

From the algorithms listed in table 6-1, the following interpretations can be made. West African rainfall is associated with surface zonal winds in the central Atlantic. Significantly, all African rainfall areas use this predictor with positive sign eg. westerly flow \rightarrow wet conditions. At zero lag the north-south SST gradient in the Atlantic Ocean is an important determinant, the south having greater influence. Cooler conditions in the southeast Atlantic contribute to a northward migration of the ITCZ over the Sahel as expected (Servain 1991). At 6-month lead surface air pressure in the north Indian Ocean is important and may relate to precursor conditions for easterly wave trains. The model fit is significant ($> 40\%$) at both simultaneous and 6-month lead for west Africa.

The zero lag model for southern Africa is closely related to the meridional gradient of SST over the Indian Ocean. When the tropics (sub-tropics) are cooler (warmer) than normal, greater rainfall is produced by a southward migration of the ITCZ and a weakening of upper westerly winds. The 6-month lead model for southern Africa uses the SW Indian SST together with zonal winds in the east Indian Ocean and the streamfunction (curl) over the central Indian Ocean. A cyclonic rotation induces an uplift of cooler subsurface water, favoring increased rainfall over southern Africa. The model only explains 26% of variance at 6 month lead.

The east African rainfall model uses zonal winds over the east Indian Ocean, but with opposite sign to the southern region. Easterly flow in the east Indian Ocean favors wet conditions concurrently and at 6-month lead. Westerly surface winds over the central Atlantic are associated with increased rainfall over east Africa both concurrently and in advance. At 6-month lead a warmer SW Indian Ocean (+swlst) creates a precursor environment for increased rainfall, with the same sign as for southern Africa.

Multiple regression models using monsoon indices are able to replicate 40 to 44% of simultaneous rainfall variance respectively for southern and east Africa. These values are statistically significant, and are largely dependent on the use of atmospheric predictors at long-lead times. This may be explained in terms of our earlier analysis, wherein winds lead the tropical oceans through various dynamical processes, from equatorial upwelling (Atlantic) to

conspiring fluxes and curl (Indian). This being the case, we may conclude that atmospheric signals in ocean monsoon regions exhibit sufficient 'memory' to qualify as candidate predictors of terrestrial climate.

To investigate how the monsoon indices influence African rainfall at different times of the year, we disaggregate the series into 3-month seasons and assess associations with the leading predictor at 6 month lead time. For West African rainfall - the more 'useful' DJF to JJA association operates for the nwl_p and cAu predictors, whilst declining values are found for the others. In the case of Southern Africa, the more 'useful' JJA to DJF association holds for the elu and cI Ψ variables, but the swl_{sst} variable shows a decline. For the bimodal East African rainfall, the cAu and elu predictors associate more closely in April than October, suggesting that the SON rains are more predictable than the MAM rains, as expected.

Discussion

African climates are dominated by the monsoon circulations that extend across the east Atlantic and west Indian Oceans. In the May to September period the Indian southwest monsoon draws moisture away from east Africa, whilst the tropical Atlantic monsoon feeds easterly waves north of the Guinea coast (Eltahir and Gong 1996; Druyvan and Hall 1996). From November to March, the NE monsoon sweeps across the west Indian Ocean delivering moisture, first to east Africa and later to southern Africa and the Mascarene Islands. The center of convective activity over the Congo basin shifts with solar angle and the seasonal monsoons. Axes of upward motion from the continental heat source extend southeastward during the austral summer to the Indian ITCZ, and westward to the Atlantic ITCZ in boreal summer. Over the central Indian Ocean the westerly monsoon flow is deep and upper easterlies are weak. Over the tropical Atlantic the westerlies are shallow and upper easterly flow is more strongly developed (Hastenrath 2001).

We have examined the way the monsoon circulations depart from normal and affect rainfall and hurricane development, using wavelet-based time series methods and multiple regression analysis. For the Indian Ocean, where prior studies have not explained the relationships between monsoon winds and SST (as in the Atlantic) we have analyzed the relationship of SST tendency with surface fluxes and entrainment for composites of warm events and cool events.

The extent and intensity of monsoon-driven convection is dependent on the interaction of local and remote ocean-atmosphere coupling processes. Our research has shed light on this subject by examining the nature and stability of ENSO transmission through monsoon indices in key areas around Africa. One of the strongest relationships is that upper zonal winds in the Atlantic often lead Niño3 SST, particularly in the 1980s (figure 6-3). This suggests the global direct circulation reacts quickly to the initial shift of convection anomalies from the western Pacific, compared with the slower nature of eastward ENSO propagation in the ocean. This direct circulation displays a shift in the 1970s, with maximum amplitude over west and southern Africa producing anomalous vertical motion that is consistent with the observed rainfall anomalies. Richard et al (2000) have found a similar shift in the relationship between southern African rainfall and ENSO. Other factors involving gradients of Atlantic SST and consequent ITCZ

migration may be of similar importance to the large scale forcing fields. In east Africa, rainfall appears to vary with anomalies of low-level winds over the monsoon region.

Another of the monsoon associations seen in the wavelet analysis is an ENSO-related zonal see-saw variation in equatorial SST between the Indian and Atlantic Oceans. SST changes in the east Atlantic are anti-phase to the equatorial Pacific and west-central Indian Oceans, (fig 6-5). This is reminiscent of an Atlantic-Pacific SST see-saw found to be important for Caribbean and Central American rainfall (Enfield and Alfaro, 1999; Giannini et al., 2000). However, our multiple regression analysis did not select these inter-ocean SST swings as a predictor of African rainfall.

Our understanding of ENSO-monsoon interactions around Africa has been applied to continental rainfall through development of multiple regression models. Regional rainfall indices were prepared using rotated principal component analysis for three coherent areas: Northwest (Sahel-Guinea), Southern (Kalahari-Zambezi) and East (Kenya-Tanzania). The statistical models for the three rainfall series make use of seven overlapping monsoon indices during the 1958-1988 period (fig 6-2). For each region about 40% of the variance is explained by three key monsoon indices, which vary from one region to another. In certain cases the regression coefficient takes an opposing sign from one region to another.

The most influential variables for west African rainfall are the surface zonal wind over the central Atlantic and the SSTs in the tropical North Atlantic and southeast tropical Atlantic. With the onset of El Niño in the Pacific, the tropical North Atlantic warms, the SE Atlantic cools and strengthened equatorial easterlies feed an anomalous low-level flow northward across the ITCZ. These are associated with a northward excursion of the Atlantic ITCZ and greater NW African rainfall. The increased tropospheric shear and greater tropical North Atlantic SSTs are consistent with subsequent reduced hurricane activity downstream in the main development region west of Africa (fig 6-4). At 6-month lead the surface pressure in the north Indian Ocean is lower prior to increased rainfall over West Africa. This area is upstream and in the same latitudinal belt as the tropical easterly jet which overlies Sahelian wave trains during boreal summer. When upper easterlies are strong, easterly waves are more active within the African ITCZ (Druryan and Hall 1996).

For southern African rainfall, SST differences between the southwest and central Indian Ocean and the rotational component of monsoon flow in the central Indian Ocean (which controls Ekman divergence and ocean entrainment) play significant roles. For east African rainfall, the surface zonal wind in the east equatorial Indian Ocean is a key determinant. Westerly (easterly) winds in the east Indian Ocean favor rainfall in southern (east) Africa, and serve to indicate the strength of the zonal direct circulation and the east-west SST gradient. The implication is that East Africa shares a maritime rainfall regime with the west Indian Ocean, whilst convection over southern Africa is inversely related.

The composite ocean thermal analysis performed for extreme warm and cool events in the west-central Indian Ocean describes their initiation and maintenance. Composite warmings begin and are maintained through the alternate or simultaneous effects of reduced evaporation and

reduced entrainment, while increased radiative fluxes also contribute. The OND season is when the fluxes most actively modify SST, and also when the ocean and atmosphere are most strongly coupled (eg. cloud depth adjusts to SST). Considering the net heat fluxes and vertical motion induced by the wind curl, the predicted amplitude and phase of SST warming and cooling conforms well with observed values. Discrepancies occur in the decay phase of the warm event, and in the onset phase of the cool event. The unexplained residuals suggest that advective processes may play an important role at those times.

A brief study of the seasonality of target-predictor relationships was made. In general, statistical associations are distributed across the year and are not particularly phase-locked. For the predictors zonal wind (elu, cAu) and pressure (nwlp), the association is stronger leading into the rainy season. However the SST predictors (seAsst, swlsst) relate more strongly leading into the dry season. This finding provides support for the use of monsoon indices in predictive models. Recognizing that our knowledge of ocean-atmosphere coupling around Africa is limited, it is suggested that greater *in-situ* measurements be gathered as part of GOOS and CLIVAR activities.

Decadal variability can also be seen in some of the monsoon indices but is not well resolved by the 1958-1988 data sets. One example is the relationship between hurricane development, North Atlantic SST and tropospheric wind shear (Fig 6-4), which is consistent with the findings of others. Another example is an increase in westerly flow aloft over the equatorial Atlantic, which corresponds well to a shift in Pacific SSTs and the global direct circulation in the late 1970s (Mestas-Nuñez and Enfield, 2001). The greater westerly flow aloft feeds an increased upper tropospheric convergence over west Africa, suggesting that reduced convection (increased subsidence) over that region is a factor in the drier Sahel conditions observed in recent decades.

In this study the heat budget of the Indian Ocean was evaluated in the context of local fluxes. It was found that only a part of the variability can be explained. The remainder comes from remote forcing by incoming rossby waves that are initiated by ENSO exchanges between the Indian and Pacific Oceans during the austral spring season (Jury and Mason 2002).

Appendix

Cross-wavelet spectrum and estimation of the instantaneous phase difference and time lag between two time series.

The Continuous Wavelet Transform (CWT) of a signal $x(t)$ with wavelet ψ is defined as:

$$W_x(b, a) = \frac{1}{a} \int_{-\infty}^{\infty} x(t) \psi^* \left(\frac{t-b}{a} \right) dt \quad (\text{eq. 6-1})$$

where a is the dilatation parameter, b is the time translation parameter and $*$ denotes the complex conjugate. Here, we use the complex Morlet wavelet:

$$\psi(t) = \pi^{-1/4} \exp(-t^2/2) \exp(i\omega_0 t) \quad (\text{eq. 6-2})$$

with $i = \sqrt{-1}$ and $\omega_0 = \sqrt{2/\ln 2} \cong 5.34$. With this wavelet, the transform coefficient $W_x(b, a)$ may be expressed in terms of real and imaginary parts, modulus and phase, and the relation between the dilation parameter a and frequency f is $f(a) = \omega(a)/2\pi = 0.874/a$.

The cross-wavelet spectrum of two series $x(t)$ and $y(t)$ is defined as:

$$W_{xy}(b, a) = W_x(b, a)W_y^*(b, a) \quad (\text{eq. 6-3})$$

where $W_x(b, a)$ and $W_y(b, a)$ are the CWT of $x(t)$ and $y(t)$ respectively and where $*$ denotes the complex conjugate. The cross-wavelet coefficient $W_{xy}(b, a)$ is a complex number and may be expressed in terms of real and imaginary parts, modulus and phase difference. Recall that if $z_1 = \exp(i\theta_1)$ and $z_2 = \exp(i\theta_2)$ are two complex numbers with phases θ_1 and θ_2 , then $z_1 z_2^* = c_1 c_2 \exp[i(\theta_1 - \theta_2)]$ is a complex number with phase: $\Delta\theta = \theta_1 - \theta_2$.

Consequently, the cross-wavelet spectrum provides an estimation of the local phase difference $\Delta\phi(b, a)$ between the two series for each point of the (b, a) time-frequency space. This local phase difference is independent of the amplitude of the series. These characteristics allow us to estimate the instantaneous phase difference between the two series $x(t)$ and $y(t)$. Keeping in mind that b corresponds to the time t , this phase difference is defined as:

$$\Delta\Phi(b) = \tan^{-1} \frac{\int_{a_1}^{a_2} \text{Im}[W_{xy}(b, a)] da}{\int_{a_1}^{a_2} \text{Re}[W_{xy}(b, a)] da} \quad (\text{eq. 6-4})$$

where $\text{Re}[W_{xy}(b, a)]$ and $\text{Im}[W_{xy}(b, a)]$ are the real and imaginary parts of $W_{xy}(b, a)$ and where $a_1 < a_2$ are the lower and upper limits of the dilatation parameter. The instantaneous time lag between $x(t)$ and $y(t)$ is then obtained from the relation:

$$T(b) = \frac{\Delta\Phi(b)}{2\pi F(b)} \quad (\text{eq. 6-5})$$

where $F(b)$ is the instantaneous frequency. We define this frequency as the first normalized moment in frequency of $W_{xy}(b, a)$:

$$F(b) = \frac{\int_{a_1}^{a_2} f(a) |W_{xy}(b, a)| da}{\int_{a_1}^{a_2} |W_{xy}(b, a)| da} \quad (\text{eq. 6-6})$$

where $f(a)$ is the frequency corresponding to the dilation parameter a and where $|W_{xy}(b, a)|$ is the modulus of $W_{xy}(b, a)$.

References

- Bigot, S., P. Camberlin, V. Moron, and P. Raucou, 1995, Modes of rainfall variability in tropical Africa and their stability through time, Proc 21st Conf Hurr. Tropical Meteorol., Miami, Amer. Met. Soc., 448-449.
- Cadet, D. L., 1985: The Southern Oscillation over the Indian Ocean. *J. Climate*, 5, 189-212.

- Camberlin, P., 1995, Drought and seasonal rainfall variance in the horn of Africa, Proc 1st Intl. Conf. Afr. Meteor. Soc., Nairobi, 253-265.
- Chambers, D. P., B. D. Tapley, and R. H. Stewart, 1999, Anomalous warming of the Indian Ocean coincident with El Niño, *J. Geophys. Res.*, 104, 3035-3047.
- Delprat N., B. Escudé, P. Guillemain, R. Kronland-Martinet, P. Tchamitchian, and B. Torrèsani, 1992, Asymptotic wavelet and Gabor analysis: extraction of instantaneous frequencies. *IEEE Trans. Info. Theory*, 38 (2), 644-664.
- Druyan, L. and T. Hall, 1996: The sensitivity of African wave disturbances to remote forcing. *J. Appl. Meteor.*, 35, 1100-1110.
- Eltahir, E. A. B., and C. Gong, 1996, Dynamics of wet and dry years in West Africa, *J. Climate*, 9, 1030-1042.
- Enfield, D. B., 1986, Zonal and seasonal variations of the near-surface heat balance of the equatorial Pacific Ocean, *J. Phys. Oceanogr.*, 16, 1038-1054.
- Enfield, D. B., and D. A. Mayer, 1997, Tropical Atlantic sea surface temperature variability at its relation to El Niño – Southern Oscillation, *J. Geophys. Res.*, 102, 929-945.
- Enfield, D. B., A. M. Mestas-Nunez, D. A. Mayer, and L. Cid-Serran, 1999, How ubiquitous is the dipole relationship in the tropical Atlantic sea surface temperatures? *J. Geophys. Res.*, 104, 7841-7848.
- Enfield, D. B., and E. J. Alfaro, 1999, The dependence of Caribbean rainfall on the interaction of the tropical Atlantic and Pacific Oceans, *J. Climate*, 11, 2093-2103.
- Fasullo, J. and Webster, P. J. 1999, Warm pool SST variability in relation to the surface energy balance, *J. Climate*, 12, 1292-1305.
- Giannini, A., Y. Kushnir, and M. A. Cane, 2000, Interannual variability of Caribbean rainfall, ENSO, and the Atlantic Ocean. *J. Climate*, 13: 297-311.
- Gray, W, 1984, Atlantic Hurricane frequency, part 1 - El Niño and 30 mb quasi-biennial oscillations influences, *Mon. Wea. Rev.*, 112, 1649-1668.
- Goddard, L, and N. L. Graham, 1999, Importance of the Indian Ocean for simulating rainfall anomalies over eastern and southern Africa, *J. Geophys. Res.*, 104, 19099-19116.
- Goldenberg, S. B., and L. J. Shapiro, 1996, Physical mechanisms for the association of El Niño and West African rainfall with Atlantic major hurricane activity, *J. Climate*, 9, 1169 – 1187.
- Huang, B., and J. L. Kinter, 2001, The Interannual Variability in the Tropical Indian Ocean and its Relation to El Niño/Southern Oscillation, *J. Geophys. Res.*, (in review)
- Harrison, M., 1986, A synoptic climatology of South African rainfall variations, PhD Thesis, Univ. Witwatersrand, Johannesburg, 341 pp.
- Hastenrath, S., A. Nicklis, and L. Greischar, 1993, Atmospheric-hydrospheric mechanisms of climate anomalies in the western equatorial Indian Ocean, *J. Geophys. Res.*, 98, 20219-20235.
- Hastenrath, S. 2001, In search of zonal circulations in the equatorial Atlantic Sector from the NCEP-NCAR reanalysis, *Intl. J. Climatol.*, 21, 37-48.
- Hastenrath, S, 2000: Zonal circulations over the equatorial Indian Ocean. *J. Climate*, 21, 2746-2756.

- Hirst, A C, and S. Hastenrath, 1983, Atmosphere-ocean mechanisms of climate anomalies in the Angola-Tropical Atlantic sector, *J. Phys. Oceanogr.*, 13, 1146-1157.
- Janicot, S., A. Harzallah, B. Fontaine, and V. Moron, 1998, West African monsoon dynamics and eastern equatorial Atlantic and Pacific SST anomalies (1970-88), *J. Climate*, 11, 1874-1882.
- Janowiak, J. E. 1988: An investigation of interannual rainfall variability in Africa. *J. of Climate*, 1, 240-255.
- Jury, M. R., and B. Pathack, 1993, Composite climatic patterns associated with extreme modes of summer rainfall over southern Africa: 1975-1984, *Theor. Appl. Climatol.*, 47, 137-145
- Jury, M. R., C. McQueen, and K. M. Levey, 1994, SOI and QBO signals in the African region, *Theor. Appl. Climatol.*, 50, 103-115.
- Jury, M. R., H. M. Mulenga, and S. J. Mason, 1999, Exploratory long-range models to estimate summer climate variability over southern Africa, *J. Climate*, 12, 1892-1899
- Jury, M. R., 2001, Composite climate structure modulating the interannual variability of African river flows, *J. Hydrology*, (in review)
- Jury, M. R., and S. J. Mason, 2001, Evolution of ENSO teleconnections around southern Africa, *Water SA*, (in review)
- Jury, M. R., Gadgil, S, G. Meyers, S. Ragoonaden, C. Reason, T. Sribimawati, F. Tangang, 2001, Motivations for an Indian Ocean observing system and applications to climate impacts and resource predictions in surrounding countries, *J Geophys. Res.*, (in review)
- Jury, M R, and Mason, S J, 2002, The evolution of ENSO teleconnections around southern Africa, *Water SA*, (submitted)
- Landsea, C. W., R. A. Pielke, A M Mestas_Nuñez, and J. A. Knaff, 1999, Atlantic basin hurricanes: Indices of climatic change, *Climatic Change*, 42, 89-129.
- Latif, M., and T. P. Barnett, 1995, Interactions of the tropical oceans, *J. Climate*, 8: 952-968.
- Lau K. M. and H. Y. Weng, 1995, Climate signal detection using wavelet transform: how to make a time series sing. *Bull. Amer. Meteorol. Soc.*, 76, 2391-2402.
- Long, M., D. Entekhabi, and S. E. Nicholson, 1998, Interannual variability in rainfall, water vapour flux and vertical motion over West Africa, *Water Resources Variability in Africa*, ed. E. Servat et al, IAHS 252, 27-33.
- Majodina, M., M. R. Jury, and M. Rouault, 2001, Ocean-atmosphere structure in the tropical Indian Ocean during a ship cruise 1995/96, *Global Ocean Atmos. Sys.*, (in press).
- Mallat S., 1998, *A wavelet tour of signal processing*. Academic Press, San Diego, CA
- McCreary, J. P., P. K. Kundu, and R. Molinari, 1993, A numerical investigation of the dynamics and thermodynamics and mixed layer processes in the Indian Ocean, *Prog. Oceanog.*, 31, 181-244.
- Mestas-Nuñez, A.M., and D. B. Enfield, 2001, Eastern equatorial Pacific SST Variability: ENSO and Non-ENSO components and their Climatic Associations, *J. Climate*, 14, 391-402.
- Meyers S. D., B.G. Kelley, and J. J. O'Brien (1993), An introduction to wavelet analysis in oceanography and meteorology: with application to the dispersion of Yanai waves, *Mon. Wea. Rev.*, 121, 2858-2866.

- Mpeta, E. J., and M. Jury, 2001, Intra-seasonal convective structure and evolution over tropical east Africa, *Climate Research*, (in press)
- Mutai, C. C., M. N. Ward, and A. W. Colman, 1998, Towards the prediction of the east Africa short rains based on sea-surface temperature – atmosphere coupling, *Intl. J. Climatol.*, 18, 975-998.
- Nicholson, S. E., 1986, The spatial coherence of African rainfall anomalies: interhemispheric teleconnections, *J. Climate Appl. Meteorol.*, 25, 1365-1381
- Nicholson, S. E., 1997, An analysis of the ENSO signal in the tropical Atlantic and western Indian Oceans, *Intl. J. Climatology*, 17, 345-375.
- Nicholson, S. E., and B. S. Nyenzi, 1990, Temporal and spatial variability in the tropical Atlantic and Indian Oceans, *Meteorol. Atmos. Phys.*, 41, 1-17.
- Peixoto, J. P., 1993, Atmospheric energetics and the water cycle, chapter 1: Nato ASI series 15, Raschke, E. and Jacob, D., eds, Springer-Verlag, 1-42.
- Reason, C. J., and Mulenga, H. 1999, Relationships between South African rainfall and SST anomalies in the southwest Indian Ocean, *Intl. J. Climatol.*, 19, 1651-1673.
- Reason, C. J. C., R. J. Allan, J. A. Lindesay, and T. J. Ansell, 2000, ENSO and climatic signals across the Indian Ocean basin in the global context, part 1, interannual composite patterns, *Intl. J. Climatol.*, 20, 1285-1327.
- Reynolds, R. W., and M. Smith, 1994, Improved global sea surface temperature analyses using optimum interpolation, *J. Climate*, 7, 929-948.
- Richard, Y., 1994, Variability of rainfall in West Africa, *La Meteorologie*, 8, 11-22.
- Richard, Y., S. Trzaska, P. Roucon, and M. Rouault, 2000, Modification of the southern African rainfall variability/-ENSO relationship since the late 1960s, *Climate Dynamics*, 16, 883-895.
- Rocha, A. M. C., and I. Simmonds, 1997, Interannual variability of south-east African summer rainfall. Part I: relationships with air-sea interaction processes. *Intl. J. Climatol.*, 17, 235-265.
- Rwelamira, J. K., and T. E. Kleynhans, 1996, SADC agricultural potential assessment – country profiles, DBSA report 124, South Africa.
- Saji, N. H., B. N. Goswami, P. N. Vinayachandran, T. Yamagata, 2001, A dipole mode in the tropical Indian Ocean, *Nature*, (in press)
- Schiller, A., 1999, How well does a coarse-resolution circulation model simulate observed interannual variability in the upper Indian Ocean?, *Geophys. Res. Lett.*, 26, 1485-1488.
- Schiller, A., J. S. Godfrey, P. C. McIntosh, G. Meyers, and R. Fiedler, 2000, Interannual dynamics and thermodynamics of the Indo-Pacific oceans, *J. Phys. Oceanogr.*, 30, 987-1012.
- Servain, J., 1991, Simple climatic indices for the tropical Atlantic Ocean and some applications, *J Geophys Res*, 96, 15137-15146.
- Servain, J., I. Wainer, A. Dessier, J. P. McCreary, 1998, Modes of climatic variability in the tropical Atlantic, 1998, Water Resources Variability in Africa, ed. E. Servat et al, IAHS 252, 45-54.
- Torrence C., and G P Compo, 1997, A practical guide to wavelet analysis, *Bull. Amer. Meteorol. Soc.*, 79, 61-78.

Ward, M.N., P.J. Lamb, D.H. Portis, M. El Hamly and R. Sebarri, 1999: Climate Variability in Northern Africa: Understanding Droughts in the Sahel and the Maghreb. In: *Beyond El Nino - Decadal Variability in the Climate System*, ed: A Navarra, Springer-Verlag, 119-140.

Webster, P. J., A. M. Moore, J. P. Loschnigg, and R. R. Leben, 1999, Coupled ocean-atmosphere dynamics in the Indian Ocean during 1997-1998, *Nature*, 401, 356-360.

White, W. B., and Cayan, D. R., 2000, A global El Nino-Southern Oscillation wave in surface temperature and pressure and its interdecadal modulation from 1900 to 1997, *J. Geophys. Res.*, 105, 11223-11242.

Woodberry, K. E., M. E. Luther, and J. J. O'Brien, 1989, The wind-driven seasonal circulation in the southern tropical Indian Ocean, *J. Geophys. Res.*, 94, 17,985-18,002.

Zebiak, S. E., 1993, Air-sea interaction in the equatorial Atlantic region, *J. Climate*, 8, 1567-1586

Table 6-1: Multi-variate models

Rainfall area	Linear regression algorithm	adjusted r^2 fit %
West Africa	+0.71(cAu) -0.44(seAsst) +0.19(nAsst)	44
West Afr-6	-0.33(nwlp) -0.25(seAsst) +0.24(cAu)	43
South. Afr	+0.63(swIsst) -0.43(cIsst) +0.22(cAu)	40
South. Afr-6	+0.27(elu) +0.26(swIsst) +0.22(cIP)	26
East Africa	-0.68(elu) +0.36(cAu)	44
East Afr-6	+0.51(cAu) -0.36(elu) +0.30(swIsst)	32

(1st lower case=area, 2nd upper case=ocean, 3rd lower case=parameter, -6 refers to lead time)

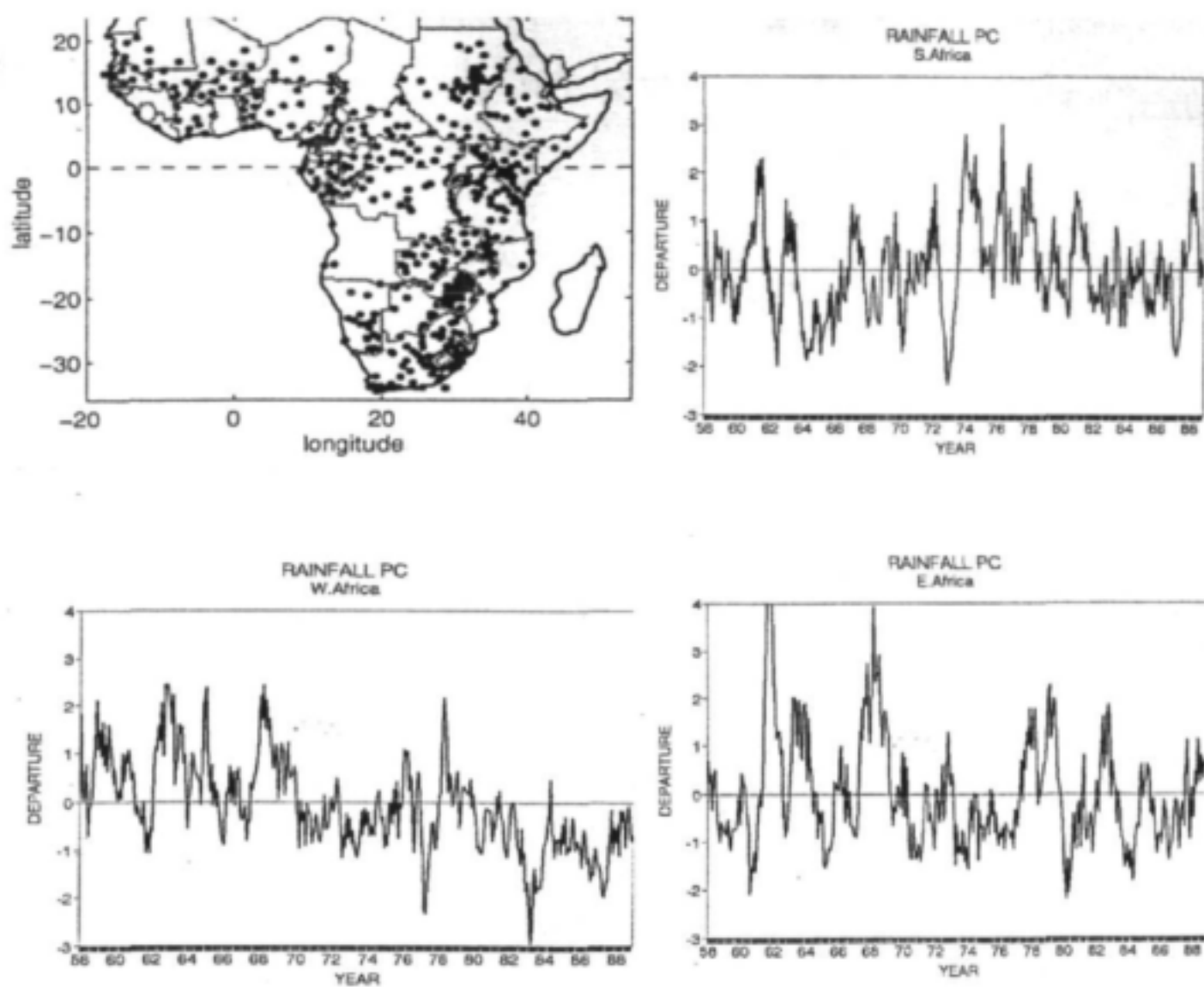


Fig 6-1 – Station distribution (upper left), rotated principal component time scores for (clockwise from upper right): southern Africa, east Africa, and west Africa.

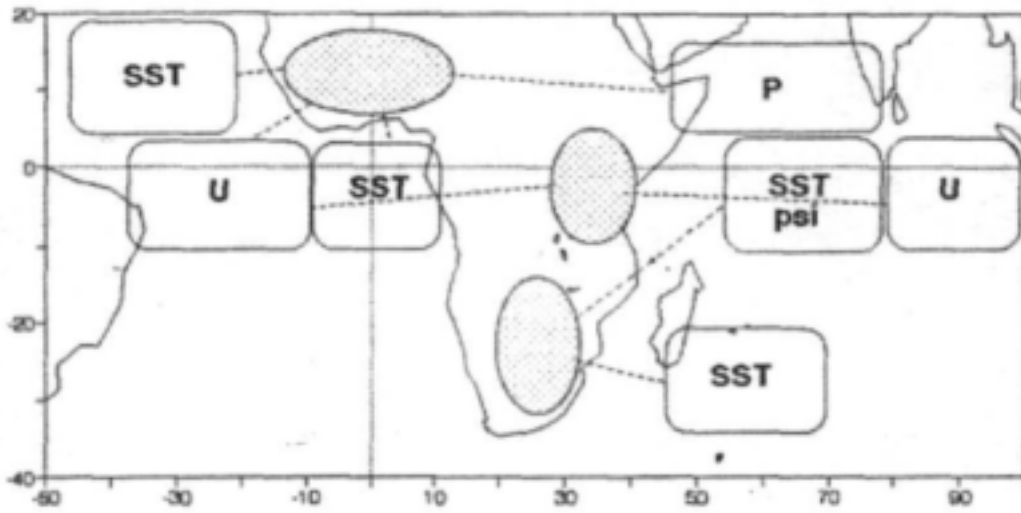


Figure 6-2 – Schematic representation of spatial loading regions for African rainfall (shaded areas). Rectangles identify tropical Atlantic and Indian monsoon index areas described in table 6-1. This serves to consolidate the predictors of African rainfall uncovered in this study.

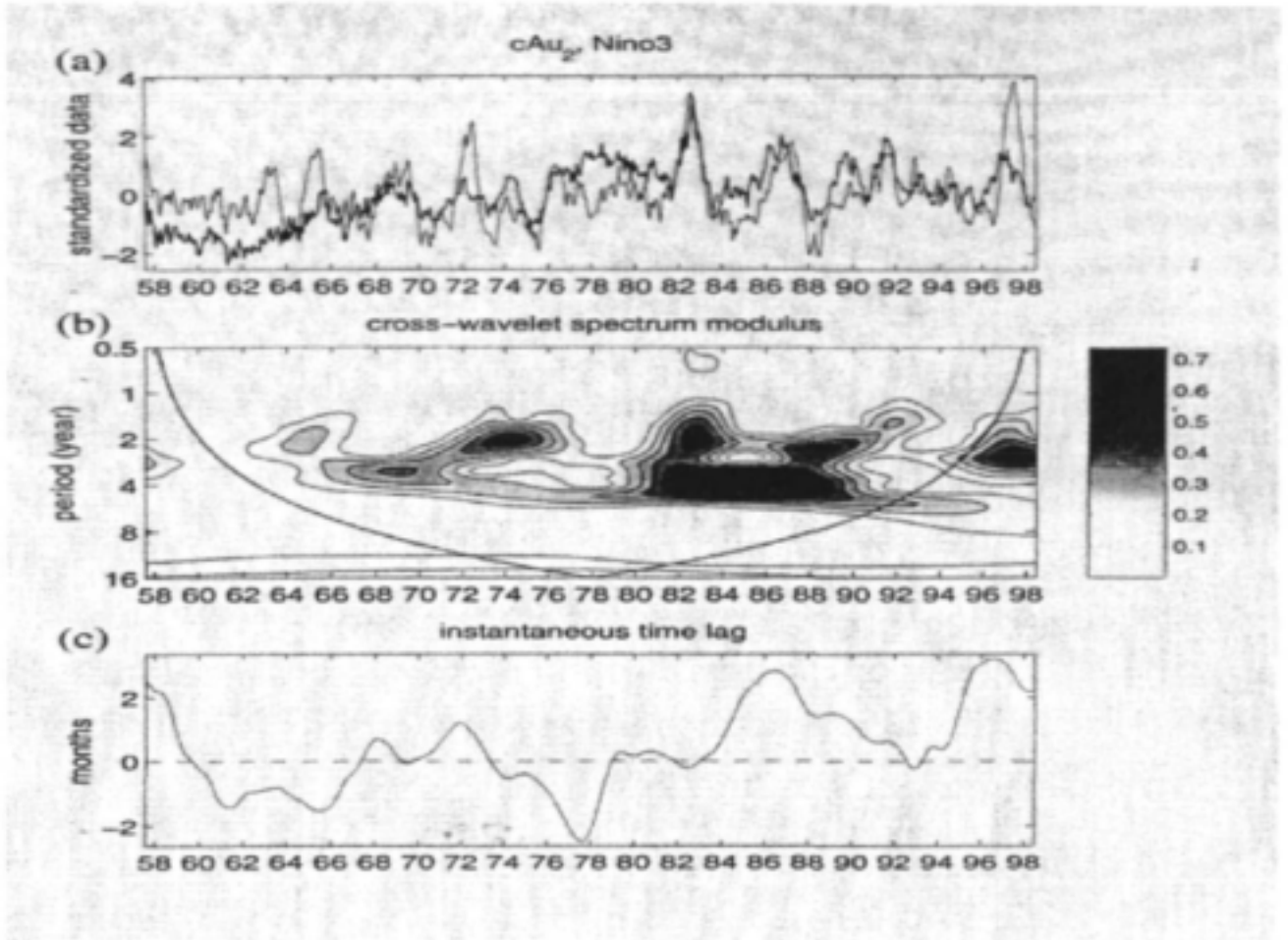


Figure 6-3 – (a) Filtered time series for Niño3 SST and upper zonal winds (bold) of the central Atlantic, (b) cross-spectrum modulus, and (c) instantaneous time lag, positive when the winds lead.

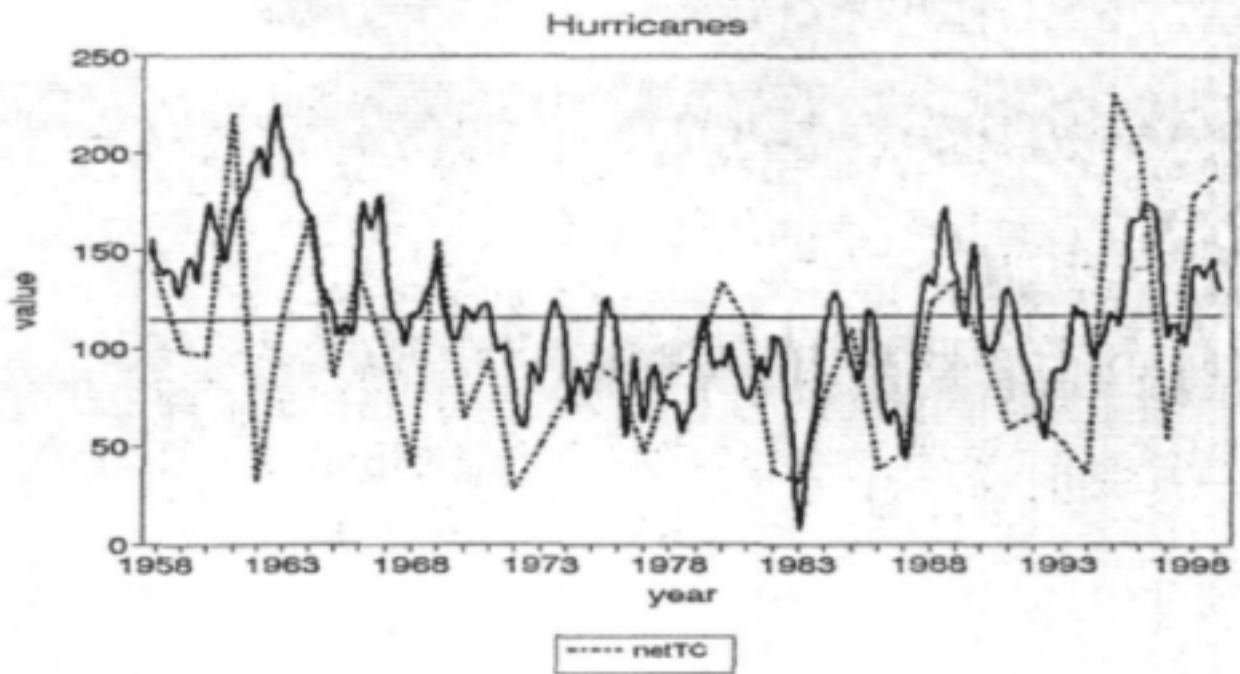


Figure 6-4 – Filtered time series of an Atlantic circulation index ($cAu - cAu_2 + nAsst$), and July-October northwest Atlantic hurricane activity (dashed), based on 'storm day' information provided by Landsea (pers. comm.).

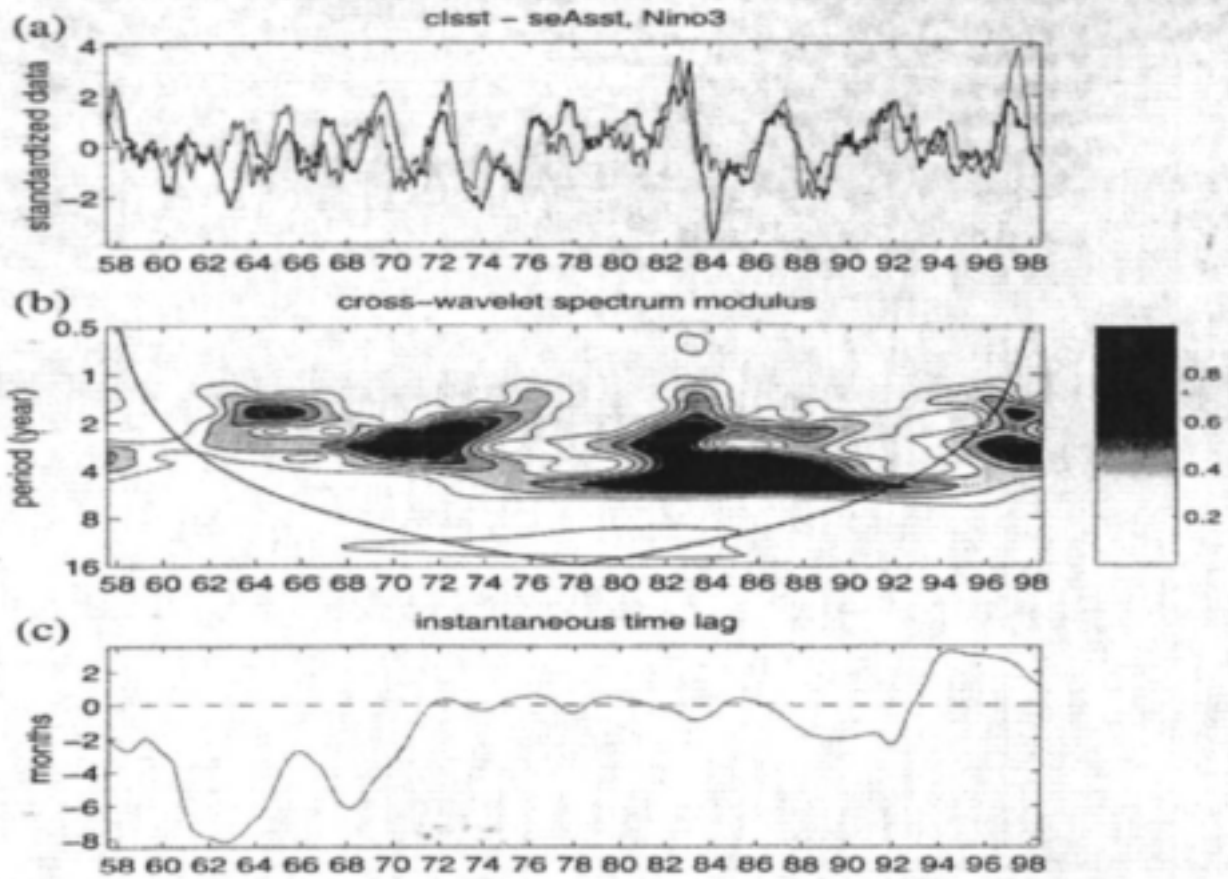


Figure 6-5 – (a) Filtered time series for the SST difference between the west-central Indian Ocean and the east Atlantic (bold) and Niño3 SST, (b) cross-spectrum modulus, and (c) instantaneous time lag, positive when the SST difference leads.

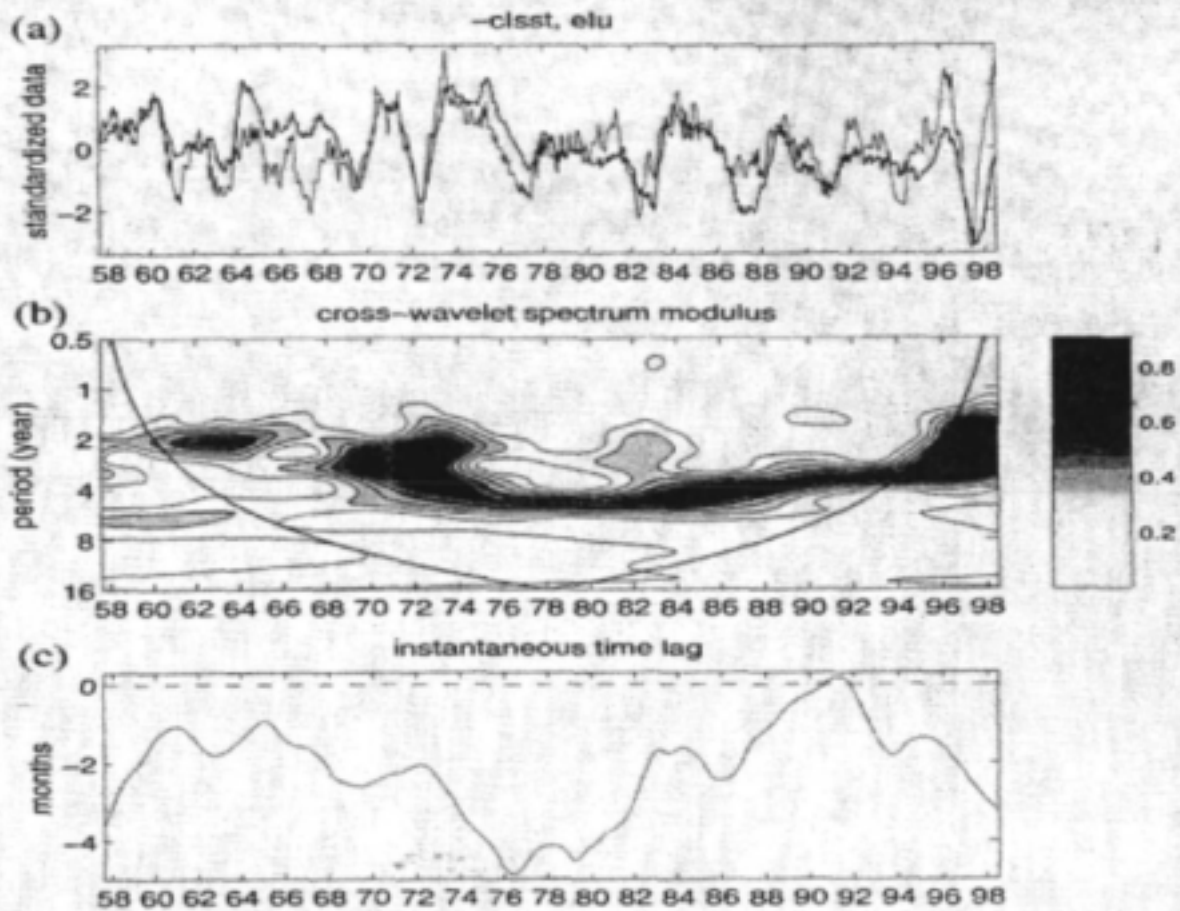


Figure 6-6 – (a) Filtered time series of SST in the west-central Indian Ocean (inverted in bold) and surface zonal winds in the east Indian Ocean, (b) cross-spectrum modulus and (c) instantaneous time lag, positive when SST leads.

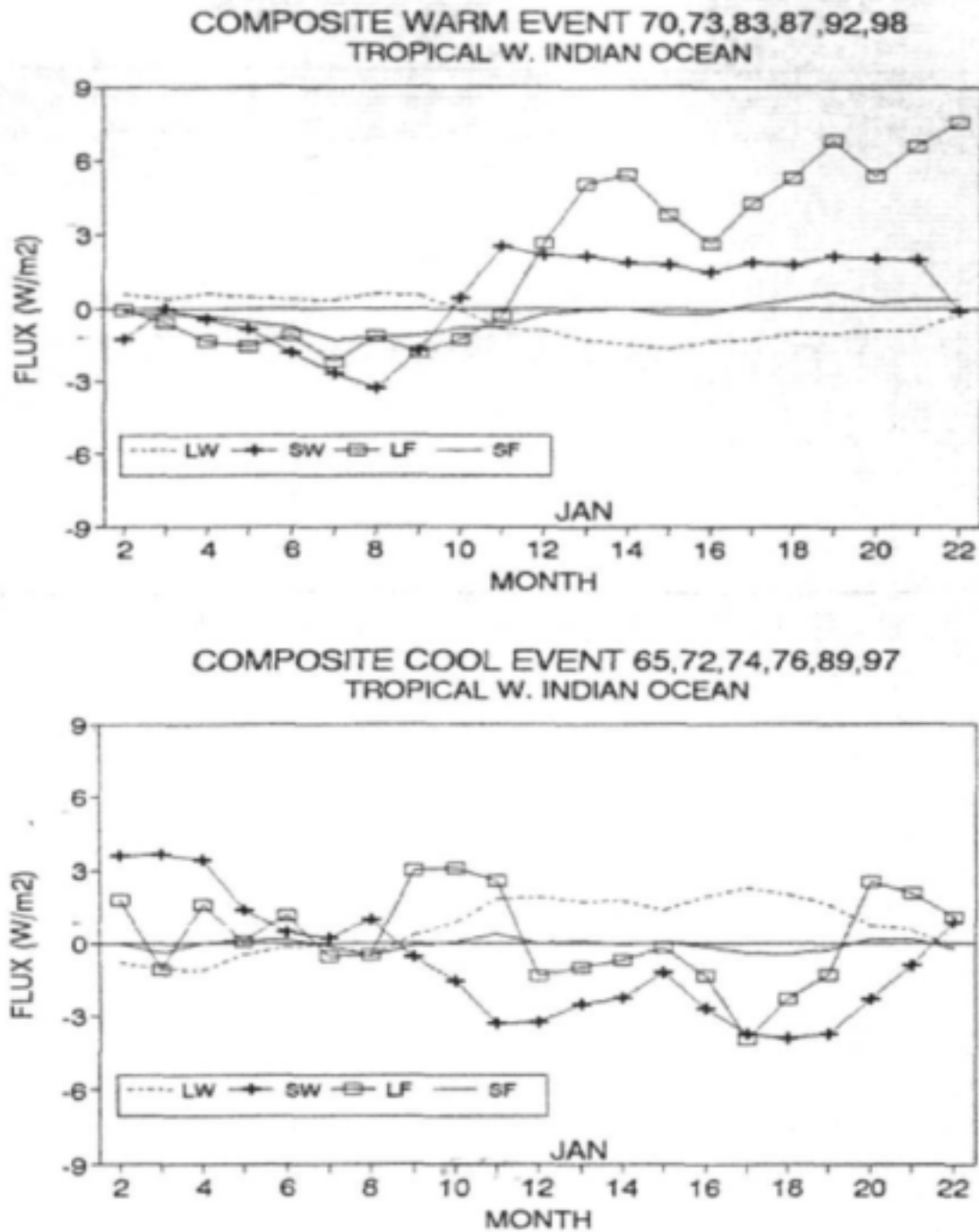


Figure 6-7 – Composite warm (a) and cool (b) events in the west-central Indian Ocean identifying surface flux components of the heat budget.

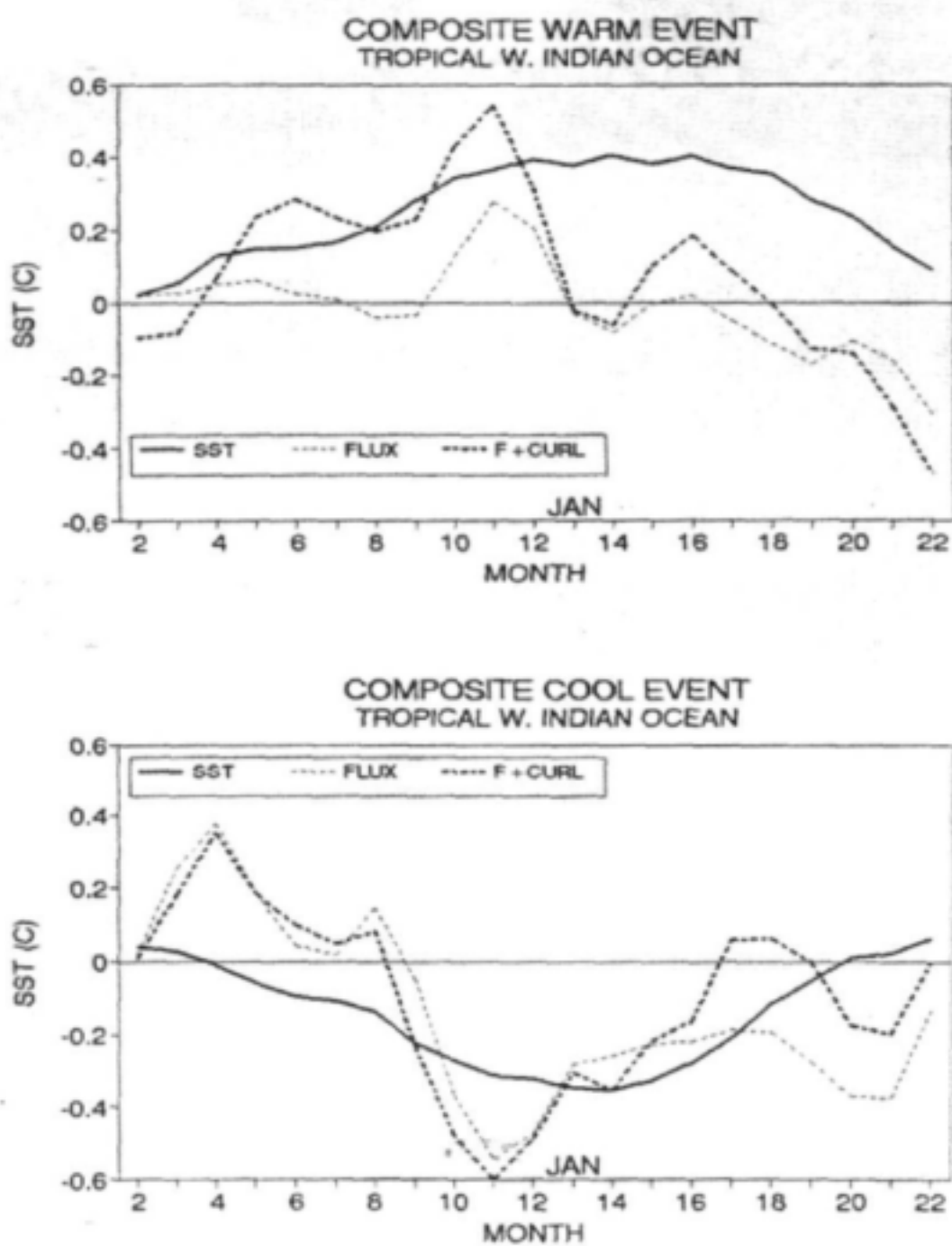


Figure 6-8 – Composite warm (a) and cool (b) events in the west-central Indian Ocean illustrating observed (bold) and predicted (thin dashed lines) SST anomalies.

Chapter 7 – Determination of predictors and targets, regionalisation and development of statistical models

Recognising that earlier work on climate prediction had uncovered 'too many' variables (Chapter 1) thereby introducing a degree of artificial skill (fig 7-1), this chapter outlines how new predictors and targets were consolidated. The analysis made use of 2° gridded mean monthly rainfall and temperature fields over the African continent from the Climate Research Unit (CRU), and COADS (Comprehensive Ocean Atmosphere Data Set) 10° gridded SST, SLP, U and V surface wind fields over the Atlantic and Indian Ocean. The period 1965-1995 was chosen for the study because of the higher integrity of meaningful ship-based data in COADS. A short description of the data follows.

COADS marine data

The Comprehensive Ocean Atmosphere Data Set (COADS) is an extensive collection of surface marine data available for the world ocean. COADS is a result of a continuing cooperative project in the National Oceanic and Atmospheric Administration (NOAA). The parameters used from this data set were Sea Surface Temperature (SST), Sea Level Pressure (SLP), Zonal (U) wind component and Meridional (V) wind component. Mean (enhanced) monthly statistics were extracted from the Indian and Atlantic Oceans in the domain 30°N-40°S, 70°W-100°E for the period 1965-1995. The period 1950-1964 was excluded because of too many missing data. The enhanced statistics, whose record period is from 1950 to 1995, were derived using 3.5 sigma trimming limits (a quality control procedure used to identify outliers with respect to climatological values). The trimming limits still allow for extreme climate events. In order to increase coverage, marine observations from ships, fishing vessels, and surface oceanographic measurements were combined. The data is accumulated into 10°x10° lat/lon grid boxes from which inter-annual patterns are extracted for the Atlantic and Indian Oceans.

CRU rainfall data

Gridded monthly rainfall and temperature data for continental Africa were obtained from the Climate Research Unit (University of East Anglia). The 2° latitude/longitude gridded mean monthly precipitation and temperature data for the period 1951 to 1995 were analysed from 2307 stations for precipitation and 1485 stations for temperature. A thin-plate spline technique was used to interpolate the mean climate surfaces as a function of latitude, longitude and elevation. The technique is robust in areas with sparse and irregularly spaced data as is the case in Africa. Hutchinson (1995) provides a theoretical description of its application to surface climate variables such as precipitation.

Indices - ENSO

El Nino is an extensive warming of the upper ocean in the tropical eastern Pacific lasting up to three seasons. The negative, or cool phase of El Nino is called La Nina. El Nino events are linked with a change in atmospheric pressure known as the southern Oscillation (SO), (Glantz, et al., 1991). The Southern Oscillation is characterised by a see-saw in atmospheric pressure between the western and eastern regions of the Pacific Ocean, with one centre of action located

south of Indonesia and the other centre located near Tahiti. The SOI, which is an index that measures the magnitude of SO is obtained by calculating the difference in atmospheric surface pressure anomalies between Tahiti and Darwin Australia. As the SO and El Nino are closely linked with each other, they are collectively known as the El Nino - Southern Oscillation, or ENSO. Another measure of the magnitude of El Nino events is sea surface temperature averaged over a specific region of the Pacific Ocean, such as the Nino3 region which extends from 150°W to 90°W and 5°N to 5°S. The return period of El Nino events is varied, ranging from two to seven years. The intensity and duration of the event are also varied yet predictable to some degree. Typically, it lasts anywhere from 14 to 22 months. ENSO events are those in which both El Nino and Southern Oscillation occur together. El Nino often begins early in the year and peaks between the following November and January. ENSO events are known to influence rainfall over the African continent (Ropelewski and Halpert, 1987; Ogallo, 1994). The Nino3 SST index from 1965 to 1995 is used in this study. The Indonesia sea level pressure anomaly index is the standardized sea level pressure over Indonesia. This index has some ENSO characteristics and has been acquired from the NOAA web site (<http://www.cdc.noaa.gov/>), from 1965 to 1995.

Quasi-biennial Oscillation Index (QBO)

The Quasi-biennial oscillation is a stratospheric zonal wind that reverses over the tropics every 12-13 months. In this study use is made of the zonal wind index (m/s) at 30 hPa of Marquardt and Naujokat, (1997). The index is a combination of values at Canton Island (3°S, 172°W) for January 1953- August 1967; Gan./Maldives (1°S, 173°E) for September 1967-December 1975; and Singapore (1°, 104°E) from January 1976-February 1999. QBO index data from January 1965-December 1995 is used in this study to match with other data sets. Naujokat (1986) documents the data, uncertainties in the early years due to lack of daily data, change in reference stations, and the general features of QBO.

Methodology

In order to study inter-annual climate variability it is necessary to consider the need for area averaging in a meaningful way, so that influences from remote sources are not confused. Many methods can be used to spatially cluster time varying fields. Among them is principal components analysis which extracts coherent patterns in spatial data. Averages are then calculated for data falling within a cluster area. In this way the data are reduced and meso-scale, intra-seasonal and topographic features are avoided. In order to understand the spectral characteristics of the resulting time series, a continuous wavelet analysis is applied. Statistical association is evaluated using Pearson's product correlation. These methods are further described in the following section.

Principal component analysis (PCA)

Principal Component Analysis (PCA) is a multivariate statistical technique having wide applications in meteorology (Lyons, 1982; Yin, 1984; Basalirwa et al., 1998). The method reduces the number of variables whilst explaining variability within the original record (Jolliffe, 1993). PCA is done when the original data contains grid point variables that are

spatially correlated, as is in the present study for gridded rainfall and temperature data over Africa; and gridded SST, SLP, U and V wind over the Atlantic and Indian Oceans. Application of PCA thus reduces the original data to sub-sets ranked in order of importance.

Principal components (PCs) or modes are produced via PCA, each consisting of an eigenvalue that quantifies the variance, a set of loadings (eigenvectors) that describe the spatial distribution (coherent patterns) and a set of time scores that define the evolution. The first PC is a linear function accounting for the highest variance, i.e. the dominant pattern. The second PC is the linear function with the next highest variance subject to being uncorrelated with the first PC. Subsequent PCs are all linear functions ranked in order of decreasing variance which are not correlated with each other or with the first and the second PCs (Jolliffe, 1990). When carrying out PCA the correlation matrix technique was chosen to avoid the analysis being dominated by high variance. This approach enables a focus on relative rather than absolute variability of the variables. The first nine rainfall PCs were retained for further analysis as they explained a large amount of variance (see table 7-1) and these could be interpreted easily. Varimax rotation was performed on the remaining nine PCs. Rotation is normally used to simplify the structure of the eigenvectors and facilitate interpretation.

Key area predictors

The number of PC modes retained to study the annual cycle was two. After removal of the seasonal cycle for the analysis of inter-annual variability - three modes were retained. In each case, for all parameters, the PCA was done first unrotated, then Varimax rotated. Rainfall PC modes for eastern and southern Africa were selected for further analysis. For SST, SLP, U and V wind: modes 1-3 for both un-rotated and rotated were considered. Key areas were identified from PC modes and time series were created by area averaging of values within maximum spatial loadings from January 1965 to December 1995. In some cases for unrotated modes, dipole patterns were evident, so data from two areas was either subtracted or added as required. In this way time series were created of 372 consecutive months for the target (rainfall and temperature) and predictor (environmental) key areas.

Correlations between key areas and PCs

Correlation analysis was done between the PC time score and respective key area time series. Key areas are considered to be superior in operational applications - as they are easier to obtain and track over time, and also they represent fixed-area anomalies that do not receive small contributions from outlying areas. The tables below define the predictor areas (7-1), their cross-correlation with key areas (7-2) and their relationship with rainfall over southern and east Africa (7-3). From these, multi-variate models were developed to predict fluctuations in terrestrial climate.

Table 7-1: Description of the PCs, their loading areas and names (parameter and ocean). For dipole regions - the name shows two oceans with a + or – sign between.

Parameter	PC Mode	Areas	Key area name
SST	PC1	60°E-90°E,10°N-10°S + 50°W-10°W,20°N-10°S	SST Ind+Atl
SST	PC2	60°W-20°W,10°N-20°N - 30°W-0°,0°-30°S	SST AtlDipole
SST	PC3	50°W-0°,10°N-10°S - 40°E-60°W, 0°-30°S	SST Ind-Atl
SST	PC1R	50°E-90°E, 0°-20°N	SST Ind
SST	PC2R	30°W-10°E, 10°N-20°S	SST eastAtl
SST	PC3R	40°W-10°W, 30°N-10°	SST northAtl
SLP	PC1	40°E-100°E,10°N-10°S + 50°W-0°,10°N-20°S	SLP Ind+Atl
SLP	PC2	60°E-90°E,10°N-20°S - 70°W-10°W,0°-30°N	SLP Ind-Atl
SLP	PC3	70°W-10°W,10°N-30°N - 30°W-0°W,10°S-30°S	SLP AtlDipole
SLP	PC1R	30°W-0°, 0°-20°S	SLP Atl
SLP	PC2R	70°E-100°E, 0°-30°N	SLP Ind
SLP	PC3R	40°W-10°W, 10°N-30°N	SLP NWestAtl
U ZONAL WIND	PC1	60°W-30°W,10°N-20°N + 40°E-90°E,20°S-40°S	U Atl+Ind
U ZONAL WIND	PC2	70°E-100°E,10°N-10°S	U Ind
U ZONAL WIND	PC3	40°W-10°W,10°S-20°S + 50°E-80°E,10°S-20°S	U Atl+Ind2
U ZONAL WIND	PC1R	60°W-10°W, 10°N-10°N	U Atl1
U ZONAL WIND	PC3R	40°W-0°, 10°S-30°S	U Atl2
V MERIDIONAL	PC1R	20°W-10°E, 10°S-40°S	V Atl1
V MERIDIONAL	PC2R	40°W-10°W, 20°N-10°S	V Atl2
V MERIDIONAL	PC3R	40°E-70°E, 20°N-10°S	V Ind

Where 'R' stands for rotated, total = 20 predictors

Table 7-3 Lagged pair-wise correlation between predictor and target indices

	Southern Africa Rainfall		East Africa Rainfall	
Environmental Key areas	CORRELATION COEFFICIENTS			
	3 Mon. lead	6 Mon. lead	3 Mon. lead	6 Mon. lead
SST Ind+Atl			-0.17	-0.2
SST AtlDipole			0.27	0.25
SST Ind-Atl	-0.30	-0.30	0.38	0.22
SST Ind	-0.15			-0.13
SST eastAtl	0.15	0.27	-0.37	-0.39
SST northAtl		0.13	-0.14	-0.15
SLP Ind+Atl	-0.34	-0.31	0.39	0.23
SLP Ind-Atl	-0.23	-0.24	0.38	0.27
SLP AtlDipole	-0.12	-0.17	0.47	0.41
SLP eastAtl	-0.29	-0.28	0.45	0.34
SLP eastInd	-0.42	-0.36	0.2	
SLP NwestAtl			0.28	0.24
ZONAL WIND Atl+Ind	-0.17			0.2
ZONAL WIND Ind	0.33	0.3	-0.44	-0.22
ZONAL WIND Atl+Ind2		0.16	-0.31	-0.25
ZONAL WIND Atl1	-0.19			-0.16
ZONAL WIND Atl2	-0.13		-0.19	-0.18
MERID. WIND Atl1	0.12			0.17
MERID. WIND Atl2	-0.17	-0.17	0.14	
MERID. WIND Ind	0.41	0.33		
QBO30	0.40	0.31		
IndSLPa	-0.42	-0.33	0.19	
SST Nino3	-0.48	-0.36		

With a degrees of freedom of 30, $r > .35$ is significant at $p < .05$

Five targets areas based on PC modes of departure data:

Rain pc1: 18 S – 30 S, 20 – 32 E south
 Rain pc3: 8 N – 4 S, 30 – 42 E east
 Temp pc1: 6 S – 20 S, 20 E – 32E central
 Temp pc2: 16 S – 28 S, 22 E – 34 E south
 Temp pc3: 6 N – 12 S, 30 E – 42 E east

Considering the continuous monthly time series with the 20 predictors listed above, and developing models over a 30 year training period yields the following results:

Target	Most Significant Predictors	Fit ($r^2\%$)
(Annual cycle)		
Rain pc1 N-S dipole Zambezi / Sahel	Vpc1 W.Indian/Guinea monsoon	93
Rain pc2 Equatorial Band	SST pc2 + 2 others eq. W. Indian/eq. W. Atlantic SST	59
Temp pc2 N-S dipole Kalahari / Sahel	SST pc2 & V pc2 eq W. Indian/eq. W. Atlantic SST NW-SE banded wind pattern	72
Temp pc3r Lower Zambezi	SST pc1 + 1 other N-S dipole of SST in both oceans	68
(Departures)		
Rain pc1 Africa south of Zambezi	U pc2r + SLP pc3 eq. E. Indian zonal wind + N-S dipole of press. in Atlantic	20
Rain pc3 Angola-Kenya dipole	U pc2 + SLP pc2 central Indian zonal wind + Indian/Atlantic Press. dipole	22
Temp pc1 Zambezi region	SST pc1 + 1 other central Indian/eq. W. Atlantic SST	70
Temp pc3 Tanzania region + NE Atlantic SST	U pc3r + SST pc3r south Atlantic zonal wind	20

We may interpret the models based on the predictors selected. The annual cycle of African rainfall is strongly controlled by the meridional (N-S) component of the tropical monsoon circulation with an explained variance of 93%. Of the models for interannual departures, the Zambezi region temperature has a high explained variance (70%), contributed by SST varying in-phase in the west Atlantic and west Indian Oceans and the global warming trend. It is suggested that the warm upper layer of these oceans undergoes a see-saw action that is in-phase. This work furthermore demonstrates that dipole (or two-area) predictors have considerable value, in addition to single-area predictors. Of the key area predictors for southern African rainfall: at zero lag the dipole in SST between the SW Indian Ocean and the western tropical Indian Ocean provides a high degree of predictability. At six month lead time the east Indian Ocean zonal wind is a useful indicator of southern African rainfall. The zonal wind is also known to produce a westward moving ocean rossby wave that induces SST changes near Madagascar some 6 months later.

One important message from this work is the importance of the annual cycle. It accounts for about half of total rainfall and temperature variance, whilst interannual departures provide only 10% of the total signal. Hence a model that predicts the amplitude of the annual cycle may have considerable value. Another point is that prediction based continuous data may help define shifts in the rainy season, in contrast with the (discontinuous) seasonal approach which is often followed.

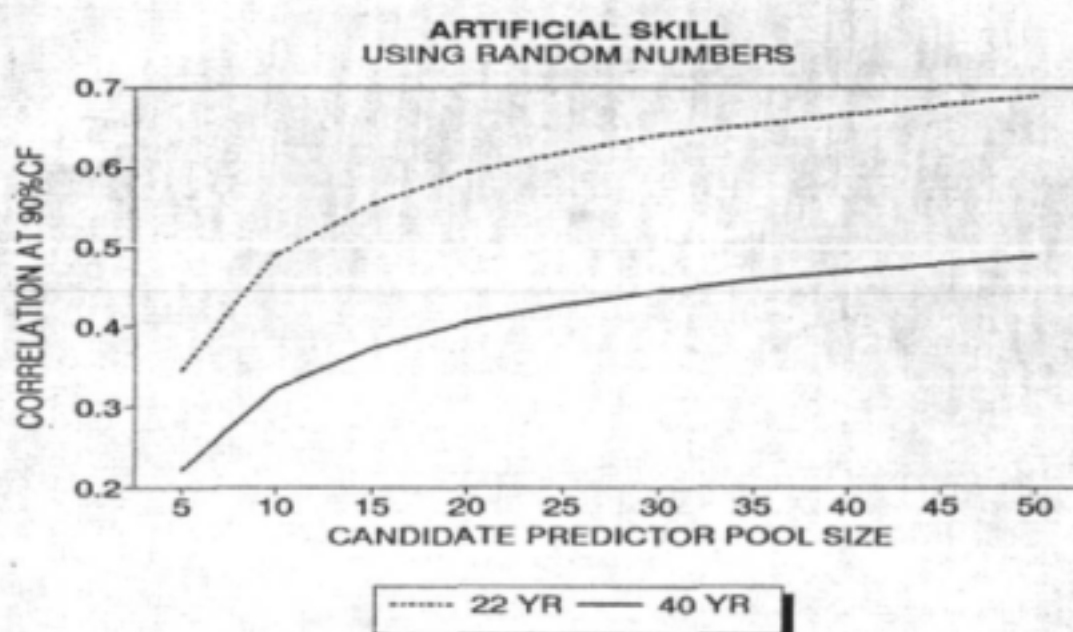


Fig 7-1 Artificial skill generated by a pool of candidate predictors ranging in size from 5 to 50, based on time series of Jury et al (1997) scrambled by Dr S Mason and iteratively used to develop multi-variate models for training periods of 22 and 40 years.

Regionalisation of target areas and formulation of models

A new approach to regionalising target rainfall data is reviewed and models are developed based on new target areas and consolidated predictors. At the outset, it is considered that the climate system offers predictability at lead-times > 3 months only at large spatial scales, where a coherent uptake of remote climatic signals is found. Here we evaluate the appropriate spatial scale for statistical prediction through principal component analysis on Africa rainfall data south of 15° N (collaborating scientist: A. Philipp, University of Wuerzburg, Germany). The rainfall data are continuous monthly departures and derive from the Climate Research Unit (CRU), University of East Anglia gridded at 0.5° resolution. Rotated principal component solutions are calculated for a varying number of PC modes from 10 to 24. The spatial loading patterns are used to define the boundaries of the PC 'clusters' and rainfall area-indices are re-constructed from the original data for each area. Then cross-correlations are computed between all area-indices within each PC solution. The correlation function is plotted for the modes 10 to 24 below. The slope is flat from 24 to 15 PCs and rises from 14 to 10. The inflection point at mode 15 (fig 7-2) suggests an optimum regionalisation for rainfall over Africa. It serves to guide the size of target area for the training of predictive models (fig 7-3). In the case of southern Africa, use of continuous monthly data may not be advisable owing to the dry winter season. So the regionalisation is re-calculated on November to March rainfall (fig 7-4). These target indices are used to develop models, based on consolidated sets of predictors.

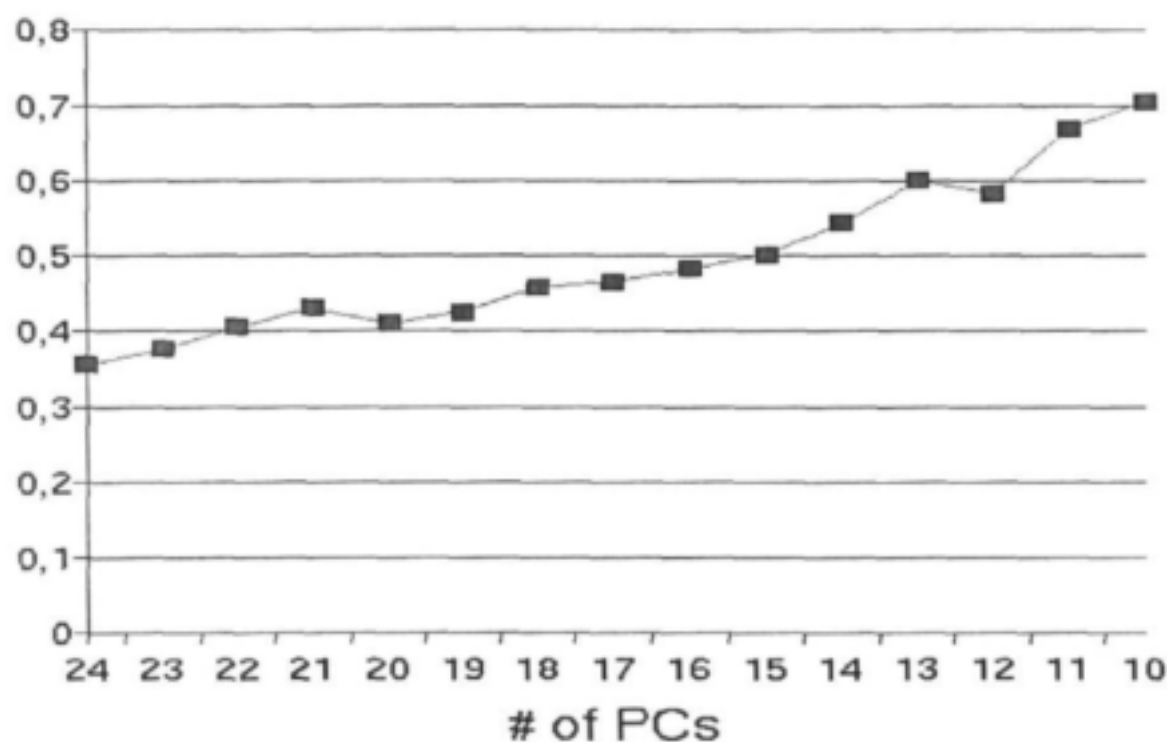


Fig 7-2 Cross-correlation of rainfall indices for various PC solutions, indicating how an optimum regionalisation is achieved.

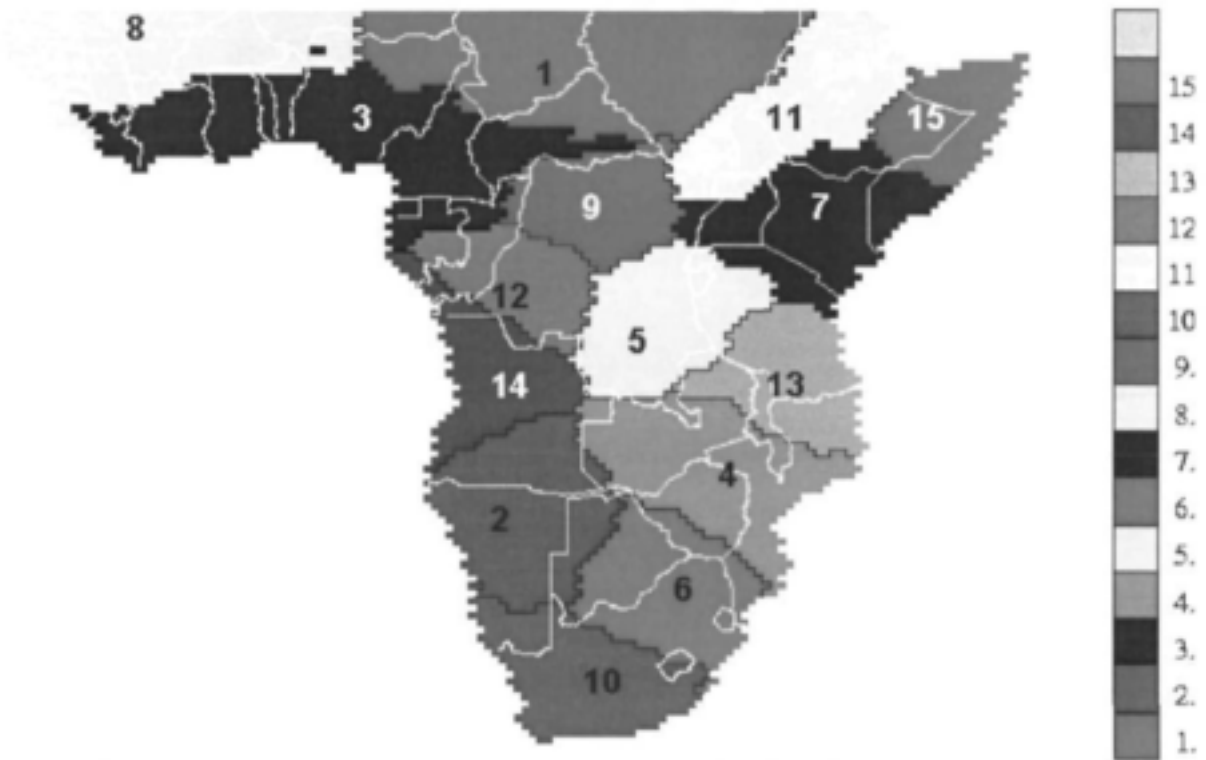


Fig 7-3 Spatial loading pattern for the optimal regionalisation.



Fig 7-4 Spatial loading pattern for selected southern African targets based on seasonal rainfall.

In table 7-2 below, multivariate algorithms are defined based on step-wise regression with new information generated from the WRC project. In some cases 'old' models out-perform newer versions, so these are retained. In some cases NCEP predictors are used as discussed earlier, in other cases COADS PC predictors are used over a 30 year period. In some cases the models exhibit significantly differing characteristics in the first and second half of the training period, so '2nd half' models are retained and the training period is 19 years. In some cases the models are trained over 39 years using the NCEP data.

Because of the 'penalty' applied to evaluate how well the predicted time series fits the observations, the model performance can be intercompared. In most cases two or three models are generated for the same target using either different lead times or different combinations of predictors. For example, the models for eastern South Africa use SST, wind and pressure in various forms to explain about 1/3 of the variance at 3-6 month lead time. Some of these are 'old' models from earlier predictor sets, whilst others achieve a better fit when trained over a shorter period, apparently due to shifts in the way the teleconnections are transmitted. It is anticipated that further refinement and consolidation of predictors will occur and lead to a unified set of predictors and statistical models. Objective cross-validations have been undertaken, however the adjusted hindcast fit provides a simple index of statistical model performance. A value of 1/3 is typical and leads to a tercile hit rate for independent periods of around 50%.

Table 7-2 Statistical models based on new regions - in use 2001+

Nov-Mar Rain	Multivariate algorithm	lead	adj r ² fit	training (yrs)
E South Africa	-.63(wiU)+.34(naSST)-.30(eiP)	JAS	33	19
E South Africa	-.44(wiU)+.38(naSST)-.28(atlw2)	SON	28	19
E South Africa	+.45(angSST)-.53(ciSST)+.49(niV)	SON	32	22 old
W South Africa	+.29(ciEvap)-.55(eiP)+.38(swiSST)	JAS	32	39
W South Africa	+.30(seaSST)+.49(eiU)+.32(QBO30)	SON	35	39
W South Africa	-.69(atlw2)-.46(eiV)	JAS	33	22 old
E Zambezi	-.26(wiU)-.53(eiP)+.32(naSST)	JAS	35	39
E Zambezi	+.36(angV)+.62(eiU)	SON	39	19
E Zambezi	-.35(atlw2)-.40(angP)	SON	34	22 old
E Botswana	+.86(wiOLR)+.56(wiP-nwiP)+.45(caU)	JAS	48	22 old
E Botswana	+.79(Upc3)-.52(Upc3r)-.26(SSTpc1)	JAS	32	30 new
N Namibia	-.70(nwiP)+.48(swaSST) [-seaSST]	JAS	40	22 old
N Namibia	-.50(Ppc2r)+.35(Upc1r)-.40(Vpc1r)	JAS	22	30 new
SA.maize	+.66(wiOLR)-.34(QBO)	SON	33	19 old

Notes on models:

- except for PC predictors: 1st letter is area, 2nd letter is ocean, 3rd letter is parameter,
- adj r^2 fit = reduced by 'penalty' applied for large predictor pool (-16), short training period (-12) and predictors in model (-4),
- 'new' = Mpeta + Philipps PCA 66-95 = 30yr, training period '39' = 59-98, '22' = 72-93, '19' = 79-98,
- models are retained that achieve > 20% adj r^2 fit, co-linear predictors are screened out,
- 'old' = 40 predictors, 'blank' = 18 key-area predictors, 'new' = 20PC predictors

Notes on Predictor Areas:

angSST-V-P=13S-3N,3W-13E, atlw2=200u, 5N-10S,40W-0
 caU=5N-10S,60-20W; naSST=7-23N,18-42W;
 seaSST=13S-3N,13W-11E; swaSST=30-45S,60-30W,
 niV-nwiP=5-15N,45-80E; ciEvap=10S-10N,60-85E
 wiU-P-OLR=5N-10S,40-60E; ciSST=10N-15S,50-80E
 eiP=10N-15S,80-95E; eiU-V=3N-10S,80-100E; swiSST=20-35S,45-65E
 SSTpc1=(10N-10S,60-90E)+(20N-10S,50-10W); Ppc2r =0-25N,70-100E
 Upc1r =10-20N,60-10 W; Upc3=(10-20S,40-10W)+(10-20 S,50-80E)
 Upc3r=10-30S,40W-0; Vpc1r=10-40S,20W-10E; Temp=16-28S,22-34E

Chapter 8 – Summary and recommendations – advances in predictability of southern African climate

This project has formulated statistical models to predict, 3 – 6 months in advance, the variability of southern African climate and water resources. The project has built on past efforts and drawn ideas from graduate students and collaborating scientists, to provide southern African water and resource managers with optimum statistical forecasts via internet website:

< www.1stweather.com/forecasts/cip_seasonal_outlook.shtml > to anticipate shifts in climate. The uptake of this predictive information could reduce economic risks by over \$1 billion per annum in South Africa. However, a predictive benefit is not so easy to achieve, given that losses from missed forecasts are twice the gains from correct ones.

In the initial stage of the project, efforts were placed on extending the results of earlier work, using the same predictors and new hydrological target data. Predictive models were formulated for a number of southern African water resources:

Target	Algorithm	r ² fit
Midmar	+0.44(aVang)+0.37(oNiV)-0.73(oAtlW)	= 64
Pongo	-0.76(aWip)+0.25(aMaurV)	= 61
Vaal	-0.71(oSlp)-0.29(aElu)+0.26(aWCI-AbP)	= 52
Gariiep	+0.39(aVang)-0.78(oSlp)-0.45(oSocnS)	= 71
Hartebees	-0.41(aElv)-0.43(aCIst)+0.44(aWCI-AbP)	= 46
Zambezi	-0.44(aArBst)-0.49(oAtlW)+0.73(oATpc2)	= 73

In one of the studies performed in 1998, hydrological anomalies over Africa were assessed using annual flow data for the Nile, Niger, Congo, Senegal, Zambezi, and Orange Rivers; and Lakes Victoria and Malawi. Significant correlations were uncovered between the various rivers hence it was concluded that drought and flood events are widespread across Africa. A composite analysis of years with high and low flow, determined a sensitivity to coupling between the zonal circulation over the tropical Atlantic and ENSO phase.

In studies developed through an exchange visit of Belgian scientist Jean-Luc Melice, scale-interactions in intra-seasonal to decadal climate variability were investigated using the continuous wavelet transform (CWT) technique applied to two long-term data sets: the Nile River flow and Durban rainfall. For Durban rainfall the annual cycle accounts for 33% of variance, whilst inter-annual fluctuations explain 10%, mainly focused on 2.3 and 4 year bands. Associations between these data sets and the Pacific pressure index of El Nino (SOI) and the Atlantic SST (N-S) dipole were uncovered and again demonstrate the widespread nature of inter-annual forcing over Africa.

In a study performed by senior student S.E. Nkosi, it was demonstrated that summer rainfall over SE Africa increases when easterly flow is present off northern Madagascar in the tropical Indian Ocean. The composite analysis of wet and dry years reveals deep easterly flow

differences in the band 5° - 20°S. Convection is reduced over the South Indian Ocean (0 - 30°S, 60° - 110°E) whilst increased over SE Africa. SSTs increase southeast of Madagascar in the latitude band 25° - 35°S and couple with an anticyclonic circulation, which transfers moisture westward to SE Africa. SST in the tropics are below normal, hence the poleward thermal gradient is reduced and the associated subtropical jet stream shifts polewards to 40°S during wet years.

The study of drought over southern Africa by N. Mwafurirwa revealed a meandering of the sub-tropical jet stream around a standing rossby wave with a ridge on 20°E and trough on 55°E. The structure is such that equatorward flow and subsidence is produced over southern Africa. In the study by M. Gwazantini, variations in key water resources in tropical southern Africa were analysed. Wet years were examined and found to be characterised by an influx of moist monsoonal air from the NE, a zonal overturning cell connected to the tropical south Atlantic, and a subtropical trough over Mozambique. Predictor indices were extracted from environmental fields exhibiting precursor signals at one season lead-time. An outcome was the development of predictive models to forecast changes in the inflow to water resources of southern Africa.

A study initiated by the project leader in 2000 led to an in-depth analysis of monsoons around Africa as predictors of rainfall. For southern African rainfall, SST differences between the southwest and central-west Indian Ocean and the rotational component of monsoon flow in the central Indian Ocean (which controls ocean dynamics) play significant roles. For east African rainfall, the surface zonal wind in the east equatorial Indian Ocean is a key determinant. Westerly (easterly) winds in the east Indian Ocean favor rainfall in southern (east) Africa, and serve to indicate the strength of the zonal direct circulation and the east-west SST gradient. The findings provide support for the use of monsoon indices in predictive models for African rainfall at two-season lead-time. Recognizing that our knowledge of ocean-atmosphere coupling around Africa is limited, it is suggested that greater *in-situ* measurements be gathered as part of GOOS and CLIVAR activities.

In the comprehensive PhD study of senior student E. Mpeta, a principal component analysis of low-resolution African rainfall and temperature, and Atlantic and Indian Ocean SST, SLP, U and V wind was done. Five regional targets and 20 predictors were formulated and models were developed over a 30 year training period, yielding the following results:

Target	Most Significant Predictors	Fit (r ² %)
Rain pc1 Africa south of Zambezi	U pc2r + SLP pc3 eq. E. Indian zonal wind + N-S dipole of press. in Atlantic	20
Temp pc1 Zambezi region	SST pc1 + 1 other central Indian/eq. W. Atlantic SST	70

The models are based on continuous time series, filtered with CWT to isolate variability in the 1.5 - 9 year band. The southern African temperature has a high explained variance

contributed by SST varying in-phase in the west Atlantic and west Indian Oceans. When the time series is detrended, some predictability is 'lost'. The work demonstrates that dipole (or two-area) predictors have considerable value. Of the key area predictors for southern African rainfall: at zero lag the dipole in SST between the SW Indian Ocean and the western tropical Indian Ocean provides a high degree of predictability. At six month lead time the east Indian Ocean zonal wind is a useful lead-time indicator of southern African rainfall.

Using a high resolution rainfall data set, the project leader interacted with German scientists to produce an optimum regionalisation of African rainfall. Rotated principal component solutions were calculated for a varying number of PC modes from 10 to 24. Cross-correlations were computed between the consequent area-indices. The correlation function displayed an inflection point at a 15-mode solution, providing a guide to the size of areas used for the training of predictive models. With a consolidated set of predictors and new targets, multi-variate models were formulated using the step-wise insertion and co-linearity screening procedures outlined earlier. The deflated hindcast fit quoted below is consistent with the tercile hit-rate from objective validation. The models that can be used to provide forecasts by October for rainfall departures in the following summer are:

Nov-Mar Rain	Multivariate algorithm	adj r^2 fit
E South Africa	-.63(wiU)+.34(naSST)-.30(eiP)	33
E South Africa	-.44(wiU)+.38(naSST)-.28(atlw2)	28
E South Africa	+.45(angSST)-.53(ciSST)+.49(niV)	32
W South Africa	+.29(ciEvap)-.55(eiP)+.38(swiSST)	32
W South Africa	+.30(seaSST)+.49(eiU)+.32(QBO30)	35
W South Africa	-.69(atlw2)-.46(eiV)	33

Statistical theory would have us completely eliminate co-linearities within these models. However, using indices of the coupled ocean - atmosphere system as predictors it is advantageous to preserve the associations. Providing these conspire and yield cumulative impacts (eg. model coefficients are consistent with correlation), model performance may be optimal. Whilst this WRC project has enabled the implementation of a variety of models to predict fluctuations of southern African climate and water resources, further work should seek to separate the spectral components of the climate system into discrete bands. Some preliminary results of this work, in collaboration with W. White, are given in fig 8-1 below. The underpinning research should consider 'slow' wave patterns that propagate zonally in the atmosphere and ocean basins, an example of which is shown in fig 8-2.

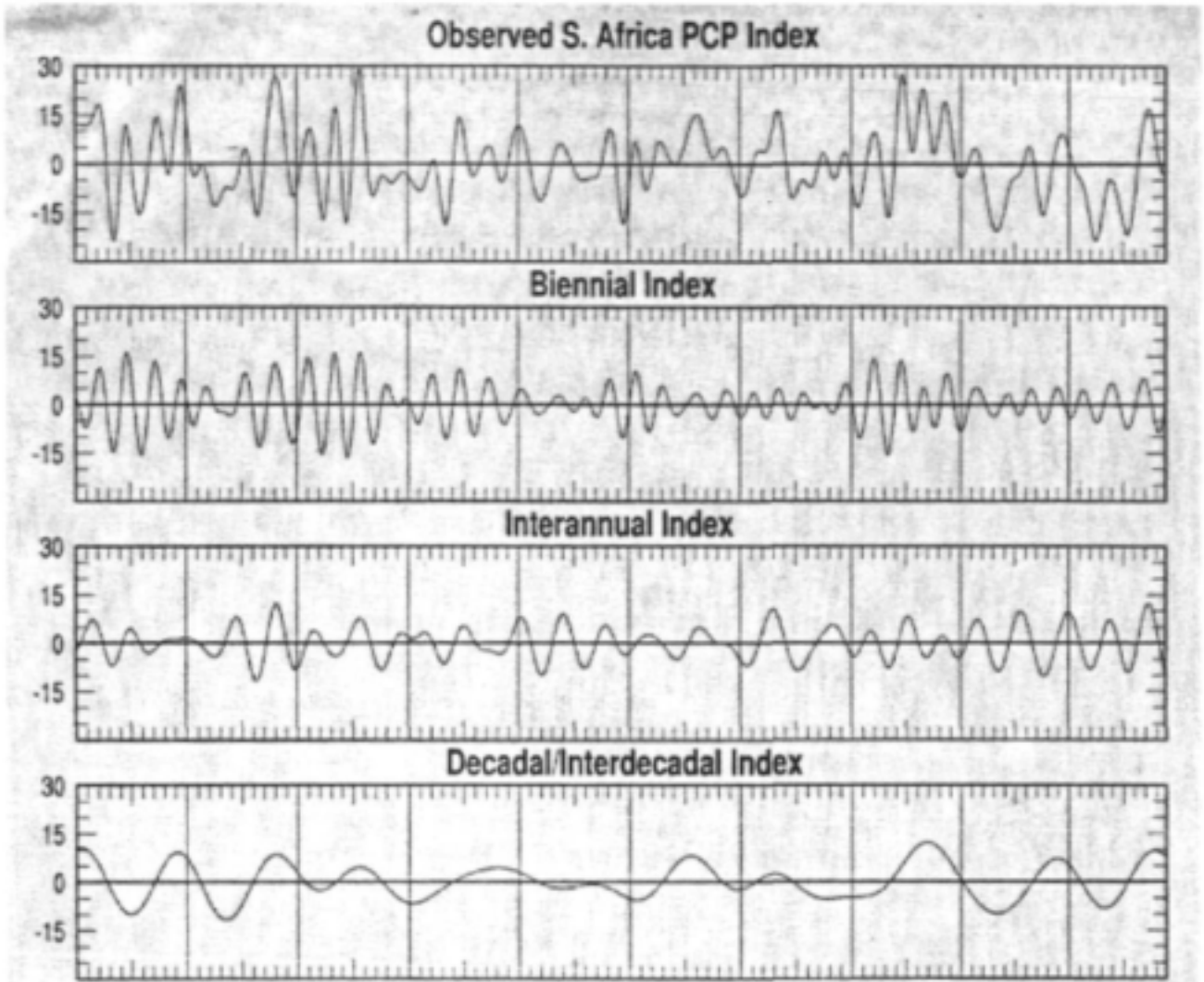


Fig 8-1 Various spectral bands within southern African rainfall over the past 100 years (from White, Scripps, 2001).

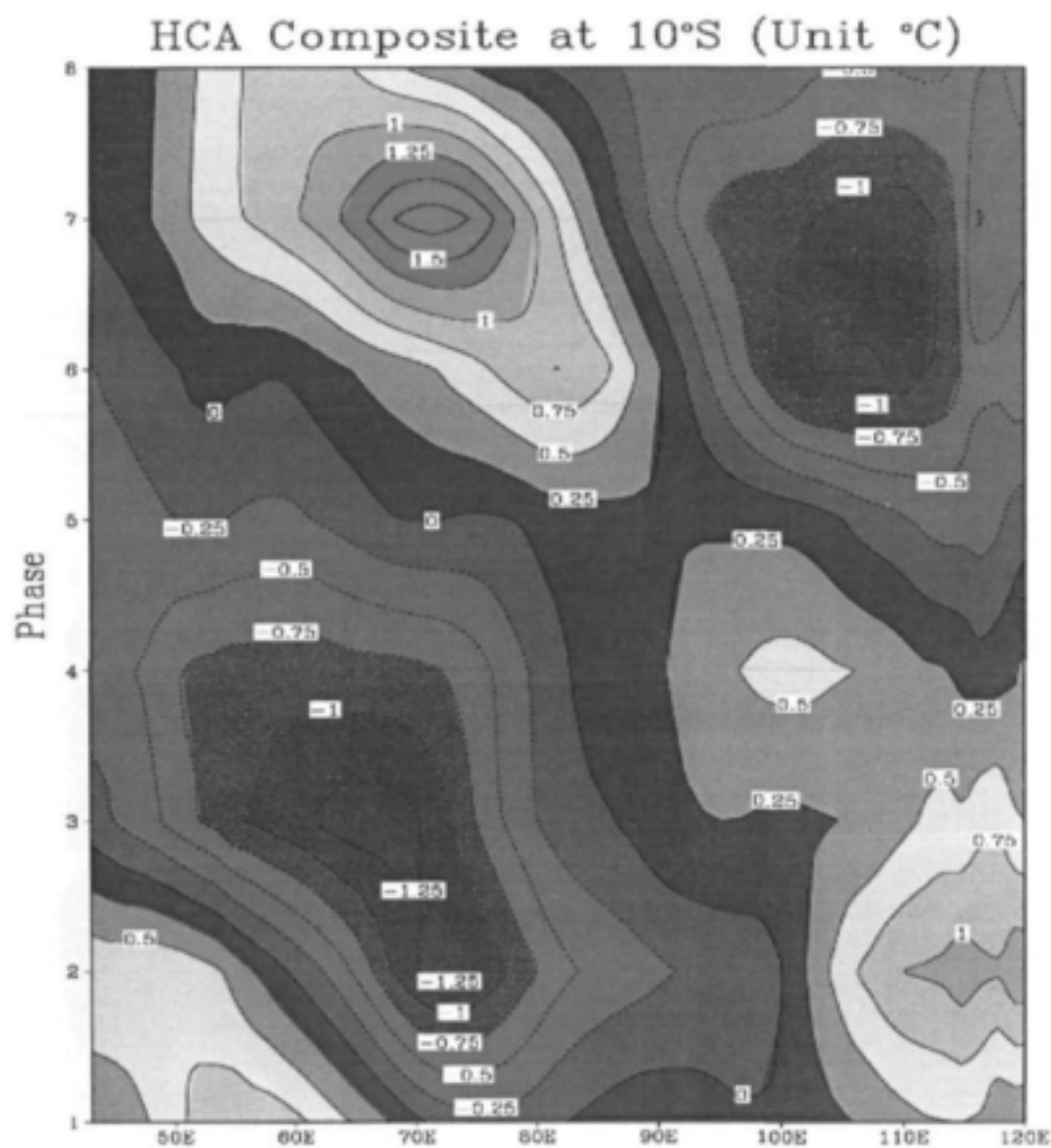


Fig 8-2 Composite rossby wave pattern plotted in hovmoller fashion for a sequence of 12 (dipole) events over the period 1958-98, based on heat content anomalies (thermocline depth) in the Indian Ocean along 10S. The y-axis represents time where each phase is about one season; x-axis is longitude. A full cycle is completed (on average) every 3.8 years. The results indicate a slow moving 'wave' shifting westward at 0.1 m s^{-1} in a predictable manner (from Huang pers comm.).

Other related WRC reports available:

Space-Time modelling of rainfall using the string of beads model: Integration of radar and rain-gauge data

AN Clothier & GGS Pegram

The String of Beads model is a stochastic rainfall model based on the combined observations of a large network of daily rain-gauges and an S-band weather radar situated near Bethlehem, South Africa. The model draws on the ideas and observations of many other rainfall modellers (mentioned at appropriate places in the report) to form an efficient means of simulating rainfall over a wide range of spatial and temporal scales.

The most successful aim was the sharing of the strengths and simplicity of the String of Beads model (SBM) with the Hydrological, in particular, the international community. In principle, the model can be adapted to varying topography and these ideas are under further development.

One of the unexpected successes of the model is that it can be used for short-term rainfall forecasting - more about this later in the summary - so although there is more to do in improving the calibration, there are already practical spin-offs which will bear fruit from this research contract.

Report Number: 1010/1/02

ISBN: 1 86845 835 0

Modelling extreme rainfall over Southern Africa

AM Joubert, SJ Crimp and SJ Mason

For sound planning and adequate warning, early recognition of conditions which give rise to heavy rainfall occurrences is vitally important. This project investigated the modelling of extreme rainfall over a range of temporal and spatial scales in Southern Africa. Firstly, with the help of the well-known CSU RAMS mesoscale model and the Wits University CRG kinematic trajectory model, new insight was gained into moisture sources and transport associated with widespread heavy rainfall periods such as the one which affected almost the entire summer rainfall region of South Africa in February 1996. Secondly, the CRG trajectory model was used to investigate air mass transport and moisture sources associated with tropical cyclone Demoina (January 1984), revealing that the primary moisture source was highly localised and associated with the vortex itself. Thirdly, in examining the difficulties experienced by some models in forecasting recent wet seasons, it appeared that premature northward progression of the westerly winds during autumn, was being simulated, resulting in too early an end to the rainfall season. Finally, a step towards overcoming problems of poor spatial resolution in GCM usage for simulating rainfall variation at inter-annual and climatological time scales, was taken with the successful nesting of the CSIRO limited area model (DARLAM) within the CSIRO9 GCM output.

Report Number: 805/1/99

ISBN 1 86845 488 6

TO ORDER: Contact Rina or Judas - Telephone No: 012 330 0340
Fax Number: 012 331 2565
E-mail: publications@wrc.org.za

Water Research Commission

Private Bag X03, Gezina, 0031, South Africa

Tel: +27 12 330 0340, Fax: +27 12 331 2565

Web: <http://www.wrc.org.za>



1868459365